Ecosystem on a Chip:

Understanding communication between plant and fungus

Zur Erlangung des akademischen Grades eines

Doktors der Naturwissenschaften

(Dr. rer. nat.)

von der KIT-Fakultät für Chemie und Biowissenschaften

des Karlsruher Instituts für Technologie (KIT)

genehmigte

DISSERTATION

von

M.Sc. Christian Metzger

Dekan: Prof. Dr. Hans-Achim Wagenknecht

Referent: Prof. Dr. Peter Nick

Korreferent: Prof. Dr. Tilman Lamparter

Tag der mündlichen Prüfung: 19. Juli 2023

I.   Eidestattliche Erklärung

Hiermit erkläre ich, dass ich die vorliegende Dissertation, abgesehen von der Benutzung der angegebenen Hilfsmitteln, selbstständig verfasst habe.

Alle Stellen, die gemäß Wortlaut oder Inhalt aus anderen Arbeiten entnommen sind, wurden durch Angaben der Quelle als Entlehnung kenntlich gemacht.

Diese Dissertation liegt in gleicher oder ähnlicher Form keiner anderen Prüfungsbehörde vor.

Karlsruhe den 25.07.2023

Christian Metzger

II.   Acknowledgement

I would like to thank Prof. Peter Nick for his guidance through a lot of my recent path. He instilled not only a fascination for botany in me, but for science at large and its place and importance in society. I want to extend my gratitude to Michael Riemann for his supervision and for proofreading the present thesis. Thanks to the entire Bota … oops! I meant, the Joseph Gottlieb Institut für Pflanzenwissenschaften for the encouraging working environment and for sharing many laughs.

Then I would like to thank two cooperation partners: Firstly, I would like to thank Leona M. Schmidt-Speicher for her great cooperation with the project. Secondly, I would like to thank Verena Höhn for her cooperation in life and for putting up with the mess I am.

Lastly, I would like to thank the cherry tree in my backyard, or rather, I would like to thank what it represents. Recently, when I stand in my kitchen in the morning, waiting for the coffee machine tirelessly doing its part, my eyes wander to the window. I am consistently astonished by the simple, yet endless beauty this tree radiates. In these small moments, a person can just exist in awe of nature. It puts immense energy into flowering to create an ever-changing masterpiece, unaware of the crumbling world around it. I would like to thank everything and everyone that creates beauty, laughter, kindness and warmth in a world that feels grimy, bitter, uncaring and cold at large. My gratitude to the people that strive to make others laugh, the artists for creating wonders, the musicians for giving rhythm to the chaos and thank everyone for caring.

III.   Abstract

English

In symbiosis, the relationship between the two species relies on the exchange and recognition of signals. In parasitism, the attacking species focuses on the avoidance of detection, whereas the host species strives to improve its ability to recognize the presence of the invader. Climate change throws off the balance that has been achieved by long evolutionary periods by weakening the host or by enabling pathogens to spread to new regions, meeting naïve hosts that are susceptible to their attacks. To reduce the devastating yield losses caused by pathogens, farmers apply chemical plant protection. Excessive use of herbi- and fungicides can be economically costly and cause unintended damage to the environmental ecosystem. Alternatively, immunoactive compounds could be used to strengthen the plant's inherent defence capabilities by exploiting the defence priming. Prior exposure to a stress stimulus causes plants to react stronger and quicker, once a pathogen attacks to shift the immune-related interaction in the favour of the host plant. In this work, we aimed to identify the mode of action of bioactive fungal metabolites of *Roesleria subterranea*, identified by our project partner at the ibwf, Mainz. Additionally, we aimed to establish methods to quantify the defence reaction of a plant cell suspension cultivated in a Microfluidic BioReactor (MBR), like measuring the concentration of Reactive Oxygen Species (ROS) and monitoring the extracellular pH. We modified the established design of the MBR to potentially cultivate fungal cells to perform co-cultivation experiments with plant and fungal cells in the same system while monitoring the cells' reaction.

Within the *R. subterranea* metabolites, we identified the AcetonAduct of Entatrevenetinon (AaE) to be a potential effector, uncoupling the synthesis of phytoalexins from the initiation of Programmed Cell Death (PCD) inherent to a successful defence reaction. For the MBR we conducted successful proof-of-concept experiments to continuously measure the pH in the MBR and detect significant differences in the H_2O_2 concentration in the outgoing medium. The cultivation of fungal cells within the MBR was possible for shorter periods and preliminary co-cultivation experiments were successful.

In summary, this work demonstrated the feasibility of multiple applications of the MBR in measuring parameters of the plant immune response and identified possible

improvements to streamline these methods. Additionally, we identified AaE as a potential effector in uncoupling phytoalexin synthesis from the PCD inherent to a successful defence reaction of the plant.

Deutsch

In jeder Symbiose ist das Verhältnis der zwei beteiligten Spezies geprägt vom Austausch und der Erkennung von Signalen. In parasitären Beziehungen, konzentriert sich die angreifende Spezies auf das Vermeiden ihrer Erkennung, während die Wirts-Spezies kontinuierlich ihre Möglichkeiten verbessert, Eindringlinge zu entdecken. Änderungen im globalen Klima ändern das Gleichgewicht, in dem sich Spezies befinden, indem sie den Wirt erheblich schwächen oder den Pathogenen ermöglichen, in neue Gebiete vorzudringen und naive Wirte zu treffen, die ihren Angriffen gegenüber anfällig sind. Um die existenzbedrohenden Ernteverluste zu reduzieren, die von Pathogenen verursacht werden, setzen Agrarwirte chemischen Pflanzenschutz ein. Dieser kann, bei exzessivem Gebrauch, den Landwirt finanziell und dem Ökosystem durch Nebenwirkungen schaden. Alternativ könnten immunoaktive Substanzen verwendet werden, um die inhärenten Verteidigungsfähigkeiten von Pflanzen zu stärken, indem man das „Defence Priming" der Pflanzen nutzt. Hier verursacht ein vorhergehender Stress Stimulus, dass die Verteidigungsreaktion einer Pflanze schneller und stärker ausfällt, sollte ein Pathogen angreifen. So wird die Interaktion zwischen Pathogen und Wirtspflanze zu Gunsten der Pflanze manipuliert. In dieser Arbeit wurde der Wirkungsmechanismus von pilzlichen Metaboliten von *Roesleria subterranea* untersucht, die von unseren Projektpartnern am ibwf, Mainz als bioaktiv identifiziert wurden. Zusätzlich wollten wir Methoden etablieren, Mikrofluidische BioReaktoren (MBR) zu nutzen, um die Verteidigungsreaktion von Pflanzenzellen zu quantifizieren, die in ihnen kultiviert werden. Es sollten die Konzentrationsmessung von Reaktiven Oxygen Spezies (ROS) und eine Beobachtung des extrazellulären pHs getestet werden. Wir haben das etablierte Design des MBR geändert und getestet, um pilzliche Zellen darin zu beherbergen, um sie in möglichen Co-Kultivierungs Experimenten unter kontinuierlicher Beobachtung zu verwenden.

Unter den *R. subterranea* Metaboliten konnten wir das AcetonAduct von Entatreventinon (AaE) als möglichen Effektor identifizieren, der in der Lage zu sein scheint, die Synthese von Phytoalexinen von dem Programmed Cell Death (PCD) einer erfolgreichen Immunreaktion der Pflanze zu trennen. Mit den MBR wurden

erfolgreiche Experimente durchgeführt, in denen wir den pH kontinuierlich messen konnten und konnten signifikante Unterschiede in der H$_2$O$_2$ Konzentration im ausfließenden Medium des MBRs messen. Das Kultivieren von Pilz-Zellen im MBR war nur für kurze Zeiträume möglich, in denen wir jedoch ein erfolgreiches Co-Kultivierungsexperiment durchführen konnten.

Zusammenfassend, konnte diese Arbeit das Potential demonstrieren, MBRs zu nutzen, um die Parameter einer pflanzlichen Immunreaktion während des Kultivierens auszulesen. Es wurden mögliche Verbesserungenmöglichkeiten im System erkannt, um die Methoden zu vereinfachen und zu beschleunigen. Zusätzlich wurde AaE als möglicher Effektor erkannt, der in der Lage zu sein scheint, die Synthese von Phytoalexinen von der Induktion des PCD zu trennen, der fester Bestandteil einer erfolgreichen Verteidigung der Wirtspflanze ist.

IV.   Contents

Table of content

Contents

Contents

Contents

Table of figures

Main figures:

Supplementary figures:

Tables:

Table of abbreviations

AaE	**A**ceton**A**duct of **E**ntatrevenetinon
BY2	**B**right **Y**ellow 2
CDA	**C**ell **D**eath **A**ssay
CTRL	**C**on**TR**o**L**
DAMP	**D**amage **A**ssociated **M**olecular **P**attern
DMSO	**DiM**ethyl **S**ulf**O**xide
eGFP	**e**nhanced **G**reen **F**luorescent **P**rotein
ETI	**E**ffector **T**riggered **I**mmunity
FABD2	**F**imbrin **A**ctin **B**inding **D**omain **2**
GFP	**G**reen **F**luorescent **P**rotein
GoI	**G**ene **o**f **I**nterest
GTD	**G**rapevine **T**runk **D**isease
JAZ1	**JA**smonate-**Z**im-domain protein **1**
LatB	**Lat**runculin **B**
LB medium	**L**ysogeny **B**roth medium
MAMP	**Mi**crobe **A**ssociated **M**olecular **P**attern
MBR	**M**icrofluidic **Bio**R**eactor
MeJA	**Me**thyl-**JA**smonate
MeOH	**Me**thanol
MS medium	**M**urashige-**S**koog medium
MTOC	**M**icro**T**ubule **O**rganizing **C**entre
OD	**O**ptical **D**ensity
OVC	**OV**ernight **C**ulture
PAL	**P**henylalanine **A**mmonia **L**yase
PAMP	**P**athogen **A**ssociated **M**olecular **P**attern
PCD	**P**rogrammed **C**ell **D**eath
PCR	**P**olymerase **C**hain **R**eaction
PR1	**P**athogenesis-**R**elated protein **1**
PRR	**P**attern **R**ecognition **R**eceptor
PTI	**P**AMP **T**riggered **I**mmunity
RL	**R**eporter **L**ine
ROS	**R**eactive **O**xygen **S**pecies
rpm	**R**otations **P**er **M**inute
RT	**R**oom **T**emperature (~25°C)
SAR	**S**ystemic **A**cquired **R**esistance
SoI	**S**ubstance **o**f **I**nterest
STS	**ST**ilbene **S**ynthase

1. Introduction

1.1 The grapevine

1.1.1 History of wine

As early as the human being has developed a mind, it has looked for ways to numb it. In many early civilizations, psycho-active substances were integral parts of religious experiences, medicine and recreational use (Crocq 2007). The transcendental state of being achieved by the proper use of these drugs was associated with the embrace of spiritualism or interpreted with a connection to the respective deities. Arguably, alcohol was the most influential drug for our species. The importance of the intoxicating beverage, achieved by having yeast digest starch or sugar-containing substances, is mirrored in the presence of alcohol-associated iconography in many prevailing religions today. In the polytheisms of the Greeks and Romans, there were deities specifically dedicated to wine, intoxication and fertility. Dionysos in Greece and Bacchus in the Roman Empire were often depicted with grapevines and their berries. The belief system of the Sumerians knew three distinct beings: Gestin, as the "mother of the vine", Pagestindug "the good vine" and Ninkas the esteemed "lady of the intoxicating fruit". (Dittrich 2015). In Christianity, many stories and allegories are told using metaphors of wine, drunkenness, vine and vineyards, with a titular character of the liturgy turning water into wine.

Even still, wine is of immense value to many cultures today. In 2021 there was a global production of wine of 261,071,000 hL, of which 19,800,000 hL were consumed in Germany alone (Database | OIV 2023). Some countries attach their local identities to the intoxicating beverage. Italy is known as the wine country and during the first local lockdowns during the COVID-19 pandemic in the year 2020 people, morbid as this humour might be chuckled at pictures of barren shelves of red wine, nestled between stocked shelves in French grocery stores. In wine-producing regions like Rhine-Palatine, many local traditions and festivities are centred around wine, the harvest and production thereof and the celebratory consumption once the strenuous harvesting season has ended.

While the roots of the grapevine dig deep into the beautiful countryside of Italy, France and the vineyards of Germany, the roots this plant digs into our history are even deeper. The earliest traces of grape wine production led to the country of Georgia in Eurasia. On remnants of pottery found in dig sites, traces of wine were found dating

back to 6,800 years BCE (McGovern et al. 2017). The production of the beverage was developed enough that our ancestors added antimicrobial resin during the ageing process, either to protect the valued good or to mask unintended aromas developing. This technique is still present today in the Greek wine variety Retsina. Findings in these dig sites hinted at the production of wine being performed in larger volumes, which has big implications. Large-scale production of wine implies the use of a domesticated grapevine. While it is possible to use wild grapevines as the substrate for winemaking, wild species of wine are often diecious, making it necessary to grow plants of both sexes and thus decreasing the yield. Early humans likely selectively cultivated the grapevine to be hermaphroditic, thus rendering every plant able to grow berries, effectively increasing the harvest. Additionally, the grapevine produces its first berries at three or more years of age, making the sedimentary lifestyle of early humans a prerequisite for large-volume winemaking. Genetic analysis of a wide range of grapevine cultivars in different locals shed light on the early history of the coexistence of grapevine and *Homo sapiens*. Evidence points towards two individual domestication events of the grapevine dating back 11,000 years (Dong et al. 2023). The last glacial period in the Pleistocene caused the fragmentation of *Vitis* populations and thus increased speciation pressure. With an amelioration of the climate towards the end of the Pleistocene two domestication events of *Vitis* occurred in Western Asia and the Caucasus. The grapevines spread westward into Europe and mixed with wild European grapevines, giving rise to a plethora of varieties resulting in the diversity in cultivars established today (Dong et al. 2023).

Since then, the cultivation of grapevine in the vineyards was further improved, with viticulturists breeding new cultivars to improve the yield and taste of the berries in either wine or table grapes. The process of turning grapes into an intoxicating beverage has also changed over the millennia, with today's process being mainly shaped by the methods established in Christian monasteries (Dittrich 2015).

1.1.2 Encroaching diseases

To meet the high demand for quality wine, local cultivars of wine are oftentimes bred to excel in the yield and taste of the berries and the resulting beverages. This coincides with deficits in the inherent resistance capabilities of the plant. The instability of plants bred with the singular focus on economic profits was demonstrated by the accidental introduction of Phylloxera to Europe in the 19th century (Granett et al. 2001). *Daktulosphaira vitifoliae* co-evolved with north American wild grapevines, which have developed partial resistance to the insect. When *D. vitifoliae* met with the naïve grapevine cultivars of Europe, it met little resistance in the vines that were bred first and foremost for their yield and taste at the cost of inherent defence mechanisms and was able to ravage the European vineyards.

Now, with the advance of climate change, more frequent and more extreme weather phenomena occur that stress plants considerably and reduce economic yield. Additionally, changing climates enable pathogens to conquer new lands and attack naïve and weakened hosts and potentially change the nature of existing symbiotic relationships, due to their ideal conditions shifting quicker than the respective host plants could develop new resistances (Elad and Pertot 2014). Already, the use of fungicides in the protection of commercial vineyards impacts the environment and the need for protection will only increase if new pathogens attack local cultivars. It is therefore of great importance to understand the interaction of pathogen and host, to understand the mode-of-action of the pathogen attack to potentially develop strategies to bolster the plant's resistance to the challenges it will inevitably face.

In the following section, we describe two examples of grapevine symbionts and what defines their relationship to the host plant.

1.1.2.1 *Neofusicoccum parvum*, a causal agent of Esca

Neofusicoccum parvum is a member of the *Botryosphaeriaceae* family and a known causal agent of the Grapevine Trunk Diseases (GTD) (Crous et al. 2006; Carlucci et al. 2015). It can live endophytically for long periods in the trunks of grapevine, causing only minor damage and primarily feeding off dead wood (Slippers and Wingfield 2007). During this stage of its life cycle, the fungus is spread from an infected vine to a new host by pruning or cutting the plant. Grapevine and *N. parvum* can coexist for years, without any obvious signs of disease. If the plant suffers a severe period of stress, the fungus can switch to an apoplectic phase, killing its host within a few days. Khattab et

al. (2022) showed that in the relationship between *N. parvum* and the grapevine, the detection of an accumulation of a single molecule can drastically alter the behaviour of the pathogen. If the grapevine suffers stress, like drought or excessive heat, the generation of new wood is disturbed. The synthesis of lignins is reduced and the intermediate trans-ferulic acid accumulates. This accumulation is detected as a sort of "surrender signal" and the fungus switches off its endophytic lifestyle, produces the phytotoxin fusicoccin A and feeds off the dying host tissue to acquire the needed nutrients to activate its sexual life cycle (Khattab et al. 2022). By producing spores, *N. parvum* can spread to a potential new host that does not suffer environmental stress.

This sudden apoplexy of, sometimes multiple grapevines at once, is known as Esca and is intensified by climate change (Beris et al. 2023). Climate change causes more frequent and more extreme weather phenomena, stressing vineyards so that endophytic symbioses of grapevine and *N. parvum* switch to apoplectic. This oftentimes affects older vines, which are known to be the most productive, thus causing massive economic losses.

This highlights the importance of researching the communication between the host plant and the pathogen. If it was known which signals are detected in these fatal interactions, we could potentially intervene. In the case of *N. parvum* and the detection of trans-ferulic acid a potential channelling of this lignin precursor towards the synthesis of phytoalexins was proposed (Khattab et al. 2022). *Neofusicoccum parvum*, because of its aggressiveness, was established as a model organism to research the interactions of plants and causal agents of GTDs.

1.1.2.2 *Roesleria subterranea*, a causal agent of dieback disease

A lesser-known fungus, *Roesleria subterranea* is, as the name suggests, a subterranean ascomycete that grows on the roots of deciduous trees and woody plants. The fungus is mainly known as a symbiont growing on the roots of the grapevine and is considered to be a minor parasite of it. The ascomycete is distributed globally and prefers cooler climates (Neuhauser et al. 2011). It has been identified in several European countries (Neuhauser et al. 2011), the United States of America (Miles and Schilder 2009) and Canada, New Zealand and finally Japan (Degawa et al. 2015). Neuhauser et al. (2011) collected reported sightings of *Roesleria subterranea* from different older and smaller publications. These publications often were very specialized

and in local languages. The vast majority of *R. subterranea* sightings were recorded on the roots of *Vitis vinifera* plants cultivated in commercial vineyards (Neuhauser et al. 2011; Miles and Schilder 2009). There are a few isolates of *Roesleria* strains found on the roots of a variety of deciduous trees (Beckwith 1924; Degawa et al. 2015). Notably, many of the plant species harbouring *Roesleria* strains belong to the family of the Rosaceae with the most notable exception being the Vitaceae. They may differ in their family but all host plants observed to be infected with *Roesleria* are situated within the Rosids clade. Notably, nearly all cases of the fungus *Roesleria subterranea* recorded are sightings of the ascomycete growing on economically important species. Therefore, there might be a certain bias within the observations. Historically and colloquially, *Roesleria subterranea* is considered a minor parasite of the grapevine (Neuhauser et al. 2011). Thus observations of *R. subterranea* and work with it were not met with appropriate interest and were published in smaller, specialized publications in local languages. Therefore the information on the fungus did not reach the viticulturists, even though there is evidence proving that *R. subterranea* can infect healthy plants and reduce their growth by 60-70 % (Miles and Schilder 2009). Neuhauser et al. (2011) determined that 46 % of dieback cases they observed in *Vitis* were caused by *Roesleria subterranea* and infected plants can die within two to three years. Regardless of the substantial damage an infection with *Roesleria subterranea* can cause, the fungus is often underestimated because a causal connection between yield loss and fungus is not immediately obvious. The aforementioned lack of widely distributed information on the fungus causes keepers of vineyards to not look for *R. subterranea* when plants succumb to dieback. This is compounded by the fact, that infection with this fungus is hard to detect. The ascomycete grows on the root of the plant, kills off tissue to feed and thus causes root rot. The resulting above-ground symptoms are very ambiguous and even if detected and correctly assigned they appear late in infection when the plant is already irreparably damaged. For early detection, the observer needs to look at the roots of the vine at a depth of at least 50 cm, but characteristic fruiting bodies of *R. subterranea* can be hard to spot, especially in the field. Neuhauser et al. (2009) established a method to isolate the DNA of the grapevine root system and screen for the presence of *R. subterranea* using species-specific primers in a PCR. The feasibility of this method is limited for field use. To screen a wide area of a vineyard, samples would need to be pooled.

Roesleria subterranea belongs to the *Roesleriaceae* family, sharing the taxon only with *Roeslerina* spp. (Yao and Spooner 1999). Using the ITS1-5.8S-ITS2 rRNA gene a phylogenetic tree was generated, suggesting *Roesleria subterranea* to be closely related to the genus *Hymenoscyphus* (Kirchmair et al. 2008), which is a member of the *Helotiaceae* family. Information on the members of the *Hymenoscyphus* genus is scarce. Some species are believed to live saprotrophically on dead leaves, like *H. albidus*. Other species are plant pathogens like *H. fraxineus* which is the causal agent of ash dieback in Europe (Gross et al. 2014; Baral et al. 2014). The order Helotiales containing the *Helotiaceae* and potentially the *Roesleriaceae* as well also harbours severe plant pathogens like *Botrytis cinerea*, a notable foliage pathogen of members within the Vitaceae. The interspecies relationships between different strains of *R. subterranea* were characterized by Kirchmair et al. (2008) and Degawa et al. (2015) using the ITS1-5.8S-ITS2 rRNA gene. Strains growing on a host of the same species regardless of the geolocation are more closely related than European strains growing on the roots of different host plants. Whereas, notably, the isolates of *R. subterranea* not on *Vitis* roots are very rare, due to the vast differences in the economic interest in the different host plants driving the identification. To generate phylogenetic trees with a higher resolution it is important to isolate more strains of *Roesleria* in more geolocations and on more roots of deciduous trees.

1.2 Plant immunity

To gain insight into what shapes the relationship of a plant with its symbiont, we need to consider the nature of the plant's immune system. The immune reaction of a plant, when faced with the attack of a potential pathogen, consists of two, more or less, distinct layers: a basal defence reaction that mounts a broad immune response against a variety of pathogens and a targeted, often intense reaction to the presence of a specific pathogen. The first, basal layer of defence is the so-called PAMP Triggered Immunity (PTI) (Jones and Dangl 2006). PAMPs are Pathogen Associated Molecular Patterns that can be recognized by membrane-bound Pattern Recognition Receptors (PRR) to trigger an immune response (Zipfel and Felix 2005). The term Microbe Associated Molecular Pattern, MAMP is also gaining more traction, since the communication between symbionts that do not necessarily define as parasitic, also relies on the detection of these patterns. Yet, in the context of plant immunity, the term PAMP is still more prevalent. While we see the value of the term MAMP, we will use the term PAMP in this work. These PAMPs are oftentimes molecules under strong evolutionary conservation pressure for the pathogen and thus, do not change rapidly, if at all. Virulent pathogens that cannot evade the detection of their PAMPs, have developed so-called effectors they can use to quench the defence reactions of a mounted PTI. The pathogen injects a variety of effectors that can influence the immune response of the host (Boller and He 2009) by binding to and directly inhibiting the PRRs initiating the PTI (Xiang et al. 2016), dephosphorylating important kinases to interrupt signalling (Zhang et al. 2007), regulating RNA metabolism, influencing the trafficking of vesicles or suppress the accumulation of phytohormones (Block et al. 2008). With the help of these effectors, some pathogens can suppress the PTI of the host, rendering them susceptible once more. Consequently, resistant plants have developed ways to detect the presence of effectors to mount the specific and often stronger Effector Triggered Immunity (ETI) (Jones and Dangl 2006). Plants can deploy so-called Nucleotide Binding-Leucine Rich Repeats (NB-LRR) to either directly detect the effector itself or, according to the guard hypothesis, by monitoring the integrity of cellular structures of the host cell (Takken and Tameling 2009) to start an immune response, once malicious modifications are detected. The signalling of both PTI and ETI employs similar mechanisms, differing mostly in sequence, intensity and frequency (Tsuda and Katagiri 2010; Thomma et al. 2011). This blurred dichotomy is also

mirrored in the defence strategies engaged, of which PTI and ETI share many but vary in intensity and duration.

To circumvent the ETI, pathogens can develop new effectors to quench the ETI reaction, which in turn, can then be detected by the plant, given they evolve the necessary NB-LRRs. This results in an arms race, that can logically only end in either party being entirely defeated and remaining susceptible or by the partners of the parasitic relationship finding some sort of mutually beneficial balance in the form of a mutualistic symbiosis. Hypotheses are stating, that all mutualistic symbioses present today, have at some point in their co-evolution started as a parasitic relationship and have, over time, developed into a beneficial partnership (Drew et al. 2021). Sometimes, the borders between classes of symbioses are hard to define, which would be perfectly explained by the evolution from parasite to mutualist taking place alongside a continuum spanning several shades of antagonisms to partners.

In the following sections, we want to highlight examples of stress signalling and defence reactions associated with plant immunity.

1.2.1 Cytoskeleton and signalling

The cytoskeleton of a cell not only gives it its shape but is an integral part of many cellular processes, signalling among them. The cytoskeleton of plants consists of two main components. The microtubules consist of α- and β-tubulin, nucleating in MicroTubule Organizing Centres (MTOC) containing γ-tubulin. α- and β-tubulin form dimers, 13 of which assemble in hollow tubes with a diameter of 25 nm (Cooper and Hausman 2016). Microtubules are dynamically unstable, with the rate of polymerization and depolymerization being regulated by the hydrolysis of the GTP bound to the tubulin monomers. The second component of the cytoskeleton is the actin filaments. The actin filaments consist of globular monomers of actin that readily polymerize and depolymerize at both ends of the filament. The monomers are bound to ATP, whereas the hydrolysis thereof regulates the rate of polymerization (Cooper and Hausman 2016). Both the microtubules and the actin filaments exhibit a polarity with the plus-end polymerizing at a considerably higher rate than the respective minus-end. Aside from their structural function in the cell, actin filaments and microtubules are heavily involved in the immune response of plants. The cytoskeleton is known to reorganize in order to facilitate the transportation of organelles and defence compounds to the site of pathogen recognition to ensure an efficient defence reaction (Wang et al. 2022a).

9

Additionally, the cytoskeleton is involved in the signalling of the defence reaction. Qiao et al. (2010) and Guan et al. (2021) showed that the dynamics of the microtubular structures influence the intensity of defence-associated gene expression. The cytoskeleton touches many aspects of stress signalling. It regulates the dynamics of Pattern Recognition Receptors (PRR) and interacts with the signalling and generation of Reactive Oxygen Species (ROS) (Cao et al. 2022). This work focuses on the immunity-related defence reaction, while previous work in our institute has established that the microtubules are an integral part of cold sensing (Wang et al. 2019).

While the cytoskeletal involvement in the defence reaction is complex and far from fully understood, it is clear, that it is an integral part of many aspects of defence reaction and signalling. The observation of the cytoskeleton can give insight into the nature of a defence reaction. In previous work, our group identified cytoskeletal differences in a PTI-like and an ETI-like defence reaction (Guan et al. 2013).

1.2.2 Ca^{2+} and the pH shift

An early signal produced by plant cells, recognizing the presence of a pathogen is a sudden influx of calcium ions from the apoplast into the cytosol of the plant cell (Jiang and Ding 2022). Plants cells actively create a low concentration of Ca^{2+} in the cytosol by sequestering the ions into organelles (Hilleary et al. 2020) and exporting them into the apoplast (Frei dit Frey et al. 2012). This homeostasis is then used to quickly transduce a signal by opening channels to create a rapid influx of cytosolic Ca^{2+}. The ions act as a second messenger by interacting with so-called calcium-binding proteins to regulate downstream defence reactions (Lecourieux et al. 2006). The homeostasis is reestablished via transmembrane transporters (Demidchik et al. 2018), giving the Ca^{2+} signature a transient nature. The precise duration, frequency and intensity of the Ca^{2+} signal are dependent on the elicitor detected and are decoded to mount specific answers to the challenge faced (Hashimoto and Kudla 2011). Being one of the earliest signalling mechanisms in plant immunity, the detection of the Ca^{2+} influx is a vital tool for researchers to determine whether an immune reaction is taking place. The detection of a Ca^{2+} influx can easily be inferred by measuring the external pH value of the apoplast because the transport of Ca^{2+} across the plasma membrane coincides with a pH shift in the extracellular matrix (Felle 2001; Felix et al. 1993). This is caused by the depolarization of the plasma membrane. While Ca^{2+} ions are transported into the cell, anions are transported out of the cell into the apoplast. The organic acid anions

entering the apoplast react with the present H^+ protons and cause an increase in the external pH (Felle et al. 2000). This phenomenon explains the quick and transient increase in pH. Additionally, the plants can also alkalize the external medium for elongated periods to inhibit the pathogens' advances by decreasing the activity of cell wall digesting enzymes (Felle 2001). Yet, the alkalization of the medium as the defence reaction exhibits a delayed onset when compared to the transient increase caused by the Ca^{2+} influx.

1.2.3 Reactive oxygen species – ROS

Another way the plant employs to signal stress and deal with invading pathogens is the use of Reactive Oxygen Species (ROS) which are a group of molecules that derive from O_2 that serve multiple functions in the organism. While ROS like superoxide (O_2^-), hydrogen peroxide (H_2O_2), singlet oxygen ($^1O_2$) and hydroxyl radicals (OH^-) are generated during photosynthesis, an accumulation of these ROS can be very damaging to the cell. These molecules are very reactive and can attack proteins, lipids in the membrane and nucleic acids thus causing irreversible damage (Gill and Tuteja 2010). Therefore the generation of ROS and antioxidants is tightly regulated to contain the potential damage they might cause (Foyer 2018).

Yet, ROS have also gained attention via their involvement in the signalling of abiotic and biotic stresses. ROS are used as a signal to infer systemic responses to wounding, salt stress, cold and heat by travelling through the apoplast of *Arabidopsis thaliana* (Miller et al. 2009). When plants suffer salinity stress, a lack of H_2O can endanger the balance of ROS and antioxidants, causing an accumulation of ROS (Parida and Das 2005) that can also be measured inside plant suspension cells (Ismail et al. 2012). During an immune reaction of the plant, the generation of ROS can function both as a signal (Lee et al. 2020) and the defence reaction itself (Keppler 1989; Peng 1992; Lamb and Dixon 1997). Detection of a PAMP by a Pattern Recognition Receptor (PRR) located at the plasma membrane of the cell causes a BIK1-mediated phosphorylation, thus activating the membrane-bound NADPH oxidase (Li et al. 2014), an enzyme that produces ROS into the apoplast. This process is entirely dependent on the presence of Ca^{2+} ions and is inhibited when the Ca^{2+} influx is blocked (Kadota et al. 2015). The transient ROS burst as a signal can be fine-tuned and regulated by the phosphorylation and dephosphorylation of the C-terminus of the NADPH oxidase by several kinases (Lee et al. 2020), amplifying the significance of the ROS burst as an important signal

in defence reactions. The oxidative burst has been shown to be a signal for Hypersensitive Response (HR) associated Programmed Cell Death (PCD) and differs in intensity when different elicitors are detected (Lamb and Dixon 1997; Chang and Nick 2012). An elongated increase in extracellular ROS with later onset is considered to be part of the defence mechanism. With an increase in ROS in the apoplast the plant can inhibit the growth of pathogenic bacteria and fungi (Keppler 1989; Peng 1992).

As can be seen in the interaction of Ca^{2+} and ROS, there is crosstalk between different signalling pathways, which can facilitate a fine-tuning of the resulting defence reaction, like Programmed Cell Death (PCD).

1.2.4 Hypersensitive Response and Programmed Cell Death

While the detection of Pathogen Associated Molecular Patterns (PAMP) by the plant results in a broad basal defence reaction, the detection of effectors, deployed by the pathogens to quench the basal defence reaction, results in a more specific and intense defence reaction of the host plant (Jones and Dangl 2006; Jones et al. 2016). Effector Triggered Immunity (ETI) shares many characteristics with PAMP Triggered Immunity (PTI) like the signalling pathways engaged and the defence mechanisms deployed, yet differing in sequence, frequency and intensity (Thomma et al. 2011). While not entirely exclusive to it, the so-called Hypersensitive Response (HR) is characteristic of the ETI (Jones and Dangl 2006; Boutrot and Zipfel 2017). The HR oftentimes culminates in the plant cells initiating Programmed Cell Death (PCD) (Balint-Kurti 2019). At first glance, this may seem counter-intuitive, for plant cells detecting a pathogen to simply kill themselves. Yet, in the context of the entire plant tissue, the sacrificing of local cells inhibits the advancement of the pathogen at the site of detection, while the surrounding tissue engages defence mechanisms to contain the potential spread of the pathogen. Certain genotypes of *Vitis vinifera sylvestris* have proven to locally accumulate stilbenes to restrict the advancement of a fungal pathogen (Khattab et al. 2021). The upstream regulation of the HR PCD includes the influx of Ca^{2+} ions (Atkinson et al. 1990) and the generation of Reactive Oxygen Species (ROS) (Chang and Nick 2012).

The association of PCD with the immune response of the plant cell can be exploited to screen for immunoactivity in plants. If the immunoactivity of a given substance or treatment was to be evaluated, a plant tissue or suspension cell line could be treated

accordingly with subsequent quantification of a resulting mortality rate to get first insights, into whether an HR reaction could be taking place.

PCD is a very local response to pathogen invasion and often coincides with the generation of defence compounds in the directly affected and nearby tissues. The generation of these secondary metabolites and other defensive preparations can be regulated via gene expression.

1.2.5 Gene expression of defence-related genes

To mount a successful defence response against an invading pathogen the attacked plant initiates the expression of a myriad of defence-related genes. The finely-tuned regulation thereof is integral to appropriately answering the challenge posed by the encroaching pathogen. Phytoalexins are secondary metabolites plants synthesize to defend themselves when a pathogen attack is recognized. The word "phytoalexin" originates from the Greek words "phyto", which means "plant" and "alekin" which translates to "to defend". Phytoalexins are a varied group of metabolites that are not chemically closely defined and span several classes like flavonoids and alkaloids. In *Vitis* species, a group of important phytoalexins is the stilbene family. When attacked by a fungus, a resistant species of *Vitis* engaged a local Hypersensitive Response (HR) with Programmed Cell Death (PCD) and an accumulation of stilbenes in the surrounding tissue to hinder the advance of the pathogen (Khattab et al. 2021). An early step in the synthesis of stilbenes is the activity and expression induction of the Phenylalanine Ammonia Lyase (PAL). This enzyme catalyses the conversion of phenylalanine towards t-cinnamic acid and thus commits it towards the phenylpropanoid pathway. Several metabolic steps later an entire family of STilbene Synthases (STS) facilitates the synthesis of the members of the stilbene family (Vannozzi et al. 2012). In *Vitis,* the number of members in the STS family is unusually large (Parage et al. 2012) with 48 members of which 32 are potentially functional. This redundancy is likely explained by differences in the promoter region of the different stilbene synthases, which enable the plant to precisely regulate the expression of the enzymes. In this work, we quantified the gene expression of PAL, STS27 and STS47 to evaluate the effects on the phenylpropanoid pathway and the synthesis of phytoalexins. STS47 is the stilbene synthase that catalyzes the generation of trans-resveratrol. Trans-resveratrol is believed to exhibit beneficial effects on human health and to partially be responsible for the French paradox (Catalgol et al. 2012).

Two phytohormones that play pivotal roles in the signalling of abiotic and biotic stresses alike are Salicylic Acid (SA) and Jasmonic Acid (JA). Both hormones are involved in the regulation of plant physiology in response to salt-, UV- and drought stresses while cross-talking with other phytohormones (Aftab and Yusuf 2021). These stress hormones are also involved in the signalling of biotic stressors like pathogens. The SA signalling pathway is said to be the major pathway employed in the detection of biotrophic pathogens, while JA signalling indicates the presence of herbivores or necrotrophs (Glazebrook 2005; Thaler et al. 2012). The interaction of phytohormones with different signalling mechanisms, transcription factors and the crosstalk between them results in a complex web of interconnection. To get insight into what signalling pathways are being engaged by the detection of an elicitor or to see where a potential effector might influence the defence reaction of a host plant, it is necessary to monitor the activity of hormone-related signalling.

In the signalling pathway of jasmonate, the transcription factor JASMONATE ZIM-domain (JAZ) acts as a repressor for the JA-dependent genes. If JA is conjugated to isoleucine (JA-Ile), it is bound by the receptor CORONATINE INSENSITIVE 1 (COI1) (Xie et al. 1998). COI1 is forming an SCF complex together with SKP1 and CULLIN which ubiquitinates JAZ repressors that are subsequently degraded via the 26S proteasome (Chini et al. 2007; Thines et al. 2007), relinquishing the repression of the JA-dependent genes. Among the genes activated by the degradation of JAZ is the gene encoding for JAZ, ensuring the JA signalling pathway negatively regulates itself, shutting down the gene expression once the JA signal subsides (Chung et al. 2008; Chico et al. 2008). Therefore, the expression of JAZ can be used as an indicator of JA signalling taking place and is commonly used as a marker gene to quantify JA-dependent stress signalling.

In many plants, the hormone Salicylic Acid (SA) is the main agent conferring the so-called Systemic Acquired Resistance (SAR). After a local detection of a pathogen, SA is synthesized and dispersed in the plant tissues. Neighbouring cells, detecting the SA induce the expression of defence-related genes to engage defence mechanisms to prepare for the containment of an invading pathogen (Tripathi et al. 2019). Very characteristic of SA signalling is the induction in gene expression of the abundant Pathogenesis-Related protein 1 (PR1) (Cameron et al. 1999) which exhibits antimicrobial effects (Gamir et al. 2017). A high level of salicylic acid SA can also be

detected during the Hypersensitive Response (HR) and the associated Programmed Cell Death (PCD) (Brodersen et al. 2005). This makes the gene expression of PR1 a suitable indicator of both SA signalling and HR-associated PCD taking place.

1.2.6 Immunity priming

Innate immunity differs vastly between animal and plant species. Higher animals have evolved specialized cells to protect their organisms from invading pathogens: T- and B-lymphocytes. These cells fight off the pathogen and create antigen- and thus pathogen-specific antibodies to help fight off repeat infections. This adaptive system does not exist in plants. With some exceptions, every single cell in a plant is inherently capable of a defence reaction (Nürnberger et al. 2004). The escalating levels of pathogen recognition and evasion thereof by the aggressor are established on an evolutionary time scale. But since the immune systems between animals and plants differ in this regard, a simple "vaccination" of plants against invading pathogens is not possible.

Previous work has shown that a preceding stimulus that activates the defence reaction of a plant can enhance the immune response of a subsequent attack (Mauch-Mani et al. 2017). This is likely due to certain transcription factors already being present, changed states of phosphorylation and/or changes in intracellular concentrations of second messengers. Should a pathogen attack during this elevated state of alertness, the resulting immune response of the plant would be faster and stronger. Since the interaction between a susceptible plant and its pathogen is very dependent on timing, a quicker response of the host could render the plant resistant to a pathogen it would generally be susceptible to. The plant mounts a strong defence reaction before the pathogen can deploy its effectors to quench the immune response of the plant. For this phenomenon, coined "priming", to occur it does not matter, whether the stimulus triggering the first and low-key defence reaction originates from a pathogen, beneficial microbes or abiotic signals (Mauch-Mani et al. 2017).

The exploitation of this phenomenon harbours great potential for a sustainable plant protection system. A substance priming the immune system of the plant is likely recognized by a receptor of the host cell. This implies two beneficial mechanisms: Firstly, receptors are very specific, thus it is unlikely that other organisms have the same reaction when treated with the same compound. This considerably decreases the likeliness of undesired side effects on the ecosystem, if this plant protection would

be applied in the field. Secondly, signals detected by a receptor are oftentimes amplified by the use of second messengers or signalling cascades ensuring that the detection of mere traces of a pathogen can trigger a suitable defence reaction mounted by the host cell. This would imply that low concentrations of the priming substance would suffice to create the desired effect, further decreasing the chance of unintended side effects.

1.3 Microfluidics

Curiosity has always been a driving factor for our species, always seeking to understand our environment and ourselves better. The foundation of the ever-evolving modern scientific method was conceived in the 17th century and relies on the abstraction of phenomena observed in the environment to deliberately adjust specific conditions of the system to observe and measure the effect. With the advancement of technology, humans have developed new ways to simulate and manipulate natural phenomena to explore their secrets. Microfluidics is a technology that can create desired microenvironments to enable high-throughput experiments that are easy to reproduce. It is a technique to create specific environments for experiments by miniaturizing a setup to handle small volumes of liquids to enable in vitro observation from single cells to small organisms exposed to finely tuned stimuli defined by the design of the microfluidic system (Sanati Nezhad 2014; Frey et al. 2022). The microfluidic systems are constructed using moulding or drilling of plastics and the flow of liquids through the system can be tightly regulated by the use of precision pumping devices and computer-assisted handling of valves. Their size and the use of specific materials can enable the observation of samples within the microfluidic system during the entire duration of the experiment.

In the recent past microfluidics have been used to facilitate laborious and time-intensive experiments and therefore increase the possible frequency of observations. Subendran et al. (2021) constructed chambers housing single larvae of the zebrafish *Danio rerio*. The chambers were designed to fix the larvae in place and to be able to continuously observe the hydrodynamics of the beating of its tail. The embryos of *Drosophila melanogaster* are a well-established model organism but are difficult to handle in large quantities due to their minuscule size. Shorr et al. (2019) designed a microfluidic device that automatically arranged large numbers of *D. melanogaster* embryos in a defined orientation, lined them up and applied equal mechanical pressure on all of them at once to observe the resulting gene expression. With classical methods, the arranging and treatment of an equal amount of embryos would have consumed a large amount of labour and would be subject to increased variations and errors due to handling. Lagoy and Albrecht (2015) conducted behavioural studies on *Caenorhabditis elegans* using microfluidics. They constructed large chambers hosting multiple individuals of *C. elegans* and used the finely controlled flow of mediums containing attractants to observe the chemotaxis of the species. Using a different

design of a chamber, they were able to determine the neuronal activity of the worms during the experiment by using transgenic individuals of the strain CX14887 and fixing the animal in place. The strain visualizes neuronal activity with a fluorescent signal. van Treuren et al. (2019) designed a microfluidic system to observe the relationship between the sea anemone *Exaiptasia pallida* and its algal symbiont. The expulsion of the algae by *E. pallida* due to external stressors is a major cause of catastrophic coral bleaching. Using their experimental design, they were able to fix larvae of *E. pallida* in traps build into the design of their microfluidic system and expose them to different environmental stressors to see, how they induce the algal expulsion. An ingenious design by Iftikhar et al. (2021) used precise flow rates and pressures established by microfluidics to create droplets containing singular fungal spores and a substance with supposed anti-fungal activity to quantify the sporulation and fungal growth inhibition caused by the substance of interest. The system was combined with an automatic observation system to evaluate the effect on many spores simultaneously.

In the plant sciences, there are microfluidic systems that enable the incubation and germination of multiple seeds of *Arabidopsis thaliana*. These systems were designed to enable the constant observation, quantification and evaluation of the growth of the root system or the shoot respectively (Busch et al. 2012; Jiang et al. 2014). Agudelo et al. (2013) designed a microfluidic system that facilitates the observation of tip-growing cells. The system was constructed to research the behaviour and chemotaxis of the pollen tube of plants, but its use could easily be extended to host other tip-growing cells like fungal hyphae. Using an intricate chip design, Allan et al. (2022) were able to fix a plant root into a microfluidic system. Installing two sets of in- and outlet in the chamber, on either side of the root, the researchers were able to create two separate flows of the medium on the two sides of the root and treat these with differing concentrations of NaCl or PEG. They subsequently observed how the resulting stress signal is transferred vertically along the length of the root and horizontally from the epidermis into the central cylinder. This one-sided treatment of the root was only achievable by microfluidics. In preliminary tests, Allan et al. (2022) were able to find flow control parameters so that the two separate streams in the microfluidic systems showed virtually no turbulences.

The Microfluidic BioReactor (MBR) is a miniaturized cell containment unit, that can hold 800 µL of plant cell suspension. The cell chamber is separated via a semi-permeable membrane from a perfusion chamber that is supplied with a liquid medium using a peristaltic pump. This system has been used before by Finkbeiner et al. (2022) to research the interaction between plant cells cultivated in separated MBRs connected via a flow of a medium. They used two MBRs containing the same cell suspension at different densities to detect a possible proliferation factor, secreted by the high-density cells to induce proliferation in the low-density culture. In many metabolic pathways, subsequent steps in the catalyzation of a given compound are separated by compartmentalization either within organelles of the same cell or between different tissues of the plant. Finkbeiner et al. (2022) were able to artificially establish a similar system by cultivating two strains of *Catharanthus roseus* that differed in their metabolic activity. Installed in a circular MBR system the combination of the cell lines was able to generate a metabolite, that each cell strain was not able to produce when cultivated alone.

1.4 Scope of the study

The nature of a symbiotic relationship between two species essentially depends on the communication between the partners. A parasitic symbiosis equates to a signalling warfare between the invading pathogen and the defending host. The host plant can detect microbial patterns as a signal of an impending attack, while the aggressor simultaneously aims to avoid detection by changing or disguising the recognized signal. In the offensive, the attacking microbes can deploy effectors to act as signals within the host cells to manipulate their defensive signalling to aid their virulence by quenching the immune response or by deliberately inducing responses that benefit the pathogen.

In this work, we aim to prove this concept by investigating whether bioactive metabolites of *Roesleria subterranea* act as a signal in suspension cell lines of certain *Vitis* lines. Our project partner at the ibwf in Mainz isolated metabolites of *R. subterranea* that proved to inhibit the sporulation of fungal spores. Our institute investigated the effects of these metabolites, Sclerodin and the Acetonadduct of Entatreventinon on the immune response and the cytoskeleton of different *Vitis* cell lines to test whether the compounds act as a signal and to elucidate the potential mode of action.

Signals that manipulate the host's immune system without damaging the plant itself have potential use in plant protection by priming the plant's defence capabilities. In this project we aimed to test the feasibility of using Microfluidic BioReactors (MBR) to identify compounds that act as immunoactive signals. The MBRs were originally designed and established by Finkbeiner et al. (2022; Finkbeiner 2019). Our project partner at the IMT of the Karlsruher Institut für Technologie, Leona M. Schmidt-Speicher, improved the design of the MBR and developed new methods to facilitate the detection of immune reactions of plant cells cultivated within. The feasibility of methods to measure the pH and the H_2O_2 concentration of the cultivated cell suspension was to be tested and the results were to inform further design improvements. Establishing and streamlining methods to non-invasively measure the immune response of plant cells cultivating within an MBR could render the MBR a potent high-throughput system to analyze the reaction of plant cells to substances of interest added to the liquid medium supplied to the microfluidic system. Additionally, the capabilities of the MBR system were to be expanded to be able to cultivate fungal

cell cultures to potentially co-cultivate plant and fungal cells within the same microfluidic system and quantify the reactions of the cell lines to the presence of the other culture.

This work aimed to make progress in the field of using the MBR system to streamline the search for immunoactive compounds that can strengthen the inherent defence capabilities of crop plants by triggering a defence reaction without damaging the plant. This causes certain components of the signalling and defence system to already be active, should an actual pathogen attack. This effectively increases the intensity and speed of the defence reaction, priming the plant to successfully fend off the invader. Using immunoactive substances to treat plants, implies the involvement of receptors recognizing the compound, thus minimizing the potential for unintended side effects on the ecosystem.

2. Materials

2.1 Cell lines

2.1.1 *Vitis vinifera* Chardonnay

In our work, the cell line *Vitis vinifera* cv. Chardonnay (Chardonnay) represented the cultivated grapevine in most experimentation. Chardonnay is a grapevine that was bred for maximized yield and taste of the wine for which it is used. This focus on efficiency and economic profit led to certain deficiencies of the plant, including the inherent immune strength and resistance of the vine. As a result of climate change, plants are challenged with new stresses like heat, drought and invading pathogens. To research the mechanisms plants use to combat these challenges it is imperative to compare plants, showing certain resistances, to plants, that are susceptible to the challenge, and identify the differences. The Chardonnay cell suspension was created by Czemmel et al. (2009) using the modified protocol from Bao Do and Cormier (1991). The cell line originates from a petiole callus and does not produce functional chloroplasts. The development thereof is halted at the proplastid stage. The wild-type of the Chardonnay line was cultivated in standard MS medium (see Chapter 2.2) without antibiotics. The cell suspension was kept on orbital shakers at 150 rpm, in the dark and at 26°C ambient room temperature. Chardonnay was subcultivated every seven days by transferring 5 mL of carry-over volume from the mother culture into 30 mL fresh MS medium.

2.1.2 *Vitis vinifera sylvestris* Ke15

Vitis vinifera sylvestris Ke15 (Ke15) is an accession of wild grapevine collected on a peninsula near Ketsch, Germany. Straightening of the Rhine river and general agricultural land use has diminished the habitat of wild grapevines to a few habitats strewn across Europe. Since the wild grapevine has been bred over numerous generations into the productive cultivars we know today, their wild relatives might be a well of resistances that the cultivars lost during their domestication. During a conservation project, multiple grapevine accessions were collected on the Ketsch peninsula and were established in the botanical garden of the KIT and screened for notable reactions to biotic and abiotic stressors. In previous work, the genotype Ke15 arose with high resistance against downy mildew and *Neofusicoccum parvum* linked to a proficient stilbene synthesis (Duan et al. 2015; Khattab et al. 2021). A cell suspension line of Ke15 was established and cultivated using a standard MS medium without antibiotics. The cell suspension was kept on an orbital shaker at 150 rpm, in

the dark at 26°C room temperature. Ke15 was subcultivated every seven days by transferring 7.5 mL carry-over volume from the mother culture into 30 mL of fresh MS-medium.

2.1.3 *Vitis rupestris*

The North American wild grapevine *Vitis rupestris* has a long history of co-evolution with many American pathogens that cause havoc in the European vineyards and has therefore developed resistance against them. *V. rupestris* shows a quick and intense cell death response upon elicitation with harpin (Chang and Nick 2012) implying an efficient Effector-Triggered Immunity (ETI) response of the vine. Due to these qualities, *V. rupestris* was used in our work to represent inherently resistant plants. A suspension cell line of the grapevine was created by inducing calli on young shoot cuttings and transferring the cells into a liquid medium (Seibicke 2002). The *V. rupestris* cell line was cultivated using a standard MS medium without antibiotics. The cells were cultivated on an orbital shaker at 150 rpm, in the dark and at 26°C room temperature. The suspension needed to be subcultivated every seven days by transferring 7.5 mL carry-over volume from the mother culture into 30 mL of fresh MS-medium.

2.1.4 BY2: *Nicotiana tabacum* Bright Yellow 2

Nicotiana tabacum is a member of the Solanaceae family and thus not closely related to the *Vitis* species we observed in this work. Yet, *N. tabacum* is a well-established model organism in plant cell biology and especially in our lab. In this work, the *N. tabacum* suspension cell line BY2 (Nagata et al. 1992) was used as a control for the methods used and in the case of the experimentation with the Microfluidic BioReactor (MBR), the cell line replaced the *Vitis* cell lines entirely due to an apparent incompatibility of *Vitis* with the MBR system (see Fig. 17). The cell line was created in 1972 from a callus induced on a *Nicotiana tabacum* seedling (Nagata et al. 1992) and propagated since. *Agrobacterium fabrum*-mediated transformation of this cell line is comparably quick, easy and well-established in our group. The wild-type of BY2 was cultivated in a standard MS medium containing no antibiotics or additives. To propagate the cell line, 1.5 mL of carry-over volume was transferred from the mother culture into 30 mL of fresh MS medium.

2.1.5 BY2 MYB14::gfp

This cell line resulted from experimentation to create a cell line that produces a green-fluorescent signal once its immune response is triggered (see Chapter 8.1). To achieve this, a construct was generated in which the gene for the Green Fluorescent Protein (GFP) was regulated by the promoter MYB14 from *Vitis vinifera,* a transcription factor which regulates the expression of biosynthesis genes of stilbenes (Höll et al. 2013; Duan et al. 2016). This gene construct was introduced into BY2 cells via *Agrobacterium fabrum* transformation. The construct contains a selective antibiotic resistance to hygromycin; therefore the transgenic cell line was cultivated in MS-medium containing 30 µg/mL hygromycin. The cell culture was cultivated on an orbital shaker at 150 rpm, in the dark at 26°C. It needed to be subcultivated every seven days by transferring 1.5 mL of the mother culture into 30 mL of fresh MS medium containing hygromycin. The cell line showed a slight baseline expression of GFP and no induction of expression under biotic or abiotic stress exposure (see sFig. 9)

2.1.6 BY2 TuA3::GFP

This cell line originates from the work of Kumagai et al. (2001). *N. tabacum* BY2 cells were transformed via *Agrobacterium* with a fusion construct of *Arabidopsis thaliana* α-tubulin and GFP. This construct contained a kanamycin resistance and was controlled by the constitutive promoter CaMV 35S, effectively labelling the microtubules of the plant cell with GFP with little to no impact on the vigour of the cell culture. This cell line is well-established in our institute. The cell culture is subcultivated weekly by transferring 1.5 mL of seven-day-old cells into 30 mL of fresh MS medium containing 100 µg/mL kanamycin in a 100 mL Erlenmeyer flask. The cell culture is cultivated at 26°C, in the dark while shaking on an orbital shaker at 150 rpm.

2.1.7 Chardonnay FABD$_2$-GFP

This cell line was generated by Guan et al. (2014) and transformed a wild-type of *Vitis vinifera* cv. Chardonnay cell line via *Agrobacterium fabrum* with a fusion construct of GFP and the Fimbrin Actin-Binding Domain 2 (FABD$_2$) of *Arabidopsis thaliana*. This construct is controlled by a 35S promoter and contains a resistance cassette to kanamycin. The constitutively expressed fusion protein effectively labels the actin filament in the living cell, with only little impact on the vigour of the cell line. The cell line is cultivated at 26°C, in the dark while shaking at 150 rpm on an orbital shaker. To propagate the cell line, 10 mL of seven-day-old cells are transferred into a 100 mL

Erlenmeyer flask containing 30 mL of fresh MS medium containing 30 µg/mL kanamycin.

2.2 Media

All cell lines observed in this work were cultivated in a medium henceforth referred to as MS medium. MS medium contains 4.3 g/L Murashige and Skoog salts (see Table 2), 30 g/L D(+)-Saccharose (see Table 2), 200 mg/L KH_2PO_4 (see Table 2), 100 mg/L Myo-Inositol (see Table 2), 1 mg/L thiamine (see Table 2) and 0.2 mg/L 2,4-Dichlorophenoxyacetic acid (see Table 2). 10 mg/mL of thiamine and 2,4-D were pre-solved in water and ethanol, respectively. After diluting all components in filtered water, the pH was adjusted to pH 5.8 using 1 M KOH. The MS-medium was divided into aliquots of 30 mL in 100 mL Erlenmeyer flasks (alternatively 15 mL in 50 mL flasks) and capped off with aluminium foil. These filled flasks were autoclaved at 121°C for 15-20 minutes. For transgenic lines, selective antibiotics were added at the time of subcultivation.

The following table contains the composition of all media used in the course of this work.

Table 1: Composition of media used in this work

application	name	composition
gel electrophoresis	0.5 % TAE Buffer	20 mM TRIS, 500 nM EDTA, ph=8.3
gel electrophoresis	5x loading buffer	1 mg/mL Bromophenol blue-Xylenecyanol in 50 % H_2O, 50 %glycerol
general	Evans Blue Solution	2.5% (w/v) Evans Blue in ddH_2O
general	LB-Medium	25 g/L LB-medium (Tryptone 10 g/L, Yeast extract 5 g/L, NaCl 10 g/L, pH=7.0) in ddH_2O
general	MS-medium	4.3 g/L Murashige-Skoog salts, 30 g/L D(+)-Saccherose, 200 mg/L KH_2PO_4, 100 mg/L Myo-Inosiltol, 1 mg/L thiamine, 0.2 mg/L 2,4 Dichlorophenoxyacetic acid
general	PDA plates	39 g/L Potatoe Dextrose Agar in ddH_2O
transformation	0.6 M mannitol	0.6 M (D)-Mannitol in ddH_2O
transformation	enzyme solution	1.5 % (w/v) cellulase-RS, 0.75% (w/v) macerozyme-R10, 0.6 M mannitol, 20 mM MES, 10 mM KCl, 10 mM $CaCl_2$, 0.1 % (w/v) BSA in ddH_2O
transformation	MMG solution	4 mM MES, 0.4 M mannitol, 15 mM MgCl in ddH_2O
transformation	Paul's medium	4.3 g/L Murashige-Skoog basal salts, 1 % (w/v) sucrose in ddH_2O, pH=5.8 (adjusted with KOH)
transformation	Paul's medium plate	4.3 g/L Murashige-Skoog basal salts, 1 % (w/v) sucrose in ddH_2O, pH=5.8 (adjusted with KOH), 0.5 % Phytagel
transformation	PEG solution	40 % (w/v) PEG4000, 0.2 M mannitol, 0.1 M $CaCl_2$ in ddH_2O
transformation	W1 solution	0.5 M mannitol, 20 mM KCl, 4 mM MES in ddH_2O
transformation	W5 solution	2 mM MES, 154 mM NaCl, 125 mM $CaCl_2$, 5 mM KCl in ddH_2O

2.3 Chemicals and consumables

The following tables contain lists of chemicals and consumables used in the experiments of this project.

Table 2: Chemicals used in the project

application	name	Company
cDNA	Oligo (dT) primer	Thermo Fisher Scientific GmbH, Im Heiligen Feld 17, 58239 Schwerte, Germany
cDNA	Reverse transcriptase buffer	New England Bioloabs GmbH, Brüningstraße 50, 65926 Frankfurt am Main, Germany
cDNA	RNase inhibitor, murine	New England Bioloabs GmbH, Brüningstraße 50, 65926 Frankfurt am Main, Germany
gel electrophoresis	Agarose NEEO ultra-quality	Carl Roth GmbH+Co.KG, Schoemperlenstraße 3-5, 76185 Karlsruhe, Germany
gel electrophoresis	Midori Green Xtra	Nippon Genetics Europe GmbH, Mariaweilerstraße 28-30, 52349 Düren, Germany
general	10x PCR Buffer	New England Bioloabs GmbH, Brüningstraße 50, 65926 Frankfurt am Main, Germany
general	2,4-Dichlorophenoxyacetic acid	Carl Roth GmbH+Co.KG, Schoemperlenstraße 3-5, 76185 Karlsruhe, Germany
general	96% Ethanol	VWR, John-Deere-Straße 7, 76646 Bruchsal, Germany
general	$AlCl_3$	Carl Roth GmbH+Co.KG, Schoemperlenstraße 3-5, 76185 Karlsruhe, Germany
general	chitosan	Sigma-Aldrich Chemie GmbH, Kappelweg 1, 91625 Schnelldorf, Germany
general	cis-hexenal	Sigma-Aldrich Chemie GmbH, Kappelweg 1, 91625 Schnelldorf, Germany
general	D(+)-Saccherose	Carl Roth GmbH+Co.KG, Schoemperlenstraße 3-5, 76185 Karlsruhe, Germany
general	Danish agar	Carl Roth GmbH+Co.KG, Schoemperlenstraße 3-5, 76185 Karlsruhe, Germany
General/qPCR	dNTP mix	BioCat GmbH, Im Neuenheimer Feld 584, 69120 Heidelberg, Germany

Materials

general	Evans-Blue	Sigma-Aldrich Chemie GmbH, Kappelweg 1, 91625 Schnelldorf, Germany
general	flg22	GeneScript Biotech, Treubstraat 1, 2288EG Rijswijk, Netherlands
general	Hygromycin	Carl Roth GmbH+Co.KG, Schoemperlenstraße 3-5, 76185 Karlsruhe, Germany
general	Kanamycin	Carl Roth GmbH+Co.KG, Schoemperlenstraße 3-5, 76185 Karlsruhe, Germany
general	KH_2PO_4	Merck KGaA, Frankfurter Straße 250, 64293 Darmstadt, Germany
general	LB-medium	Carl Roth GmbH+Co.KG, Schoemperlenstraße 3-5, 76185 Karlsruhe, Germany
general	MeJA	Sigma-Aldrich Chemie GmbH, Kappelweg 1, 91625 Schnelldorf, Germany
general	Methanol	Carl Roth GmbH+Co.KG, Schoemperlenstraße 3-5, 76185 Karlsruhe, Germany
general	$MgCl_2$	Thermo Fisher Scientific GmbH, Im Heiligen Feld 17, 58239 Schwerte, Germany
general	Murashige-Skoog basal salts	Duchefa Biochemie B.V, A. Hofmanweg 71, 2031 BH Haarlem, Netherlands
general	Myo-Inositol	Duchefa Biochemie B.V, A. Hofmanweg 71, 2031 BH Haarlem, Netherlands
general	NaCl	Carl Roth GmbH+Co.KG, Schoemperlenstraße 3-5, 76185 Karlsruhe, Germany
general	NaN_3	Carl Roth GmbH+Co.KG, Schoemperlenstraße 3-5, 76185 Karlsruhe, Germany
general	nuclease-free water	Lonza Group Ltd, Am Rinnentor 13, 64625 Bensheim, Germany
general	Phytagel	Duchefa Biochemie B.V, A. Hofmanweg 71, 2031 BH Haarlem, Netherlands
general	Rifampicin	Carl Roth GmbH+Co.KG, Schoemperlenstraße 3-5, 76185 Karlsruhe, Germany
general	Streptomycin	Sigma-Aldrich Chemie GmbH, Kappelweg 1, 91625 Schnelldorf, Germany

Materials

general	thiamine	Merck KGaA, Frankfurter Straße 250, 64293 Darmstadt, Germany
general	Zeocin	VWR, John-Deere-Straße 7, 76646 Bruchsal, Germany
transformation	BSA	Carl Roth GmbH+Co.KG, Schoemperlenstraße 3-5, 76185 Karlsruhe, Germany
transformation	CaCl$_2$	Carl Roth GmbH+Co.KG, Schoemperlenstraße 3-5, 76185 Karlsruhe, Germany
transformation	celluase-RS	Duchefa Biochemie B.V, A. Hofmanweg 71, 2031 BH Haarlem, Netherlands
transformation	D(-)-Mannitol	Carl Roth GmbH+Co.KG, Schoemperlenstraße 3-5, 76185 Karlsruhe, Germany
transformation	KCl	Carl Roth GmbH+Co.KG, Schoemperlenstraße 3-5, 76185 Karlsruhe, Germany
transformation	macerozyme-R10	Yakult Deutschland GmbH, Forumstraße 2, 41468 Neuss, Germany
transformation	MES	Carl Roth GmbH+Co.KG, Schoemperlenstraße 3-5, 76185 Karlsruhe, Germany
transformation	PEG4000	Carl Roth GmbH+Co.KG, Schoemperlenstraße 3-5, 76185 Karlsruhe, Germany
qPCR	SYBR-Green	Biozym Scientific GmbH, Steinbrinksweg 27, 31840 Hessisch Oldendorf, Germany
qPCR	GoTaq Buffer	Promega GmbH, Gutenbergring 10, 69190 Walldorf, Germany
cell mortality	harpin	Yves Kessler Vegetationstechnik Garten- & Landschaftsbau GmbH, St.-Michael-Straße 16, 82319 Starnberg, Germany

Table 3: Consumables used in this project

application	name	company
general	Cellstar Cell Culture Dishes, PS, 35x10mm, with vents, sterile	Greiner Bio-One GmbH, Maybachstraße 2, 72636 Frickenhausen, Germany
general	pipette tips 10 µL	Diagonal GmbH & Co. KG, Havixbeckerstraße 62, 48161 Münster, Germany
general	pipette tips, 1000 µL	Diagonal GmbH & Co. KG, Havixbeckerstraße 62, 48161 Münster, Germany
general	pipette tips, 200 µL	Diagonal GmbH & Co. KG, Havixbeckerstraße 62, 48161 Münster, Germany
general	Reaction vials Mµlti® SafeSeal assorted colours, 0.5 ml	Carl Roth GmbH+Co.KG, Schoemperlenstraße 3-5, 76185 Karlsruhe, Germany
general	Round filters ROTILABO®	Carl Roth GmbH+Co.KG, Schoemperlenstraße 3-5, 76185 Karlsruhe, Germany
general	Sealing film PARAFILM®, 100 mm	Carl Roth GmbH+Co.KG, Schoemperlenstraße 3-5, 76185 Karlsruhe, Germany
MBR	3M™ Greenback Printed Circuit Board Tape 851, Green,	3M Deutschland GmbH, Carl-Schurz-Strasse 1, 41453 Neuss, Germany
MBR	Dispensing needle interior-Ø 0.15mm	MARTIN GmbH, Industriestrasse 17, 82110 Germering, Germany
MBR	Luer hose connectors ROTILABO®, Female / hose inner Ø 1.6 mm	Carl Roth, Schoemperlenstraße 3-5, 76185 Karlsruhe, Germany
MBR	Pump tubing Tygon® LMT 55, 0.13mm Øint, 1.93mm Øext	Tour Saint-Gobain, 12 place de l'Iris, 92400 Courbevoie, France
MBR	SP-HP5-SA	PreSens Precision Sensing GmbH, Am BioPark 11, 93053 Regensburg, Germany
MBR	Tygon 3350 tubing, 1.6mm Øint, 3.2mm Øext, 0.8mm wall thickness	Tour Saint-Gobain, 12 place de l'Iris, 92400 Courbevoie, France
qPCR	96 Well 0.1 mL 8-TubeStrip Platte, reißbar, weiß,	Biozym Scientific GmbH, Steinbrinksweg 27, 31840 Hessisch Oldendorf, Germany
qPCR	96 Well 8-Cap Strip Platte, reißbar, farblos	Biozym Scientific GmbH, Steinbrinksweg 27, 31840 Hessisch Oldendorf, Germany
qPCR	PCR SingleCap 8er-SoftStrips 0.2 mL, farblos	Biozym Scientific GmbH, Steinbrinksweg 27, 31840 Hessisch Oldendorf, Germany
qPCR	SafeSeal SurPhob Spitzen, 100 µL, steril	Biozym Scientific GmbH, Steinbrinksweg 27, 31840 Hessisch Oldendorf, Germany
qPCR	SafeSeal SurPhob Spitzen, 1000 µL, steril	Biozym Scientific GmbH, Steinbrinksweg 27, 31840 Hessisch Oldendorf, Germany
qPCR	SafeSeal SurPhob Spitzen,10 µL, extra lang, steril	Biozym Scientific GmbH, Steinbrinksweg 27, 31840 Hessisch Oldendorf, Germany

2.4 Devices and software

The following tables list devices and software used in this work.

Table 4: Devices used in this project

application	name	company
gel electrophoresis	Invitrogen Sage Imager Blue-Light Transilluminator	Thermo Fisher Scientific GmbH, Im Heiligen Feld 17, 58239 Schwerte, Germany
gel electrophoresis	Mupid One Electrophoresis System	Nippon Genetics Europe GmbH, Mariaweilerstraße 28-30, 52349 Düren, Germany
general	Biomedis Tuttnauer	biomedis Vertriebsgesellschaft mbH, Kerkerader Straße 2, 35394 Gießen, Germany
general	Biometra TSC ThermoShaker	Analytik Jena GmbH, Konrad-Zuse-Straße 1, 07745 Jena, Germany
general	Büchner funnel	Carl Roth, Schoemperlenstraße 3-5, 76185 Karlsruhe, Germany
general	Eppendorf BioPhotometer D30	Eppendorf SE, Barkhausenweg 1, 22339 Hamburg, Germany
general	Eutech EC-PH510	Thermo Fisher Scientific GmbH, Im Heiligen Feld 17, 58239 Schwerte, Germany
general	GFL 3033	LAUDA-GFL: Gesellschaft für Labortechnik mbH; Schluze-Delitzsch-Straße 4; 30938 Burgwedel; Germany
general	IKA KS 260 basic	IKA-Werke GmbH & Co. KG, Janke & Kunkel-Straße 10, 79219 Staufen, Germany
general	Memmert BE 600	Memmert GmbH + Co. KG.; Äußere Rittersbacher Straße 38; 91126 Schwabach; Germany
general	Nanodrop 1000 Spectrophotometer	Peqlab Biotechnologie GmbH, Carl-Thiersch-Straße 2B, 91052 Erlangen, Germany
general	Qiagen 85210 TissueLyser Universal Laboratory Mixer-Mill Disruptor	QIAGEN, Qiagen Straße 1, 40724 Hilden, Germany
general	T100 Thermal Cycler	Bio-Rad Laboratories GmbH, Kapellenstraße 12, 85622 Feldkirchen, Germany
general	Thermo Scientific Maxisafe 2020	Thermo Fisher Scientific GmbH, Im Heiligen Feld 17, 58239 Schwerte, Germany
general	Vacuubrand MZ 2C	Vacuubrand GmbH + co KG, Alfred-Zippe-Straße 4, 97877 Wertheim, Germany

Materials

general	VWR MicroStar 17	VWR International GmbH; Hilpertstraße 20a; 64295 Darmstadt; Germany
MBR	Peristaltic Pump, REGLO Digital Compact, 4-Channel 12-Roller	Cole-Parmer GmbH, Futtererstraße 16, 97877 Wertheim, Germany
MBR	pH-1 SMA HP5	PreSens Precision Sensing GmbH, Am BioPark 11, 93053 Regensburg, Germany
MBR	Spark Multimode Microplate reader	Tecan Group AG, Seestrasse 103, 8708 Männerdorf, Switzerland
microscopy	Zeiss Axio Imager Z1, Apotom, Axiocam 503 mono, HXP120, Power Supply 230	Carl Zeiss AG, Carl-Zeiss-Straße 22, 73447 Oberkochen, Germany
microscopy	Zeiss Axio Observer.Z1, Yokogawa Confocal scanning system CSU-X1	Carl Zeiss AG, Carl-Zeiss-Straße 22, 73447 Oberkochen, Germany
qPCR	CFX Connect Optics Module	Bio-Rad Laboratories GmbH, Kapellenstraße 12, 85622 Feldkirchen, Germany
qPCR	CFX Connect Thermal Cycler	Bio-Rad Laboratories GmbH, Kapellenstraße 12, 85622 Feldkirchen, Germany
transformation	Nalgene reusable bottle top filter	Thermo Fisher Scientific GmbH, Im Heiligen Feld 17, 58239 Schwerte, Germany
transformation	Sorvall LYNX 4000 Superspeed Centrifuge	Thermo Fisher Scientific GmbH, Im Heiligen Feld 17, 58239 Schwerte, Germany

Table 5: Software used in this project

application	name	company
gel electrophoresis	Intas GDS software	INTAS Science Imaging Instruments GmbH, Gustav-Bielefeld-Straße 2, 37079 Göttingen, Germany
general	Fiji ImageJ	https://imagej.nih.gov/ij/
general	OriginPro 2022b	Origin Lab Corporation, One Roundhouse Plaza, Suite 303, Northampton, MA01060, USA
general	Serial Cloner	open source, http://serialbasics.free.fr/Serial_Cloner.html
microscopy	ZenBlue	Carl Zeiss AG, Carl-Zeiss-Straße 22, 73447 Oberkochen, Germany

2.5 Kits and enzymes

The following tables contain lists of kits and enzymes experiments in this work were performed with.

Table 6: Kits used in this project

application	name	company
general	Roboklon Universal RNA Kit	Roboklon GmbH, Kantstraße 65, 10627 Berlin, Germany
MBR	Amplex™ Red Hydrogen Peroxide/Peroxidase Assay Kit	Invitrogen, Thermo Fisher Scientific, Dieselstraße 4, 76227 Karlsruhe, Germany
transformation	Gateway LR Clonase II Enzyme-Mix	Invitrogen, Thermo Fisher Scientific, Dieselstraße 4, 76227 Karlsruhe, Germany
transformation	Roti-Prep plasmid mini	Carl Roth, Schoemperlenstraße 3-5, 76185 Karlsruhe, Germany

Table 7: Enzymes used in this project

application	name	company
cDNA	MuLV-Reverse transcriptase	New England Bioloabs GmbH, Brüningstraße 50, 65926 Frankfurt am Main, Germany
general	Qiagen RNase-Free DNase Set	QIAGEN, Qiagen Straße 1, 40724 Hilden, Germany
general	Taq DNA polymerase	New England Bioloabs GmbH, Brüningstraße 50, 65926 Frankfurt am Main, Germany
qPCR	GoTaq polymerase	Promega GmbH, Gutenbergring 10, 69190 Walldorf, Germany
restriction	AflIII	New England Bioloabs GmbH, Brüningstraße 50, 65926 Frankfurt am Main, Germany
restriction	ClaI	New England Bioloabs GmbH, Brüningstraße 50, 65926 Frankfurt am Main, Germany
restriction	EcoRV-HF	New England Bioloabs GmbH, Brüningstraße 50, 65926 Frankfurt am Main, Germany

2.6   Primers and bacterial strains

The following tables list primers and the bacterial strains used in this project's work.

Table 8: Primers used in this work

name	5'-3' sequence	annealing °C
prMYB14_hoe29_fw	CTACTGACGTGCACTAGCCT	60
prMYB14_hoe29_rv	GCAAGGCGATCCCTATGAATG	60
STS27_fw	CCCAATGTGCCCACTTTAAT	60
STS27_rv	CTGGGTGAGCAATCCAAAAT	60
STS47_fw	TGGAAGCAACTAGGCATGTG	60
STS47_rv	GTGGCTTTTTCCCCCTTTAG	60
UbQ_fw	GAGGGTCGTCAGGATTTGGA	60
UbQ_rv	GCCCTGCACTTACCATCTTTAAG	60
PAL_fw	TCCTCCCGGAAAACAGCTG	60
PAL_rv	TCCTCCAAATGCCTCAAATCA	60
PR1_fw	TGCTAACCAGAGATTGGCCATTG	60
PR1_rv	CGCATCGGTGCCTGTCAATGAA	60
JAZ1_fw	TGCAGTCTGTTGAGCCAATACATA	60
JAZ1_rv	CACGTTTCCGGACTTCTTTACAC	60

Table 9: Bacterial strains used in this project

use	name	company
transformation	*A.fabrum* LB4404	Invitrogen, Thermo Fisher Scientific, Dieselstraße 4, 76227 Karlsruhe, Germany
transformation	*E.coli* DB3.1	Invitrogen, Thermo Fisher Scientific, Dieselstraße 4, 76227 Karlsruhe, Germany
transformation	*E.coli* DH5a	Invitrogen, Thermo Fisher Scientific, Dieselstraße 4, 76227 Karlsruhe, Germany

2.7 *Roesleria subterranea* and its metabolites

Our project partners at the ibwf in Mainz collected a strain of *Roesleria subterranea* (IB-Rüd01-16) on the roots of a grapevine rootstock in a commercial vineyard in Rüdesheim, Germany. The identity of the strain was confirmed by cultivation and subsequent morphological characterization and ITS sequencing (personal communication, Stefan Jacobs, ibwf). They screened the fungal metabolites of the strain for their bioactivity and finally identified and isolated two compounds that proved to inhibit the sporulation of *Magnaporthe oryzae* and *Phytophthora infestans* spores. These compounds are Sclerodin and the AcetonAduct of Entatrevenetinon (AaE). Both chemicals were isolated, lyophilised and sent to our institute to test their effects on the physiology and immune system of plant cells. Upon arrival, both substances were solved in Methanol (MeOH) to create stock solutions of 10 mM each. The stock solutions were stored in the dark at –20°C.
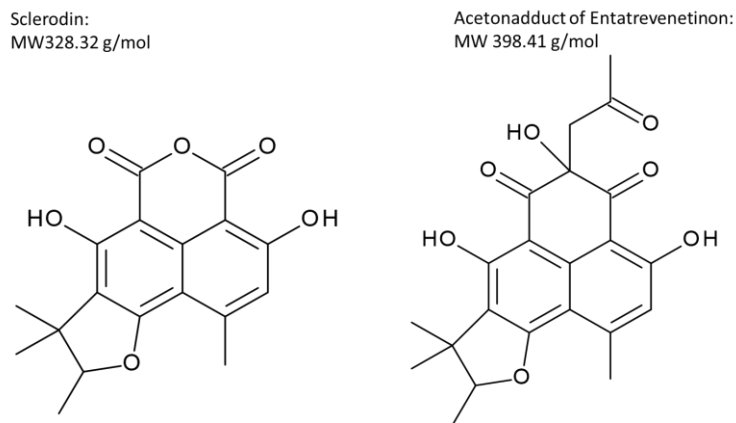

Fig. 1: Structures of Sclerodin and AaE: The structures of Sclerodin and the AcetonAdduct of Entatrevenetinon (AaE) were provided by Stefan Jacob, ibwf Mainz

2.8 Microfluidics: an abstract ecosystem

2.8.1 Microfluidic BioReactor (MBR)

The Microfluidic BioReactors (MBR) originally designed by Finkbeiner et al. (2022) were constructed with two distinct chambers divided by a semi-permeable membrane (pore size 5 µm). The design of the MBRs was further developed and improved by Leona M. Schmidt-Speicher at the Institute of Microstructure Technology (IMT). Plant or fungal cells can be placed into the cell chamber through openings in the top layer. The perfusion (or supply) chamber is connected to two in- and outlets. These outlets can be fitted onto a tubing which connects the MBR to the peristaltic pump and potentially to other reactors in sequence. Fresh medium is pumped into the perfusion chamber from where solubles can perfuse through the membrane into the cell chamber. Thus the cells contained within the chip are continuously supplied with fresh nutrients. Vice versa, waste products and other metabolites can perfuse from the cell chamber into the perfusion chamber and will be transported off by the unidirectional medium flow. The system can be installed in a way that the medium runoff will either be fed into the medium supply, generating a circular system, into a waste receptacle or subsequent bioreactors. The MBRs are fabricated using polycarbonate plates (Finkbeiner et al. 2022) in a fashion that cells within the cell chamber are observable using brightfield microscopy.
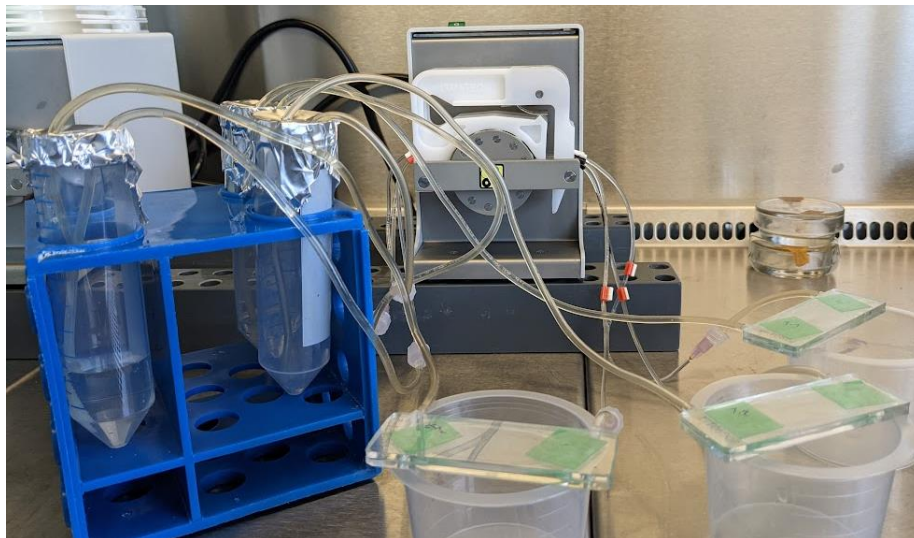

Fig. 2: Exemplary setup of three singular MBRs: Three microfluidic bioreactors were installed using a peristaltic pump to create a unidirectional medium flow. The medium runoff of the MBR was fed back into the medium source thus creating a circulating system.

2.8.2 *Neofusicoccum parvum*

The ascomycete *Neofusicoccum parvum* is considered a causal agent of Grapevine Trunk Diseases (GTD) (Carlucci et al. 2015). The fungus generally lives peacefully in the trunk of the grapevine but switches to an aggressive lifestyle upon detecting an accumulation of the metabolic intermediate ferulic acid (Khattab et al. 2022). Ferulic acid is an intermediate in the synthesis of lignin and accumulates if the host plant is disturbed in the generation of new wood, which may be caused by severe drought or heat. *N. parvum* may detect ferulic acid as a sort of "surrender signal" indicating that its host suffers extreme conditions and may perish soon. It switches to its more aggressive sexual life cycle and produces the phytotoxin fusicoccin A (Khattab et al. 2022) to kill off its host to gain the additional nutrients necessary for its sexual reproduction. The resulting spores can subsequently be spread to and infest new hosts that may not suffer suboptimal conditions.

Neofusicoccum parvum is a fungal model organism to research plant pathogens and potentially look at its interaction with the host plant. For this set of experiments *N. parvum* was cultivated on Potatoe Dextrose Agar (PDA) plates (see Table 1). Every two weeks a small disk of hyphae-imbued agar was transferred from the old plate to a fresh PDA plate. To transfer the fungus into a liquid medium, a small disk of one-week-old hyphae-imbued agar was transferred into 15 mL of liquid MS-medium (see Table 1) and incubated in the dark at 28°C while shaking at 150 rpm. After one week of incubation, the resulting hyphae cluster was cut into small pieces and transferred into 15 mL of fresh MS medium. The fungal hyphae should now grow more or less homogenous in the suspension culture and need to be subcultivated weekly by transferring 750 µL of hyphae suspension from the old culture into 15 mL of fresh MS medium.

2.9 Constructs

2.9.1 pDonor vector containing the MYB14 promoter

The promoter region of MYB14 from *V. sylvestris* was supplied by Duan et al. (2016) and was contained in a donor plasmid: pDonor::prMYB14
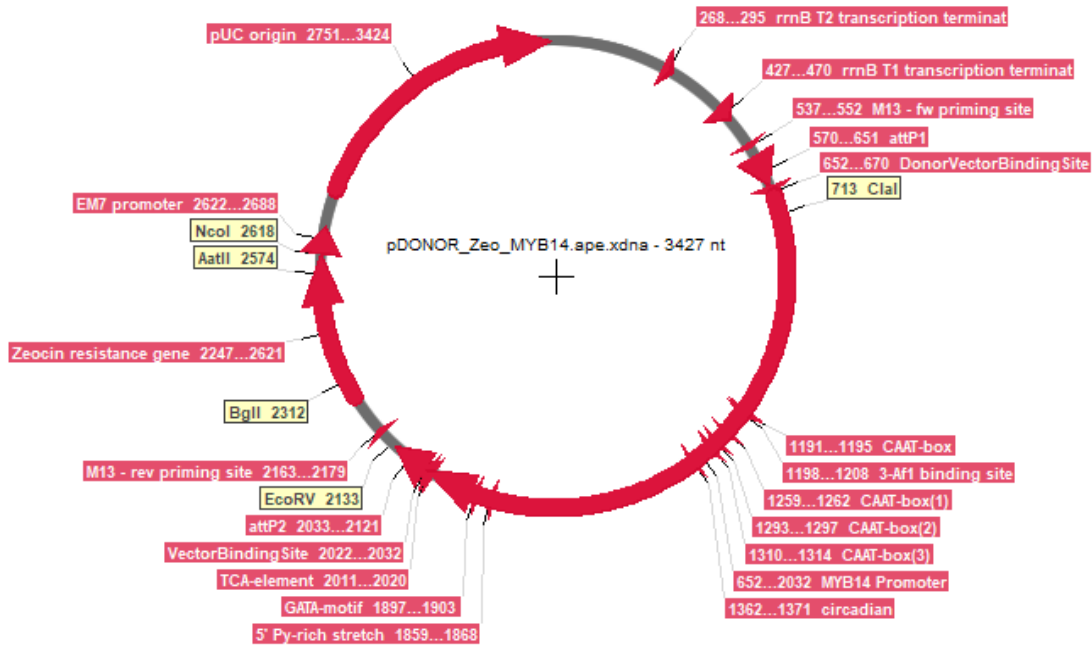
Fig. 3: Graphic map of pDonor::prMYB14: The 3,427 nt plasmid contained the promoter region of MYB14 derived from *Vitis vinifera sylvestris* genotype Hö29 and a zeocin resistance cassette for antibiotic selection in bacteria.

The backbone of the donor plasmid contained a cassette for a zeocin resistance. Thus, zeocin was used as the selective antibiotic.

2.9.2 pMDC107 Gateway vector containing the prMYB14::GFP construct

The pMDC107 Gateway Vector was supplied from our bacterial stock collection.
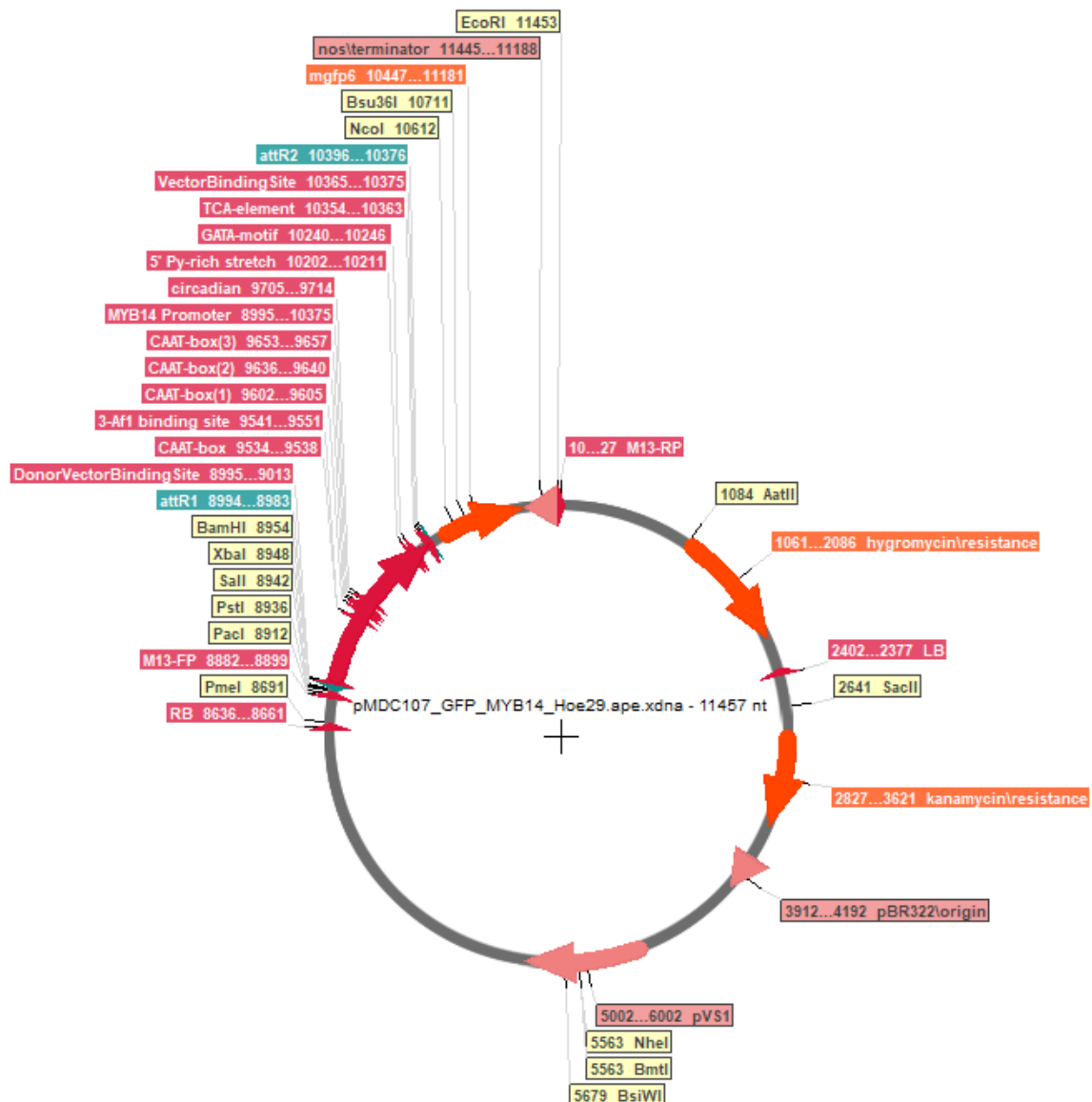
Fig. 4: Graphic map of pMDC107 prMYB14::GFP: The 11,457 nt big plasmid contained the gene for eGFP controlled by the *Vitis* promoter MYB14. The backbone of the plasmid contained a kanamycin resistance for bacterial selection, while the T-region of the plasmid contained a hygromycin resistance cassette for the selection of transgenic plant cells.

This vector (prMYB14::GFP) could be used by *A. fabrum* to transform plant cells. Between the LB and the RB region, we cloned in the promoter region of MYB14 from Duan, right in front of the gene for eGFP. This T-DNA also contained a resistance cassette for hygromycin selection in plants. The plasmid's backbone contained the resistance against kanamycin for bacterial selection.

2.9.3 Control Gateway Vector p2FGW7-FABD$_2$-GFP
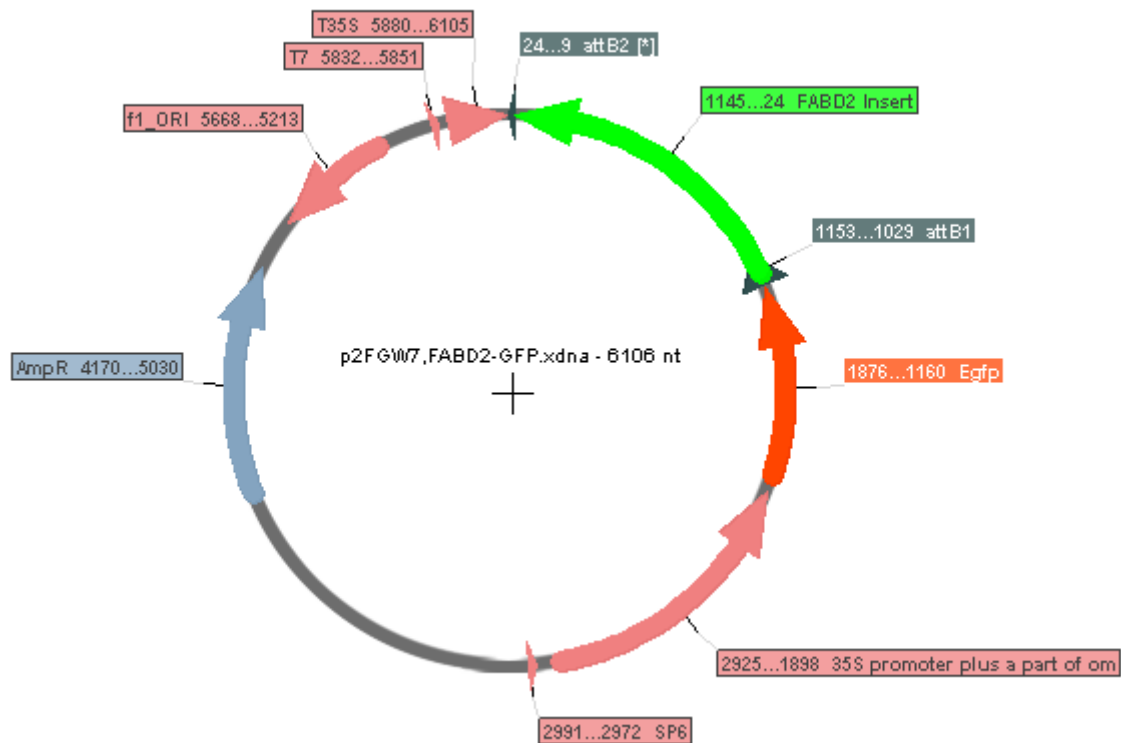
Fig. 5: Graphic map of p2FGW7-FABD2-GFP: The 6,106 nt big plasmid contains a fusion of FABD2 to eGFP controlled by the constitutive promoter 35S. Additionally, the plasmid contains a resistance cassette for ampicillin (AmpR).

The gateway vector p2FGW7-FABD$_2$-GFP contained a fusion of the Fimbrin Actin Binding Domain 2 (FABD$_2$) with eGFP controlled by the constitutive promoter 35S. Plant cells transformed with this vector constitutively produce a green fluorescent fusion of FABD$_2$ which binds to the actin filament of the cell, effectively marking the actin cytoskeleton of the cell.

3. Methods

3.1 Subcultivation of cell lines

The cell lines used were subcultivated in a seven-day cycle. After seven days a certain carry-over volume of old cell suspension was transferred from the "mother" cell culture to the fresh "daughter" Erlenmeyer flask containing autoclaved MS-medium. The volume of the carry-over depends on the growth rate of the specific cell line. The volumes used in this work are empirically established. In an established cell line, this process results in a starting culture with a stable cell density after subcultivation. To standardise this process even further, one could measure the density of the mother culture (cell fresh weight per mL suspension) and calculate the carry-over volume on a case-to-case basis to set a starting cell density for the culture. For specific information on a specific line, please see Chapter 2.1.

3.2 General methods

3.2.1 Restriction digestion

An isolated vector plasmid can be digested by specific restriction enzymes to get a first hint regarding the integrity of the sequence of the plasmid. With a known sequence, the plasmid can be digested *in silico* by one or more restriction enzymes to get a characteristic arrangement of resulting fragments. This calculation was performed using the software SerialCloner (see Table 5). To digest the plasmid in vitro, 1 µg of the plasmid was added to 5 µL of a compatible reaction buffer for the restriction enzyme to be used. 10 U of each enzyme was added and the volume was adjusted to 50 µL with ddH$_2$O. After 60 min of incubation, the resulting fragments could be visualised via electrophoresis to confirm the bands that have been calculated *in silico*.

3.2.2 PCR and Colony PCR

The Polymerase Chain Reaction (PCR) is a process that uses the activity of a polymerase and specifically designed DNA primers to amplify a specific region of a template DNA/RNA. A master mix of ingredients was created and aliquoted. Subsequently, the template DNA was added and the final mixture was treated in a thermocycler to create ideal conditions for the polymerase to amplify the desired region. To create the PCR master mix the following ingredients were mixed per sample: 10.9 µL of ddH$_2$O, 2.0 µL of 10x PCR buffer (see Table 2), 0.4 µL of dNTP mix (10mM) (see Table 2), 0.8 µL of the forward primer, 0.8 µL of the reverse primer and 0.1 µL of the Taq DNA polymerase (5 U/µL) (see Table 7). Of this master mix 15 µL were

aliquoted into 0.2 mL reaction tubes for each sample and 5 μL of template DNA of the sample was added. These aliquots were treated in a thermocycler according to a standard PCR protocol (see Table 10) and subsequently visualised via gel electrophoresis (see Chapter 3.2.3). Colony PCR was oftentimes used to check whether colonies growing on plates containing selective antibiotics were the desired cells. Colonies were picked from the plate with the tip of a pipette and mixed into the PCR mix by pipetting. The cells were lysed in the first heating step of the PCR, thus making the DNA template available to the polymerase enzyme. Choosing primers to amplify a region on the introduced plasmid would produce a PCR product in samples of colonies that were successfully transformed. For the colony PCR, the aforementioned master mix was slightly different since the template DNA was added differently. In this case, 15.4 μL of ddH$_2$O was added. This mix was aliquoted in volumes of 20 μL into 0.2 mL reaction tubes and the picked colonies were added by pipette mixing. The tubes were treated in a thermocycler with a standard PCR protocol (see Table 10) and the resulting amplification product was visualised via gel electrophoresis (see Chapter 3.2.3).

Table 10: PCR protocol for thermocycler

94°C	1:00 min	
94°C	0:30 min	
60°C	0:30 min	35x
68°C	0:30 min	
68°C	2:00 min	
12°C	storage	

3.2.3 Gel electrophoresis

To visualise DNA, plasmids, fragments thereof or PCR products these can be loaded onto agarose gels containing MIDORI[Green] Xtra (see Table 2). Depending on the fragment size to be observed, the agarose gel can be created using different concentrations of agarose (see Table 2). In our case, 1 % (w/v) agarose was solved in 40 mL of 0.5 % TAE buffer (see Table 1) using a microwave to heat the mixture until the agarose was entirely solved. After letting the solution cool until it was just touchable, 2.4 µL of MIDORI[Green] Xtra was added and mixed. The gel was poured into a casting mould with a comb to create the needed number of pockets. Once the gel has cooled for 20 min it was transferred into a gel chamber (see Table 4) filled with 0.5 % TAE buffer. The samples were mixed with 5x loading buffer (see Table 2) and loaded along with a ladder marker into the pockets of the submerged gel. Subsequently, the chamber was closed and a voltage of 100 V was applied for 20 min. The gel with the separated fragments was visualised with the Invitrogen Sage Imager Blue-Light Transilluminator (see Table 4) and the Intas GDS software (see Table 5).

3.3 *Roesleria subterranea* and the Acetonadduct of Entatrevenetinon

3.3.1 *Roesleria subterranea* and its metabolites

The relationship between two species is shaped by the communication between them. Whether a host species detects structural molecules of its pathogen to mount a defence reaction or whether two species in a mutualistic symbiosis find and adjust their balance, this communication relies on the production and detection of chemical signals. In understanding the signalling between two given species lies the potential to manipulate or exploit these signals to influence the behaviour of the species involved. The ascomycete *Roesleria subterranea* lives on the roots of deciduous trees and the roots of grapevine. It can be considered a significant pathogen of the host (Neuhauser et al. 2011) as it kills off the host's tissue to feed, effectively destroying the vital root system of the plant. As with most symbioses, the interaction of *R. subterranea* and the *Vitis* plant likely relies on a complex back and forth of the plant detecting the fungus and the ascomycete in turn either evading detection or circumventing the mounted defence reaction using effectors (see Chapter 1.2). By understanding the communication and potentially identifying the signals used, it might be possible to shape the interaction, maybe even finding easy-to-produce substances that might boost the plant's inherent immune system to successfully repel *R. subterranea*.

Our cooperation partner at the ibwf in Mainz has identified several metabolites of *Roesleria subterranea* that proved bioactive by inhibiting the sporulation of *Magnaporthe oryzae* and *Phytophthora infestans* spores (personal communication, Stefan Jacob, ibwf). The partners in the DialogProTec project then tested these bioactive compounds to see, what effects, if any, they show on the physiology of plants. Researchers at the IMBP in Strasbourg (France) looked at the impacts of the components on the roots of *Arabidopsis thaliana*, while we at the KIT in Karlsruhe (Germany) made observations of the effect of the compounds on the physiology and immunity reactions of plant suspension cells. We aimed to elucidate the reaction of cells of different *Vitis* lines to these molecules to potentially shed light on the relationship between *Roesleria subterranea* and its host and to see if these compounds act as sginals and would be potential candidates for substances used for plant immunity priming (see Chapter 1.2.6).

3.3.2 Mortality induced by *R. subterranea* compounds

A quick and established method to screen for potential immunoactivity of a given substance is to perform a Cell Death Assay (CDA). During the Hypersensitive Response (HR) associated with the Effector Triggered Immunity (ETI) plant cells engage the Programmed Cell Death (PCD) to restrict the advancement of the potential pathogen attacking the tissue. Therefore, the observation of an increase in cell mortality could function as a preliminary indication of an immune response taking place. Whether the mortality originates in a deliberate defence reaction of the cell needs to be confirmed with subsequent experiments.

To see whether the *Roesleria* metabolites Sclerodin or AcetonAduct of Entatrevenetinon (AaE) induce cell death, four different cell suspension lines were treated with them and cell mortality was quantified using the Evans Blue selective staining protocol (see Chapter 3.4.2). In this work, the following cell lines were used: We did testing on *Vitis vinifera* cv. Chardonnay (see Chapter 2.1.1) to represent susceptible *Vitis* plants and *Vitis vinifera sylvestris* genotype Ke15 (see Chapter 2.1.2) was used because this wild relative of our local cultivars proved to be quite resistant to many diseases our cultivars are susceptible to. Additionally, the reaction of the cell line *Vitis rupestris* (see Chapter 2.1.3) was also tested. *V. rupestris* is a North American wild relative of the grapevine and is known to be resistant to many pathogens ravaging our vineyards and to excel in quick HR and immunity-related PCD. Finally, all

experiments were also performed on BY2 wild-type cells as an established model organism in our institute as a control group for the methods used.

All cell lines were exposed to the Substance of Interest (SoI) on the day of subculturing. After subcultivating the lines according to their respective protocol (see Chapter 2.1), the cell suspensions were aliquoted into 2 mL volumes into 35x10 mm Petri dishes (see Table 3). A triplicate of untreated cells was created for each cell line. As a control for the effect the solvent of Sclerodin and AaE, a solvent control with the effective concentration of 0.5 % MeOH was performed in triplicate. Finally, the cells were treated with the respective SoI by adding 50 μM of the SoI into the cell suspension. After adding the substances, where applicable, the cell culture dishes were sealed off using a sealing film (see Table 3). The dishes were then placed on an orbital shaker (see Table 4) and cultivated at 150 rpm in the dark at 26°C.

Cell mortality was quantified at different time points, depending on the experiment; samples of both the Sclerodin and the AaE treatment were taken 48 hours after elicitation. For the AaE treatment, a time course was also created, taking samples at 4 h, 8 h and 48 hours post elicitation. To take the sample, the culture dish was opened, 200 μL of cell suspension was extracted and the dish was subsequently resealed. Cell mortality in the samples taken was quantified using the Evans Blue selective staining protocol (see Chapter 3.4.2).

3.3.3 Cytoskeletal effects induced by *R. subterranea* compound AaE

The cytoskeleton of the plant cell and the reorganization thereof can be part of the signalling pathway in defence (Wang et al. 2022b; Sofi et al. 2023). The disintegration of the cytoskeleton is a common occurrence in Programmed Cell Death (PCD). To observe how the AcetonAduct of Entatrevenetinon (AaE) affects the cytoskeleton of the plant, two cell lines have been treated with 50 μM of AaE. The cell lines BY2 TuA3:GFP and Chardonnay FABD$_2$-GFP can be used to either visualize the microtubules or the actin filament in the living cell respectively (see Chapters 2.1.6 and 2.1.7). To treat the lines with the fungal metabolite, five-day-old cells were aliquoted into 1 mL volumes in 1.5 mL reaction tubes. For each treatment, three individual biological replicates were created, including a negative control and two known disruptors of the respective cytoskeletal elements along with the appropriate solvent controls. The cell suspension of BY2 TuA3:GFP in the reaction tube was complemented with 50 μM of AaE, 10 μM of Oryzalin, 0.1 % DMSO or 0.5 % MeOH.

The cell line Chardonnay FABD$_2$-GFP was treated with 50 µM AaE, 10 µM latrunculin B, 0.1 % DMSO or 0.5 % MeOH. The samples were incubated for 60 minutes at 26°C in the dark while shaking at 150 rpm on an orbital shaker. After 60 minutes the samples were observed using the Spinning Disc microscope (see Table 4). The structures of the cytoskeleton were visualised using an excitation filter of 488 nm, an emission filter of 509 nm wavelength and an exposure time of 500 ms to observe the GFP fused to molecules associated with the respective cytoskeletal structure. Three or more pictures of representative cells were taken with the z-stack function of the ZenBlue software (see Table 5). The stack was placed to visualize the cell starting with the outmost layer of the cortex and ending in the estimated middle of the cell. The individual layers were fused using an orthogonal projection.

3.3.4 Effect of AaE on the expression of defence-related genes

In a successful defence reaction in plants, Programmed Cell Death (PCD) coincides with the induction of defensive genes. These can include genes that are associated with the signalling of biotic stresses and the genes that are involved in the synthesis of defence compounds, like the so-called phytoalexins. To further illuminate the reaction the observed plant cell lines exposed to the presence of the *Roesleria subterranea* metabolite AcetonAdduct of Enatrevenetinon (AaE), the expression patterns of commonly observed defence-related genes were quantified. We measured the gene expression in the *Vitis* lines *Vitis vinifera sylvestris* genotype Ke15, *Vitis rupestris* and *Vitis vinifera* cv. Chardonnay. Additionally, we tested *Nicotiana tabacum* cv. BY2 wild-type cells as a well-established control group. We quantified the gene expression of Phenylalanine Ammonia-Lyase (PAL) and the STilbene Synthases 27 and 47 (STS27 and STS47) to get insight into the metabolic pathway that results in the generation of phytoalexins. We also looked at the expression patterns of Pathogenesis-Related protein 1 (PR1) and JAsmonate-Zim-domain protein 1 (JAZ1) as marker genes for the involvement of the salicylic acid and jasmonate signalling pathways, respectively.

The exposure of the cell lines to AaE was started on the day of subculturing. The newly-generated cell culture was aliquoted into 2 mL volumes inside cell culture dishes (see Table 3). Of each treatment, three biological replicates were created for each cell line. The samples were complemented with either 50 µM of AaE or 0.5 % methanol (MeOH) as the solvent control. After adding the elicitor, the culture dishes of the treated samples and the untreated control group (CTRL) were sealed using a sealing film (see

Table 3). All samples were incubated at 26°C, in the dark while shaking at 150 rpm on an orbital shaker. Samples were taken 4 hours post-elicitation. The cell suspension was filtered using a Büchner funnel (see Table 4), filter paper, a side-arm flask (see Table 4) and a vacuum pump (see Table 4). 150-200 mg of dried cells were transferred into Safe-Seal reaction tubes (see Table 3) containing a milling steel bead and immediately frozen in liquid nitrogen. By using the steel beads contained in the Safe-Seal tubes, the samples were homogenized in a mix-mill disruptor (see Table 4). Subsequently, the total RNA of the samples was extracted using the Roboklon Universal RNA KIT (see Table 6) following the protocol included. The optional DNA digestion step was performed using the RNase-Free DNase Set by Qiagen (see Table 7). The quality of the extracted total RNA was confirmed (see sFig. 3) via gel electrophoresis (see Chapter 3.2.3).

The total RNA was converted into complementary DNA (cDNA) using a MuLV-Reverse transcriptase (see Table 7). 1 µg of RNA is mixed with 1 µL of 10 mM dNTP mix (see Table 2) and 0.4 µL of 500 ng/µL Oligo (dT) in a 0.2 mL reaction tube (see Table 3). The total volume was adjusted to 16 µL with ddH$_2$O. In a thermocycler, the sample was heated to 65°C for 5 minutes. The samples were transferred on ice, while the MuLV-transcriptase (0.25 µL), with the corresponding buffer (2.00 µL), RNase inhibitor (0.5 µL) and ddH$_2$O (1.25 µL) were added to each sample. Subsequently, the samples were incubated at 42°C for 60 minutes, at 90°C for 10 minutes and then cooled at 12°C until retrieved. The finished cDNA was stored in the freezer at –20°C.

To quantify the gene expression within the samples, a real-time quantitative PCR (RT-qPCR) was performed. We used a protocol based on the work of Svyatyna et al. (2014). For each sample, technical triplicates were performed. To achieve this, a master mix of 61.8 µL was complemented with 3.25 µL of 1:10 diluted cDNA, mixed and subsequently split into three technical replicates of 20 µL, therefore accounting for volumes lost due to pipetting. The master mix contained final concentrations of 200 nM per primer (see Table 8 for sequences), 200 nM of each dNTP (see Table 2), 1x GoTaq buffer (see Table 2), 2.5 mM MgCl$_2$ (see Table 2), 0.5 U GoTaq Polymerase (see Table 7) and 1x SYBR Green (see Table 2). The RT-qPCR was performed using the Bio-Rad CFX Connect Optics Module and CFX Connect Thermal Cycler (see Table 4) and the material in Table 3. The gene expression of the genes of interest; PAL, STS27, STS47, PR1 and JAZ1, was standardized to the unaffected

housekeeping gene ubiquitin (see Table 8) using a calculation based on the work of Livak and Schmittgen (2001) to calculate a fold induction of the observed sample:

$$fold\ induction: 2^{-\Delta\Delta C^t}$$
$$\Delta C^t{}_{GoI}(x) = C^t{}_{GoI}(x) - C^t{}_{Ubq}(x)$$
$$\Delta\Delta C^t(x) = \Delta C^t{}_{GoI}(x) - \Delta C^t{}_{GoI}(CTRL)$$

In this calculation X represents the sample, GoI stands for Gene of Interest and CTRL is the mean of the ΔC^t values of the negative control. This results in a fold induction of a gene of interest standardized to the expression of the gene in the untreated negative control of the respective cell line.

3.4 Microfluidics: an abstract ecosystem

3.4.1 Microfluidics: establishing a system

Immunoactive substances can be used to prime plants to increase their inherent defence capabilities against pathogen attacks (Mauch-Mani et al. 2017). Therein lies a huge potential to alleviate the environmental impact of herbi- and fungicide use. The immunoactivity of such substances often relies on the detection thereof and signal transduction, which implies both potential signal specificity and amplification. Therefore these substances have a low potential for unintended side effects on the ecosystem and can be applied at low concentrations. Detection and identification of immunoactive components rely on observing multiple physiological phenomena and gene expression. The application of microfluidic techniques harbours great potential to establish a high-throughput screening for the immunoactivity of soluble molecules. Finkbeiner et al. (2022) developed and designed a Microfluidic BioReactor (MBR) that can cultivate plant cells in a cultivation chamber, supplied via a unidirectional medium flow. The medium flow is generated by a peristaltic pump. Plant cells inside the microfluidic chip can be exposed to substances of interest by adding these to the medium supplied to the system. To evaluate the immunoactivity of the substance it is key to establish quantification methods to measure the defence reactions of cells within the MBR system. Leona M. Schmidt-Speicher of the institute IMT at Karlsruher Institut für Technologie developed and designed quantification methods within the reactor. In cooperation with them, our institute tested the application of these methods on plant cells exposed to elicitors or pathogens.

3.4.2 Cell mortality assay

Cell mortality in the plant cells was quantified via the selective staining protocol using Evans Blue. The cells were separated from the medium they were cultivated in by using handmade filters. These filters were crafted by truncating a 2.0 mL reaction tube and sealing off one opening with a mesh with a 20 µm pore size. The filters were placed on an absorbent tissue paper and the 100-200 µL of the cell suspension to be quantified were transferred onto the filter. The medium was absorbed and the filter containing the dried cells was transferred into 2.5 % Evans Blue solution (see Table 2) so that the cells were completely submerged in the solution. After an incubation period of 5 minutes, the filter was placed onto the tissue paper until any excess Evans Blue solution was absorbed. The filters were then placed into ddH$_2$O and continuously rinsed with clean ddH$_2$O until the majority of excess Evans Blue was separated from

the cells. The cells were transferred into reaction tubes and visualised via brightfield microscopy. The Evans Blue molecules only enter dead or dying plant cells through holes in the plasma membrane and cell wall. Therefore only dead cells appeared blue or darkened under the microscope. Using the "Tiles" function of the apotome microscope (see Table 4) and the respective software ZenBlue (see Table 5) large overview pictures were taken. Cells were counted using the "Multipoint" tool of the ImageJ software (see Table 5) and the cell mortality was calculated using the following formula:

$$cell\ mortality\ [\%] = \frac{\#dead\ cells}{\#dead\ cells + \#alive\ cells} * 100$$

3.4.3 MBR plant cell cultivation

The cell chamber of the Microfluidic BioReactor (MBR) can hold a volume of 800 μL, whereas the effective volume can vary due to random warping of the membrane that separates the cell chamber from the perfusion chamber. Plant cells cultivated within the MBR are supplied with a medium via a unidirectional flow generated by a peristaltic pump. The cells can be exposed to substances of interest by solving these in the medium supplied. Given the ability to read out the reaction of the plant cells within the MBR, this enables high-throughput screening of substances.

To check the feasibility of the method, the MBRs supplied were checked for potential leaks and potential cell lines were tested for their compatibility to be cultivated in the MBR. Pump tubing (see Table 3) was installed onto the peristaltic pump (see Table 4) using the clamp included with the multichannel pump. Dispensing needles (see Table 3) were inserted at either end of the pump tubing and connected to Tygon pumping (see Table 3) using Lür connectors (see Table 3). Tubing was then connected to the medium source and the MBR. The peristaltic pump was set to maximum speed (137 μL/min) to quickly fill the tubing and was stopped, once the medium entered the inlet of the MBR. Using a truncated tip of a 1000 μL pipette (see Table 3) 800 μL of cell suspension could be transferred to the cell chamber of the MBR. The opening of the cell chamber next to the inlet was sealed using biocompatible tape (see Table 3) and the MBR was placed upright so the remaining air pockets in either cell or perfusion chamber could easily leave the MBR while resuming the filling process. Once the medium reached the outlet of the MBR, the remaining opening of the cell chamber was sealed and the MBR was placed horizontally. The pump rate of the peristaltic pump

could now be reduced to 30 µL/min. The outgoing tube of the MBR could be connected to a waste receptacle, to a subsequent MBR or it could be returned to the medium source, installing a circular system. During the cultivation, the MBRs were kept in the dark.

To evaluate the compatibility of a given cell line with MBR cultivation the cells' mortality was quantified. The cells were extracted from the cell chamber after seven days of cultivation by pipetting them through one opening of the cell chamber and cell mortality was subsequently quantified using the selective staining protocol with Evans Blue (see Chapter 3.4.2). This was compared to cells cultivated to the established method in our lab. The cell suspension was subcultivated (see Chapter 3.1) into 30 mL of fresh MS medium in an Erlenmeyer flask and cultivated in the dark at 26°C while rotating on an orbital shaker at 150 rpm. These control samples were taken after seven days of cultivation and mortality was quantified via Evans Blue selective staining (see Chapter 3.4.2).

To test the feasibility of using the MBR to treat cells with a given substance and observe a phenomenon caused by the said substance, BY2 cells were cultivated in the MBR and treated with 27 µg/mL harpin, as a known elicitor of ETI-associated PCD. Using the aforementioned setup solitary MBRs were installed and loaded with BY2 wild-type cells. The source tubing of the peristaltic pump was put into a standard MS medium (see Chapter 2.2) and the outgoing tube of the MBR was connected to a waste receptacle. Triplicates of both the harpin treatment and the untreated CTRL were both equilibrated in the MBR by supplying the cells with standard MS medium for 60 minutes. After equilibration, the source medium of the harpin-treated samples was replaced by an MS medium containing 27 µg/mL harpin. Cell mortality in all samples was quantified after two days of incubation by pipette extracting cells out of the cell chamber and using the selective staining protocol with Evans Blue (see Chapter 3.4.2).

3.4.4 MBR fungal cell cultivation and co-cultivation

Microfluidic BioReactors (MBR) can be used to co-cultivate different cell types modularly installed in separate MBRs in sequence. Cells being co-cultivated could be intra- and interkingdom. Finkbeiner et al. (2022) demonstrated that cells cultivated in connected MBRs interact with one another. Results culminating from the following experiments were partially published in the aforementioned paper.

To evaluate the possibility to cultivate cell types of different kingdoms within the MBR setup, the cultivation of *Neofusicoccum parvum* suspension (see Chapter 2.8.2) in the MBR was tested. *N. parvum* was cultivated in two variants of MBRs differing in the pore size of the membrane separating the cell and perfusion chambers. Plant cells were cultivated in MBRs with a pore size of 5 µm. For the cultivation of fungal cells, MBRs were constructed using a membrane with a pore size of 1 µm, since fungal hyphae are considerably smaller in size. Both MBRs with 5 µm and 1 µm pore size were connected to the peristaltic pump (see Table 4), and ultimately the medium source by Tygon tubing (see Table 3). A unidirectional medium flow was generated by using pump tubing (see Table 3) which was connected via dispensing needles (see Table 3) and Lür connectors (see Table 3) to the general Tygon tubing. The peristaltic pump was operated at a pump rate of 137 µL/min until the medium reached the inlet of the MBRs. 800 µL of *N. parvum* suspension (see Chapter 2.8.2) was transferred into the cell chamber of the bioreactor using a truncated tip of a 1000 µL pipette. The opening of the cell chamber closest to the inlet of the MBR was sealed off using biocompatible tape (see Table 3). The MBR was placed vertically to enable air pockets to escape the MBR chambers while resuming the pump activity. Once the medium reached the outlet of the MBRs the MBRs were placed horizontally and the pump rate was kept at 137 µL/min. The outgoing medium was guided into a waste receptacle using tubing. During the intended seven-day cultivation, the MBRs were kept in the dark. The setup was observed daily. Once cultivation was stopped, the growth patterns of the hyphae growing in the MBR were observed using bright field microscopy via the apotome microscope (see Table 4).

To attempt a co-cultivation of interkingdom cell types within the same MBR setup, MBRs containing BY2 wild-type cells were installed in a sequence of MBRs containing *N. parvum* suspension to observe the reaction of the BY2 cells to the presence of the *N. parvum* cells. For both cell lines, MBRs with a membrane pore size of 5 µm were used. The ascomycete is known to produce phytotoxins to kill off plant cells when stressed. Therefore, the reaction of the BY2 cells was read out via their cell mortality. A respective control group was established using a singular chip, only containing BY2 cells and supplied from the same medium source as the co-cultivation sample. Pump tubing (see Table 3) was installed on the peristaltic pump (see Table 4) using the included clamps. Dispensing needles (see Table 3) were inserted at either end of the pump tubing and connected to general Tygon tubing (see Table 3) using Lür

connectors (see Table 3). The medium-supplying tubes of both co-cultivation and CTRL were inserted into the same standard MS medium (see Chapter 2.2) source. In the CTRL MBRs, the medium runoff was directly guided into the waste receptacle. In the co-cultivation group, the outlet of the first MBR is connected to the inlet of the second MBR in sequence. The outlet of the latter MBR was connected to the waste.

Fig. 6: Exemplary setup of a co-cultivation setup with respective CTRL: In the co-cultivation treatment two MBRs were installed in sequence connecting the outlet of the first chip to the inlet of the latter using Tygon tubing. The first chip was loaded with a cell suspension of *N. parvum*, whereas the latter MBR was used to cultivate BY2 wild-type cells. The outlet of the second MBR was connected to the waste receptacle. A control group was established by installing a singular MBR filled with a cell suspension of BY2 wild-type. Both groups were supplied with the same MS medium at a pump rate of 30 µL/min. In the actual experimentation, there were three replicates of both treatments run simultaneously.

The peristaltic pump (see Table 4) was operated at a pump rate of 137 µL/min until the MS medium reached the inlet of an MBR. The pumping was then arrested and the MBR was filled with 800 µL of the respective cell suspension using a truncated tip of a 1000 µL pipette. The cells were inserted into the opening of the cell chamber closest to the outlet of the MBR while tilting the bioreactor to facilitate an even distribution of the suspension in the chamber. The BY2 wild-type culture was seven days old, while the *N. parvum* suspension was used a day after subcultivation. Subsequently, the opening closest to the inlet of the MBR was sealed off using biocompatible tape (see Table 3). The reactor was then placed vertically to allow air pockets to leave the chambers of the MBR easily while the pumping process was resumed. Once the

medium reached the outlet of the MBR the remaining opening of the cell chamber was sealed off and the MBR was placed horizontally in its final position. Once all MBRs were loaded, the pump rate of the peristaltic pump was reduced to 30 µL/min. Both co-cultivation and CTRL were cultivated for two days while darkening the clean bench used.

After two days of cultivation, BY2 cells of each sample were extracted using a truncated 1000 µL tip. A sufficient amount of cell suspension was gathered through an opening in the top layer of the cell chamber and cell mortality was quantified using the Evans Blue staining protocol (see Chapter 3.4.2).

3.4.5 MBR measurement of transgenic fluorescence

Within this work, we intended to generate a transgenic cell line that would produce a green fluorescent signal, once its basal immune defence was engaged. This was attempted by cloning the promoter of MYB14 from *Vitis vinifera sylvestris* Hö29 in front of a gene translating to eGFP. Ultimately, this proved unsuccessful (see Chapter 8.1). This cell line would have been loaded into the MBR and treated with known elicitors of plant immunity to observe the generated green fluorescent signal directly by putting the entire MBR under a fluorescence microscope. Since the transgenic cell line was not established, no experiments with the cell lines in the MBR were performed.

3.4.6 MBR pH measurement

An early signal used in the signalling of a basal defence reaction of the plant is an influx of Ca^{2+} ions (Lecourieux et al. 2006). This transport of Ca^{2+} coincides with a change in the extracellular pH, due to the movement of ions across the membrane (Jabs et al. 1997; Nürnberger and Scheel 2001) and the depolarization of the cell membrane (Felle 2001). Measuring the extracellular pH is a well-established method of detecting a basal defence reaction.

Leona M. Schmidt-Speicher designed connector screws to create an interface to measure the pH of the cell suspension within the MBR. In this work, the pH was measured using optic means with the pH-1 SMA HP5 system developed by PreSens Precision Sensing GmbH (see Table 4). This system uses glass fibre to send light to a sensor spot placed in the medium to be measured. The sensor spot reflects the light signal and the sensor interprets the pH of the medium using the parameters of the light reflected. Depending on the pH of the solution the sensor spot is in, it reflects the light differently. Schmidt-Speicher designed a connector screw that can be screwed into

one of the top layer openings of the MBR cell chamber. An SP-HP5-SA sensor spot (see Table 3) was placed on the bottom part of the screw. Upon installation, this part was situated inside the cell chamber. The glass fibre was then fixed into an opening on the upper part of the screw, situated outside of the MBR. The sensor spot was calibrated for the required range of pH using the multipoint calibration tool included in the software of the sensor. It was calibrated using aliquots of MS medium adjusted to the pH values of pH 9, pH 7, pH 6, pH 5 and pH 4. If not in use, the connector screw with the sensor spot was stored in a standard MS medium, which was replaced regularly.
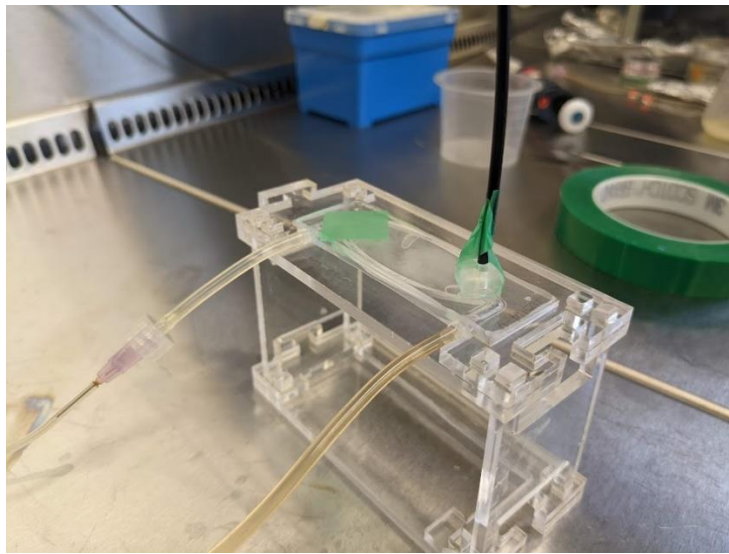

Fig. 7: pH measurement within the MBR system: In the MBR system, the pH was measured by optic means. A light signal was sent via the glass fibre to a sensor spot that reflected the light, which changed depending on the pH of the solution the sensor is in. The sensor interpreted the change in the reflected light to measure the pH of the solution. Using a connector screw designed by Leona M. Schmidt-Speicher, the sensor spot was placed inside the cell chamber of the MBR while the glass fibre was connected to the spot on the outside through dentation in the screw top. The glass fibre was fixed in position using biocompatible tape. The pH was measured every 30 seconds.

To set up the measuring of the pH within the MBR, a pumping tube (see Table 3) was installed onto the peristaltic pump (see Table 4) using the included clamp. The pumping tubing was connected to general Tygon tubing using dispensing needles (see Table 3) and a Lür connector (see Table 3). One side of the pumping tube was connected to the medium supply using Tygon tubing (see Table 3) and the other end was connected to an MBR. The peristaltic pump was operated at 137 µL/min pump rate until the medium reached the inlet of the MBR. It was then stopped and 800 µL of a seven days old BY2 cell suspension was introduced into the cell chamber through an opening using

a truncated tip of a 1000 µL pipette. The cell chamber opening closest to the inlet of the MBR was sealed using biocompatible tape (see Table 3) and the MBR was placed upright to facilitate the expulsion of any remaining air pockets upon resuming the pumping process. Once the medium reached the outlet of the MBR the remaining opening of the cell chamber was sealed by inserting the aforementioned connector screw and the glass fibre was installed and fixed with the biocompatible tape (see Table 3). The outlet of the MBR was connected to a waste receptacle using Tygon tubing. The peristaltic pump was operated continuously at 137 µL/min.

Before starting any measurement of the pH, the system was equilibrated for 90 minutes. Subsequently, a baseline pH is measured for 30 minutes. To induce an extracellular alkalization the cells were treated with 25 µg/mL of chitosan. In previous work, it was shown that this concentration of chitosan induces a defence reaction in *Vitis rupestris* with an accompanying alkalization of the cell medium (Sofi et al. 2023). The chitosan stock of 10 mg/mL was solved in 1 % acetic acid. Therefore in addition to the chitosan treatment, a solvent CTRL with acetic acid was performed as well. After the 30-minute pre-measurement, either the chitosan or the respective solvent was added to the medium supplied to create a final concentration of 25 µg/mL chitosan and 0.0025 % acetic acid respectively. After adding the substance of interest, the pH was continuously measured for two hours. The pH was measured every 30 seconds. Due to the availability of a single pH-1 SMA HP5 system replicates of either chitosan treatment or solvent CTRL were not performed simultaneously but separately.

To standardize the pH measurements, the ΔpH was calculated. The values of each 30-minute baseline measurement were averaged and defined as the $pH_{baseline}$. To calculate the ΔpH of each timepoint of the measurement its respective $pH_{baseline}$ was subtracted from the absolute pH value at timepoint t.

$$\Delta pH_t = pH_t - pH_{baseline}$$

These calculations were performed per replicate and subsequently, the replicates were used for statistical analysis. $\Delta\Delta pH_{chitosan}$ was calculated by subtracting $\Delta pH_{solvent}$ from the $\Delta pH_{chitosan}$ to correct for the shift in pH that the solvent of chitosan has caused.

3.4.7 MBR pH measurement - chitosan double pulse

To see, whether the MBR system could be used to deliver two distinct impulses of a given signal, we conducted an experiment to treat BY2 cells with 25 µg/mL of chitosan at two different subsequent time points, separated by a period of supplying standard MS medium. We established a control group to see, whether the second pulse of chitosan caused a defence reaction of bigger amplitude if a preceding stimulus of chitosan was present and if this potential difference was measurable with the MBR system. The MBR setup was installed and BY2 cells were introduced in the system as detailed in Chapter 3.4.6. The system was equilibrated for 45 minutes and a baseline pH was measured for 30 minutes. After measuring the baseline, the first treatment of either 0.0025 % acetic acid or 25 µg/mL chitosan was performed, by transferring the supply tube into an MS medium containing the respective elicitor for 10 minutes. Subsequently, the supplied medium was reverted to standard MS medium and the pH was measured for 45 minutes before the second treatment with either acetic acid or chitosan was repeated for another 10 minutes, as mentioned before. After the second treatment, the pH was measured for 45 minutes and the experiment was concluded. During the entire experiment, the pH was measured every 30 seconds and ΔpH was calculated as detailed in Chapter 3.4.6. Three separate experiments were performed in triplicates each. First, the BY2 cells were treated with 0.0025 % acetic acid in both the first and second treatments as solvent control (slvCTRL). In the second experiment, the first treatment was performed with 0.0025 % acetic acid while the cells were treated with 25 µg/mL of chitosan in the second treatment (singlePulse). In the third experiment, the cell suspension was treated with 25 µg/mL of chitosan in both treatments (doublePulse).

3.4.8 MBR H_2O_2 measurement

The generation of Reactive Oxygen Species (ROS) in plants can function both as a signal to biotic and abiotic stresses (Lee et al. 2020) and as the actual defence mechanism (Keppler 1989; Peng 1992; Lamb and Dixon 1997). In our institute, Ismail et al. (2012) previously showed that the application of salt stress induced an increase in ROS levels as part of a signalling pathway. In this work, the feasibility of quantifying ROS levels in the runoff of the Microfluidic BioReactor (MBR) system was to be evaluated. To induce an increase in ROS, BY2 wild-type plant cells were cultivated in an MBR and were treated with 150 mM NaCl, a known elicitor of ROS induction (Ismail et al. 2012).

To treat the *N. tabacum* BY2 wild-type cells within the MBR system, a single MBR was installed per treatment. Pump tubing (see Table 3) was installed on a peristaltic pump (see Table 4), connected to general Tygon tubing (see Table 3) via dispensing needles (see Table 3) and Lür connectors (see Table 3). This tubing was used to connect the inlet of the MBR to the pump and finally a medium source. The peristaltic pump was operated at a pump rate of 137 µL/min creating a unidirectional flow of MS medium (see Chapter 2.2) to the perfusion chamber of the MBR. Once the medium reached the inlet of the MBR the pumping process was arrested and 800 µL of a seven days old BY2 wild-type cell suspension was transferred into the cell chamber of the MBR via pipetting the suspension through an opening of the cell chamber with a truncated tip. Subsequently, the opening of the cell chamber closest to the inlet of the MBR was sealed off using biocompatible tape (see Table 3) and the MBR was placed vertically while the pumping was resumed at 137 µL/min. This facilitates the expulsion of remaining pockets of air from the cell chamber. Once the medium reached the outlet of the MBR, the remaining opening was sealed with biocompatible tape and the MBR was installed in the final horizontal orientation. The outlet of the MBR was connected to a waste receptacle using Tygon tubing. In both the salt treatment and the negative control treatment the system was pre-flushed with a standard MS medium (see Chapter 2.2). After the entire system was filled, the source tube of the salt treatment was transferred into an MS medium containing an additional 150 mM NaCl. The pump was continuously operated at 137 µL/min for 60 minutes. After this hour, medium runoff from both treatments was collected in subsequent technical triplicates. To quantify the ROS levels in this medium the Amplex^{TM} Red Hydrogen Peroxide/Peroxidase Assay Kit (see Table 6) was used according to the respective protocol. In addition to the samples, a standard curve was created and measured to quantify the absolute levels of H_2O_2 and the induction thereof. The fluorescence intensity in the samples of the treatments and the standard curve was measured with a Spark Multimode Microplate reader (see Table 4).

3.4.9 Cleaning of the MBR system

With the notable exception of the Microfluidic BioReactors (MBR) that were operated for the cultivation of the *N. parvum* culture (see Chapter 4.2.3), MBRs could be reused when cleaned properly. After the respective experiment concluded, the system was first run dry by removing the source tube from the medium source and operating the peristaltic pump (see Table 4) at a pump rate of 137 µL/min for a short while. In the pH measurement experiments (see Chapter 3.4.6), the connector screw with the SP-HP5-SA sensor spot was uninstalled and transferred into a standard MS medium (see Chapter 2.2) for storage. The entire system was then flushed with 70 % ethanol for 30 minutes and subsequently run dry. The MBR was then rinsed by holding the opening of the cell chamber directly under a tap for desalinated water. It was then incubated in 70 % EtOH for 60 minutes, removed from said ethanol and dried overnight. The tubing was rinsed inside and outside with desalinated water and 70 % EtOH and autoclaved before reuse.

4. Results

4.1 *Roesleria subterranea* and the Acetonadduct of Entatrevenetinon

4.1.1 Mortality induced by *R. subterranea* compounds

To check whether the metabolites of *Roesleria subterranea* Sclerodin or the AcetonAduct of Entatrevenetinon (AaE) induce an increase in cell mortality that might potentially be associated with a defence reaction, three *Vitis* cell lines and BY2 were treated with 50 µM of the respective substance. For Sclerodin and AaE the mortality was quantified after 48 hours of incubation by extracting samples and applying the Evans Blue selective staining protocol (see Chapter 3.4.2).
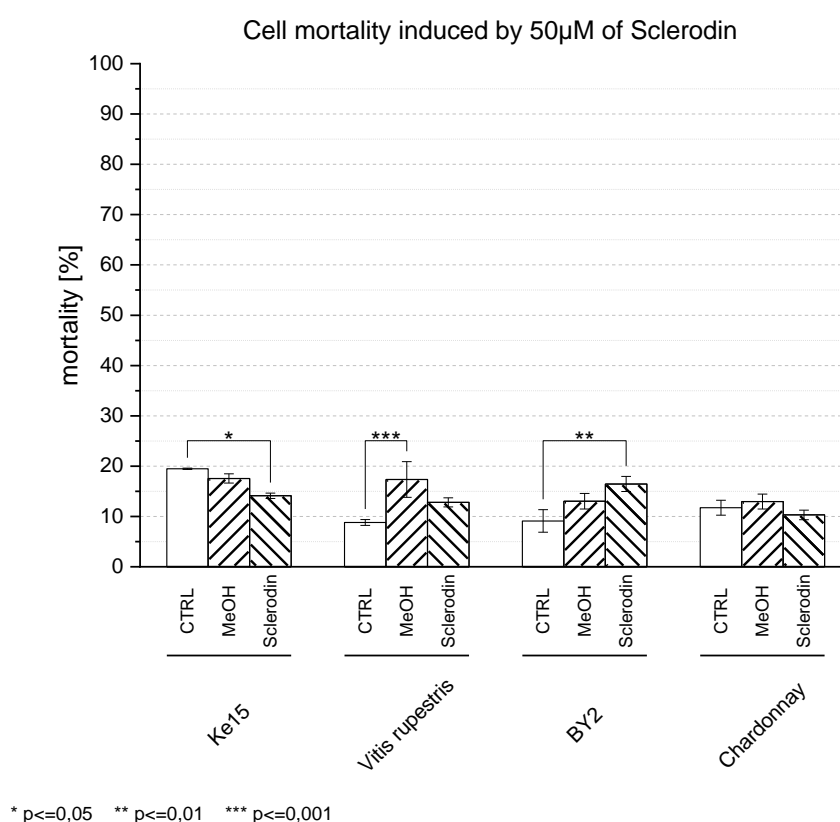

* p<=0,05   ** p<=0,01   *** p<=0,001

Fig. 8: Sclerodin-induced mortality after 48 h: The cell lines were aliquoted into volumes of 2 mL and treated with 50 µM Sclerodin, 0.5 % methanol (MeOH) or were untreated (CTRL). Samples were incubated at 26°C, in the dark, while shaking at 150 rpm on an orbital shaker. Samples were extracted after 48 h and mortality was quantified via Evans Blue staining (see Chapter 3.4.2). Each treatment was performed as three biological replicates and statistical analysis was performed via Fisher LSD ANOVA with a significance level of 0.05.

When treating Ke15, *V. rupestris*, Chardonnay and BY2 with 50 µM of Sclerodin and the respective solvent control we observed only minor differences in cell mortality exhibited by the lines. In Ke15 there was a slight but significant decrease in mortality

when comparing the Sclerodin-treated sample with the respective negative CTRL. In *V. rupestris* there was a significant increase in cell mortality when treated with the solvent, MeOH. In BY2 the treatment with Sclerodin caused a significant but small increase in mortality when compared to the negative CTRL. In Chardonnay, the treatments caused no significant change in cell mortality. Yet in all cell lines, the change in mortality induced by Sclerodin was never significantly different from the respective solvent control (MeOH).
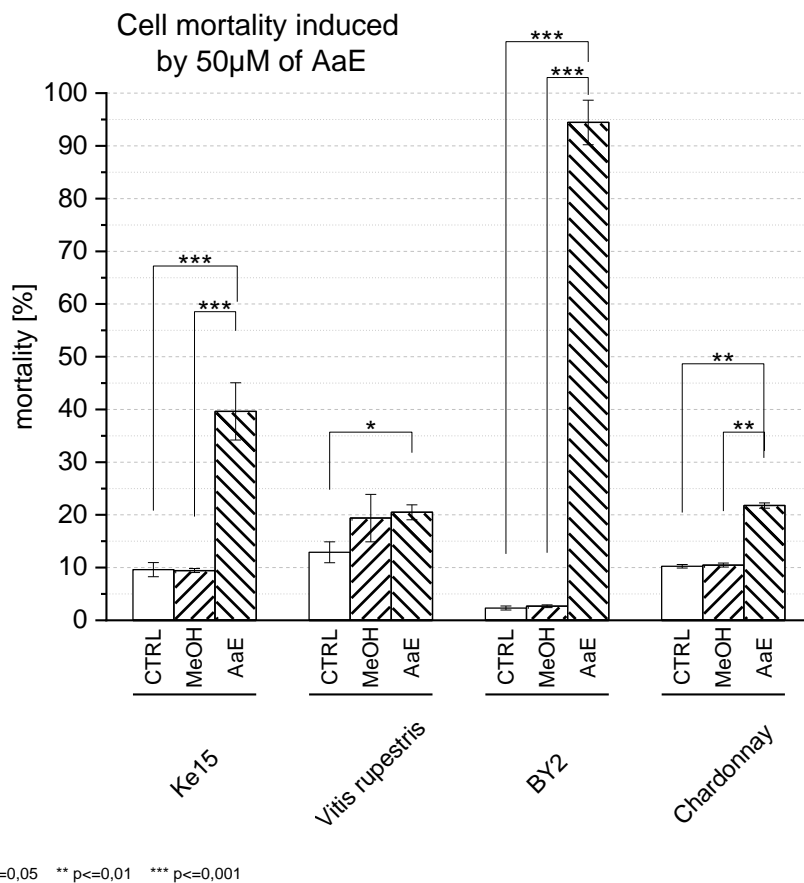

Fig. 9: AaE-induced mortality after 48 h: 2 mL aliquots of all cell lines were treated with 50 µM of AaE, 0.5 % methanol (MeOH) or were entirely untreated, respectively. The samples were incubated at 26°C, in the dark while shaking on an orbital shaker at 150 rpm. Samples were extracted after 48 h and cell mortality was quantified via Evans Blue staining (see Chapter 3.4.2). Treatments were performed as biological triplicates and significance levels were calculated using the Fisher LSD ANOVA with a significance level of 0.05.

The treatment with 50 µM of AaE caused major shifts in cell mortality in the cell lines Ke15, *V. rupestris*, BY2 and Chardonnay. In Ke15 50 µM of AaE caused an increase in mortality to 39.63 % (SE ± 5.43) which is significantly higher than the respective MeOH control with 9.44 % (SE ± 0.66) and negative CTRL with 9.61 % (SE ±1.35). In

Vitis rupestris, we observed a baseline mortality of 12.91 % (SE ± 1.97) in the negative CTRL. Comparing the AaE treatment to the CTRL a small but significant increase to a rate of mortality of 20.49 % (SE ± 1.42) was quantifiable. Yet, this difference is not significantly different from the respective solvent control (MeOH) with a mortality rate of 19.39 % (Se ± 4.51). In BY2 we observed an extreme increase in cell death in the AaE-treated samples. The mortality rate increased to 94.45 % (SE ± 4.22) which was significantly higher than both negative CTRL and MeOH control with mortality rates of 2.33 % (SE ± 0.38) and 2.68 % (SE ± 0.26) respectively. Treating the Chardonnay cell suspension line with 50 µM of AaE caused a significant increase in cell mortality to a rate of 21.77 % (SE ± 0.51) when compared to the respective controls. The negative CTRL of Chardonnay exhibited a cell mortality rate of 10.25 % (SE ± 0.32) and the MeOH control showed a mortality of 10.47 % (SE ± 0.38).
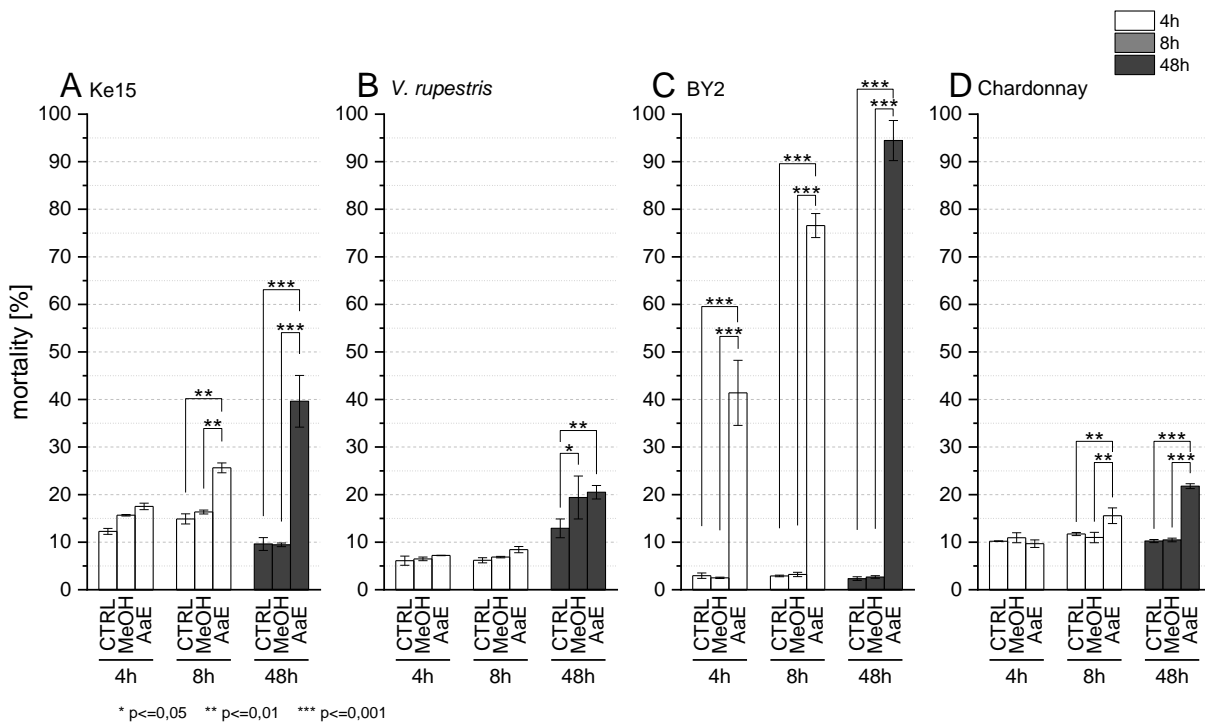

Fig. 10: Timecourse of AaE-induced mortality: 2 mL aliquots of each cell line were treated with 50 µM of AaE and the respective solvent control of 0.5 % methanol (MeOH) and untreated control (CTRL). The samples were incubated at 26°C, in the dark while shaking on an orbital shaker at 150 rpm. Samples were extracted and quantified via Evans Blue staining (see Chapter 3.4.2) at 4 h, 8 h and 48 h post-elicitation. Biological triplicates were generated and statistical analysis was performed via Fisher LSD ANOVA with a significance level of 0.05.

The cell mortality caused by AaE was further investigated by quantifying the mortality at earlier time points. Additional samples were taken at 4 and 8 hours post-elicitation

and quantified via Evans Blue selective staining protocol (see Chapter 3.4.2). When treating the Ke15 suspension cell line with 50 µM of AaE, there is no significant increase in cell mortality observable 4 hours post-elicitation. After 8 hours of incubation, the cell mortality in the AaE-treated sample was significantly increased with 25 % (SE ± 1.03) when compared to the respective negative and solvent controls. At the 48 hours time point, the mortality rate of the AaE treatment is significantly higher than its respective controls and reaches 39.63 % (SE ± 5.43). In *Vitis rupestris* the treatment with AaE and its solvent did not cause a significant increase in cell mortality at the time points 4 and 8 hours when compared to their respective negative CTRL. At the 48 hours time point post-elicitation the treatments with methanol and AaE exhibited elevated levels of cell mortality when compared to the negative CTRL. Yet, there is no significant difference between the AaE-treated sample and the methanol control (MeOH) with mortality rates of 20.49 % (SE ± 1.42) and 19.39 % (SE ± 4.51) respectively. BY2 cells exhibited high levels of cell mortality at all three time points when treated with 50 µM of AaE, significantly higher than their respective controls in all cases. The mortality increased from 41.39 % (SE ± 6.85) at the 4 hours time point to 76.57 % (SE ± 2.53) at 8 hours post-elicitation. At the 48 hours time point, the cell mortality rate induced by AaE reached 94.45 % (SE ± 4.22). In Chardonnay, the 50 µM AaE treatment caused no significant change in mortality at the 4 hours time point. After 8 hours of incubation, the mortality rate increased significantly from its respective controls to 15.55 % (SE ± 1.65) and increased even further at the 48 h time point to 21.77 % (SE ± 0.51) while still being significantly higher than the respective controls.

4.1.2 Cytoskeletal effects induced by *R. subterranea* compound AaE

To see whether the AcetonAdduct of Entatrevenetinon (AaE) has an effect on the actin filaments within the plant cell, cells of the Chardonnay FABD$_2$-GFP line were treated with 50 µM of AaE. Additionally, a positive control with latrunculin B (LatB) was performed. LatB binds to actin monomers, effectively stopping the filaments from polymerizing. Biological triplicates of AaE- and LatB treatment were carried out with their respective solvent control of MeOH and DMSO, respectively, and an entirely untreated negative CTRL.
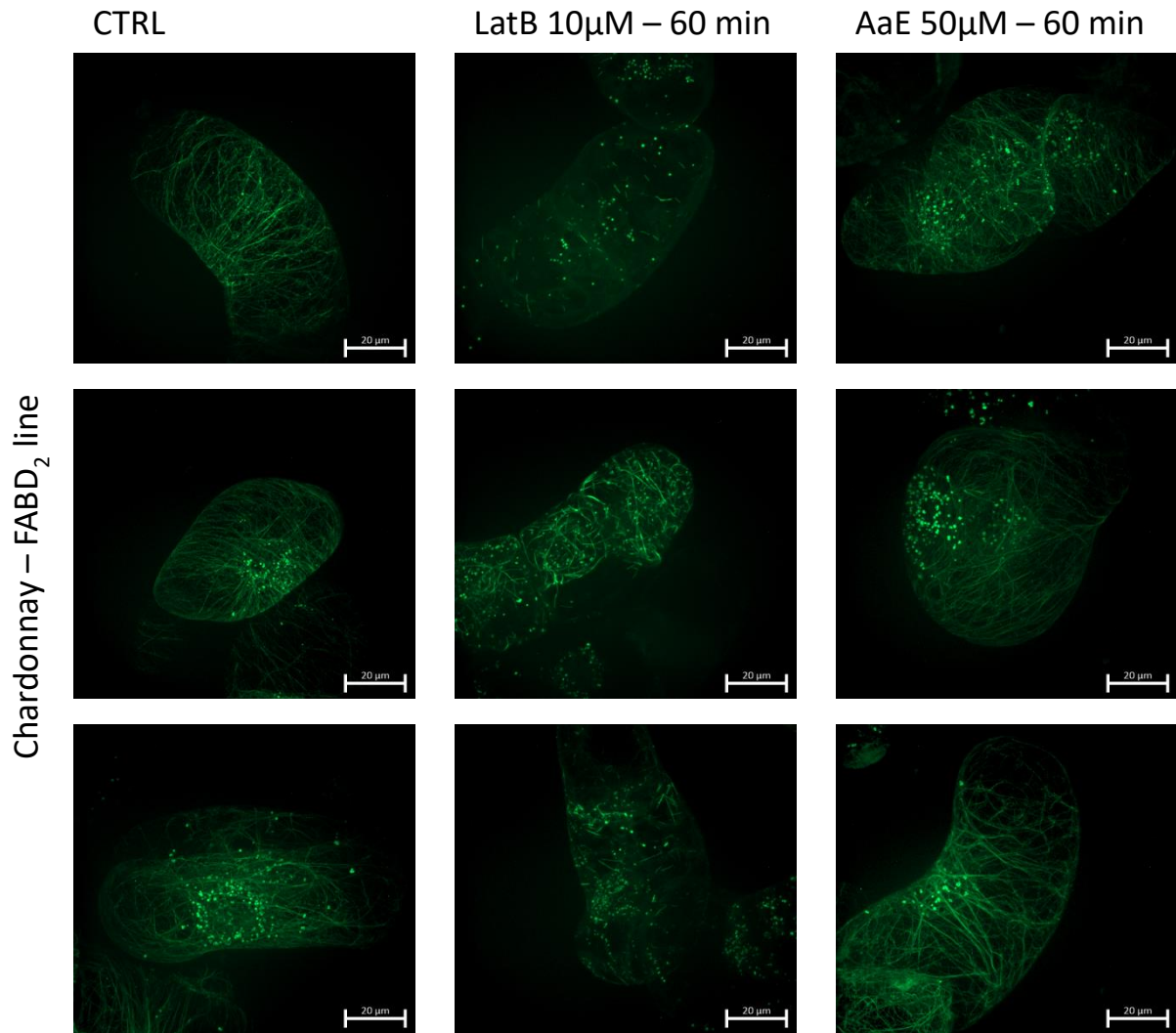
| | CTRL | LatB 10µM – 60 min | AaE 50µM – 60 min |

Fig. 11: Effects of AaE on the actin filament of Chardonnay – FABD2-GFP: Cells of the transgenic line Chardonnay-FABD$_2$-GFP were treated with 50 µM of AaE and 10 µM of latrunculin B (LatB) for 60 minutes. The fluorescence was visualised using excitation filters of 488 nm and emission filters of 509 nm wavelength. For solvent controls please see sFig. 1.

The negative control (CTRL) treatment of Chardonnay FABD$_2$-GFP cells exhibited an undisrupted habitus. The fluorescent signal could be seen as fine filaments spanning the cortex of the cell with occasional aggregates of intense signals visible in the outskirts of the nucleus and rarely in the cell cortex (see Fig. 11). Treating the cells for 60 minutes with 10 µM of LatB caused the majority of the green fluorescent signal to disintegrate. The signal appeared more diffuse with the filaments visible in the CTRL appearing to be broken into smaller pieces. Additionally, the appearance of signal aggregates was more common and more evenly distributed in the cell cortex. In the AaE-treated samples, the aggregates of the signal were slightly more commonly found than in the CTRL samples, yet the filaments of the green fluorescent signal appeared

undisrupted as seen in the CTRL samples. The solvents had little effect on the signal detected in the cells (see sFig. 1).

To visualise the effect of AaE on the microtubules of the plant cell, cells of the BY2 TuA3:GFP cell culture were treated with 50 µM of AaE and 10 µM of oryzalin respectively for 60 minutes. Additionally, there were samples of negative control (CTRL) and solvent controls of MeOH and DMSO. All samples were performed in biological triplicates.
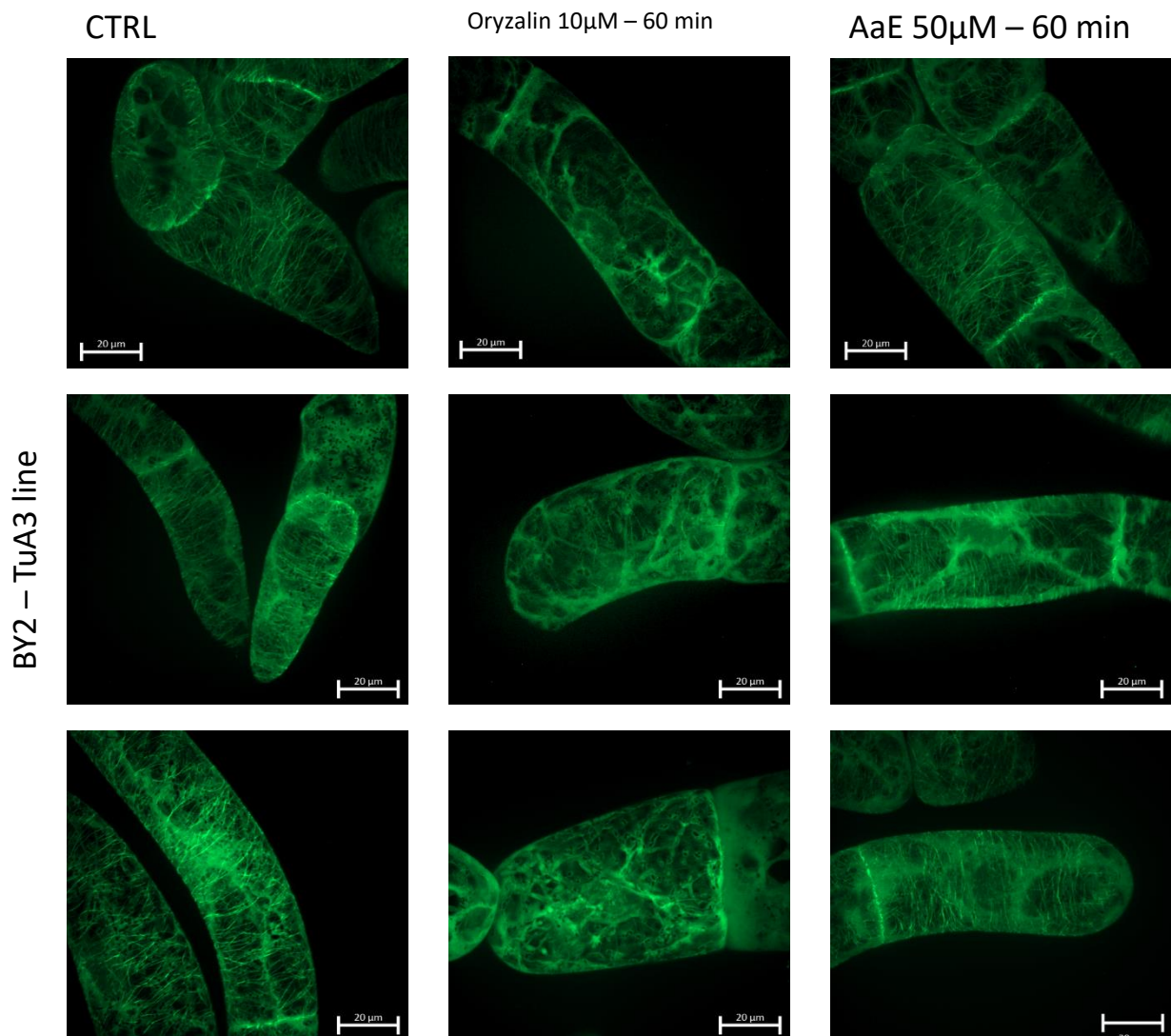
Fig. 12: Effects of AaE on the microtubules of BY2 TuA3:GFP: The cell lines BY2 TuA3:GFP was treated with 50 µM of AaE and 10 µM of oryzalin respectively for 60 minutes. The pictures were taken using fluorescence filters with 488 nm of excitation wavelength and 509 nm of emission wavelength with an exposure time of 500 ms. For the solvent controls please see sFig. 2.

The untreated samples of BY2 TuA3:GFP exhibited an undisturbed habitus of the cell line. The green fluorescent signal has shown a background signal but also formed

visible filaments spanning across the cortex of the cell. In the oryzalin-treated samples, the filaments have almost entirely disintegrated. There was a strong diffuse green fluorescent background signal with occasional, broken filaments. In samples treated with AaE, there was also a strong background signal of green fluorescence, yet the filaments of the signal seem to be similar to the ones exhibited in the negative CTRL. The controls for the solvents of the elicitors, MeOH and DMSO had little effect on the intracellular signals (see sFig. 2).

4.1.3 Effect of AaE on the expression of defence-related genes

To quantify the gene expression of commonly observed defence-related genes in plant cell lines exposed to 50 µM of AaE, cells of Ke15, *V. rupestris*, Chardonnay and BY2 were treated with AaE for 4 hours, and their total RNA was extracted and converted to cDNA (see Chapter 3.3.4). Gene expression was quantified using RT-qPCR and fold induction of the gene of interest was calculated relative to the expression of the housekeeping gene in the negative control. We looked at the expression pattern of the genes PAL, STS27 and STS47 to get insight into the metabolic activity of the synthesis of phytoalexins. We also quantified the expression of PR1 and JAZ1 as markers for the salicylic acid and jasmonate signalling respectively.
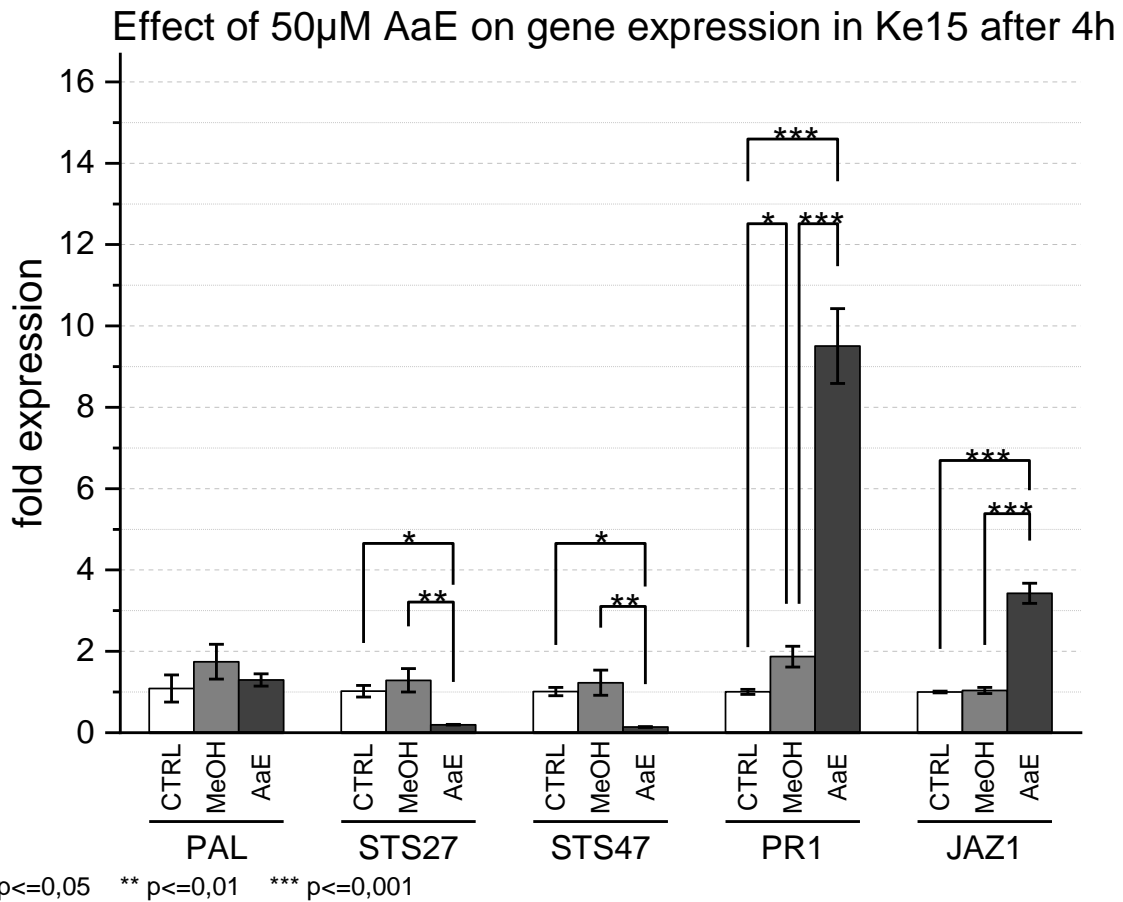
Effect of 50µM AaE on gene expression in Ke15 after 4h

* p<=0,05   ** p<=0,01   *** p<=0,001

Fig. 13: Gene expression with 4 h 50 µM AaE treatment in Ke15: Suspension cells of *V. vinifera* Ke15 were treated with 50 µM of AaE for 4 hours, and RNA was extracted and converted into cDNA. Gene expression in the samples was quantified using RT-qPCR and the fold induction was standardized to the housekeeping gene ubiquitin in the negative CTRL. Significance was calculated using the Fisher LSD ANOVA with a significance level of 0.05.

In Ke15, the exposure to 50 µM of AaE caused no significant difference in the expression of PAL after 4 hours of incubation. Both stilbene synthases STS27 and STS47 exhibited a significant and almost ten-fold reduction of expression when AaE was present (see Fig. 13). STS27 was at a 0.20-fold (SE ± 0.01) expression and significantly different from both negative and MeOH control. STS47 exhibited a 0.14-fold (SE ± 0.01) expression. This value was significantly different from the respective controls. The expression of PR1 was significantly induced to a level of 9.5-fold (SE ± 0.92) (see Fig. 13). The fold induction of the AaE treatment was significantly higher than both negative CTRL and the MeOH treatment. The MeOH treatment showed a slightly but significantly higher expression of PR1 than the respective negative control with a 1.87-fold (SE ± 0.26) induction. In the presence of

AaE, the expression of JAZ1 was significantly increased 3.43-fold (SE ± 0.25) when compared to both the negative and the solvent control (see Fig. 13).
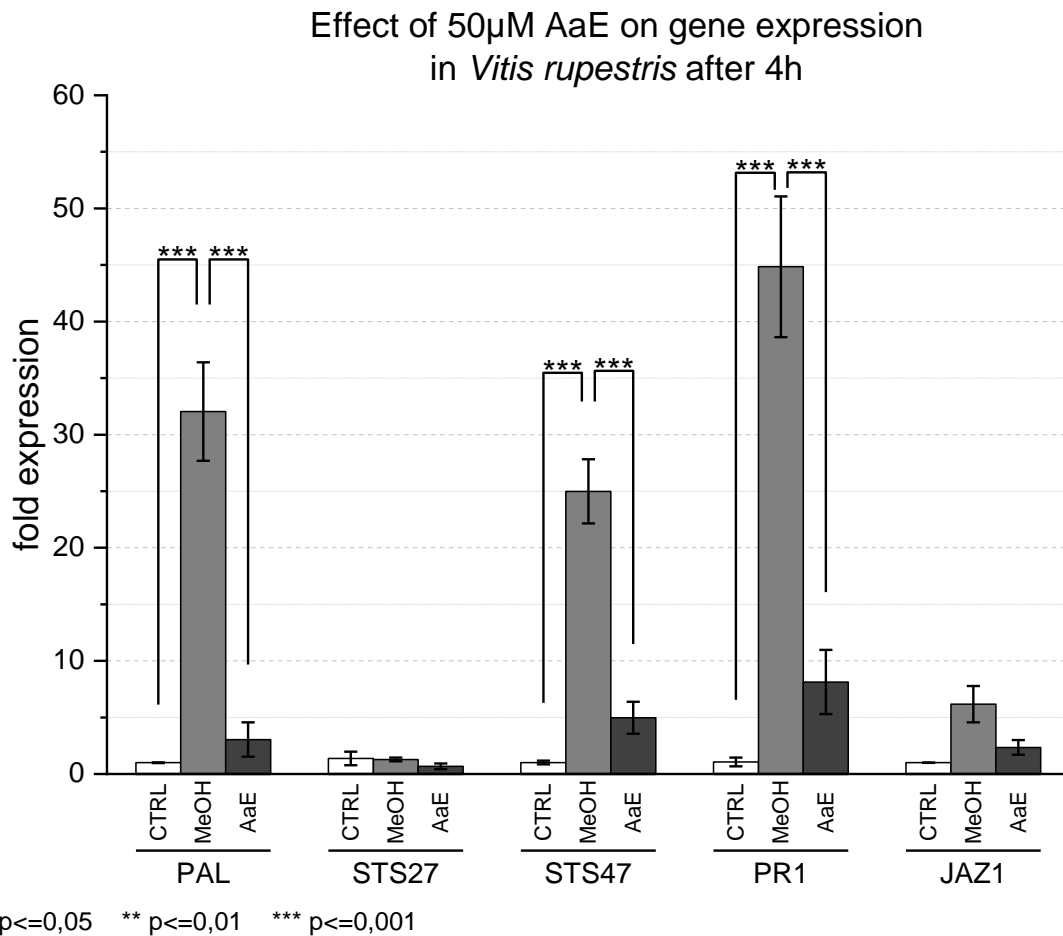

Fig. 14: Gene expression with 4 h 50 µM AaE treatment in *V. rupestris*: Cells of the suspension line *V. rupestris* were treated for 4 hours with 50 µM of AaE and the respective solvent control. Total RNA was extracted and converted into cDNA. Expression patterns of the genes were quantified using RT-qPCR. The fold induction was calculated and standardized to the housekeeping gene ubiquitin in the negative CTRL. The significance of differences was calculated via ANOVA using the Fisher LSD with a significance level of 0.05.

In *Vitis rupestris*, the treatment with 50 µM of AaE did not significantly change the expression of PAL when compared to the negative CTRL. Yet, the solvent control, 0.5 % methanol caused a 32.05-fold (SE ± 4.35) induction of PAL (see Fig. 14). This is significantly higher than both the negative control and the AaE treatment. The AaE treatment caused no significant change in the expression of STS27 (see Fig. 14). The gene STS47, on the other hand, was significantly induced by a factor of 24.99 (SE ± 2.83) due to the methanol treatment. The STS47 expression in the AaE

treatment was significantly reduced when compared to the MeOH control but did not significantly differ from the expression in the negative control (see Fig. 14). In PR1 the expression increased 44.85-fold (SE ± 6.22) when treated with 0.5 % methanol. This expression was both significantly higher than the negative control and the 50 µM AaE treatment (see Fig. 14). The gene expression due to AaE was increased to 8.14-fold (SE ± 2.83) but failed to be significantly different from the negative control. The JAZ1 expression in *V. rupestris* showed a tendency to be increased in the methanol control and the AaE treatment to be reduced when compared to said control, yet all treatments failed the tests for significance (see Fig. 14).
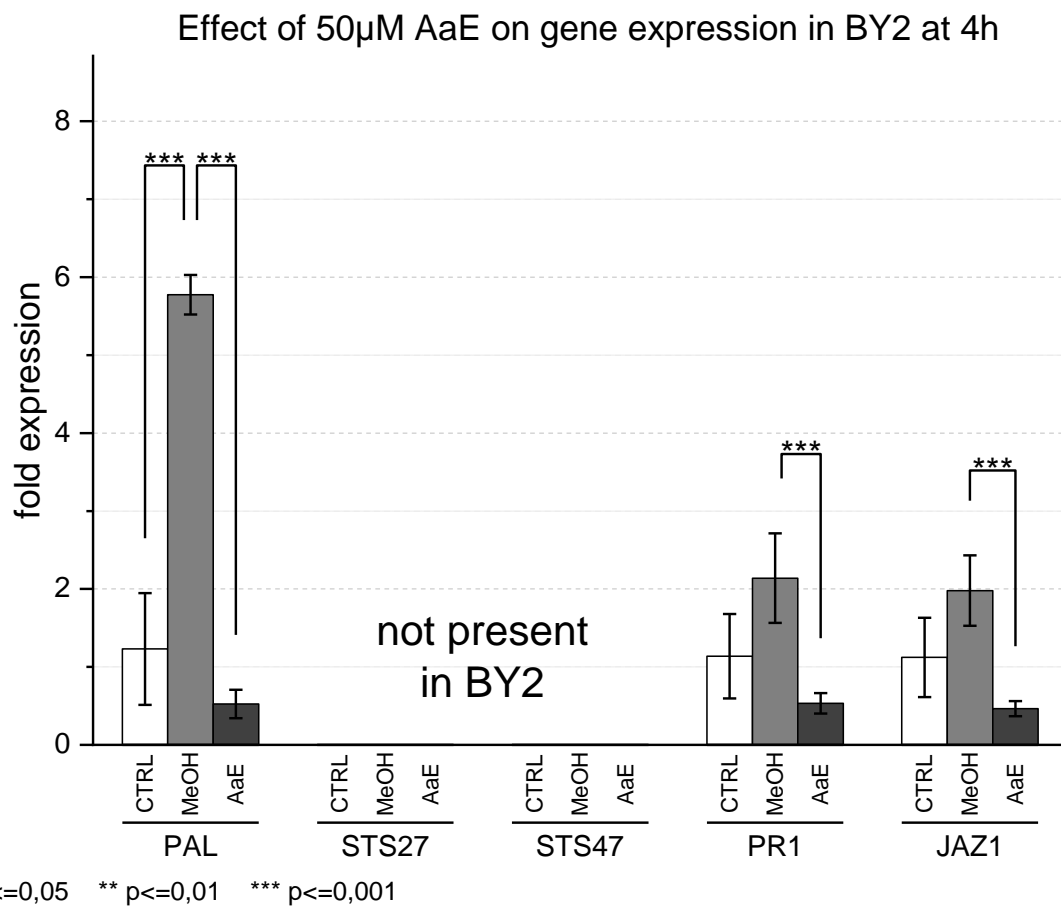
Fig. 15: Gene expression with 4 h 50 µM AaE treatment in BY2: BY2 wild-type cells were treated with 50 µM of AaE. After 4 hours, the total RNA was extracted and converted into cDNA. The gene expression in the samples was quantified via RT-qPCR and fold induction was calculated by standardizing to the expression level of the housekeeping gene ubiquitin in the negative CTRL. The significance of the differences was calculated via the Fisher LSD ANOVA using a significance level of 0.05.

The expression levels of the defence-related genes were tested in BY2 using the same primers as were used in the *Vitis* lines. The primers were designed for use in *Vitis* and thus, did not perfectly bind to the respective primer sites in the *Nicotiana tabacum* line. This was reflected in the melting curve analysis of the RT-qPCR (data not shown). This resulted in the standard error of the measurements in BY2 being bigger as compared to the *Vitis* lines. In BY2 the solvent of AaE, methanol did significantly induce (5.77-fold (SE ± 0.25)) the expression of PAL when compared to both the negative CTRL and the AaE treatment (see Fig. 15). The expression of PAL in the AaE-treated sample did not significantly differ from the expression level in the negative control. *N. tabacum* does not have naturally occurring stilbene synthases, therefore the expression levels of STS27 and STS47 were not able to be reliably quantified and were therefore omitted. PR1 and JAZ1 showed similar expression patterns. For both genes, the treatment with 0.5 % MeOH showed a tendency to induce an increased expression of the respective gene, yet failed to be significantly different from the negative control, due to high error margins (see Fig. 15). In both genes, the expression in the AaE-treated sample was significantly lower than compared to the respective methanol control, but not when compared to the negative CTRL.
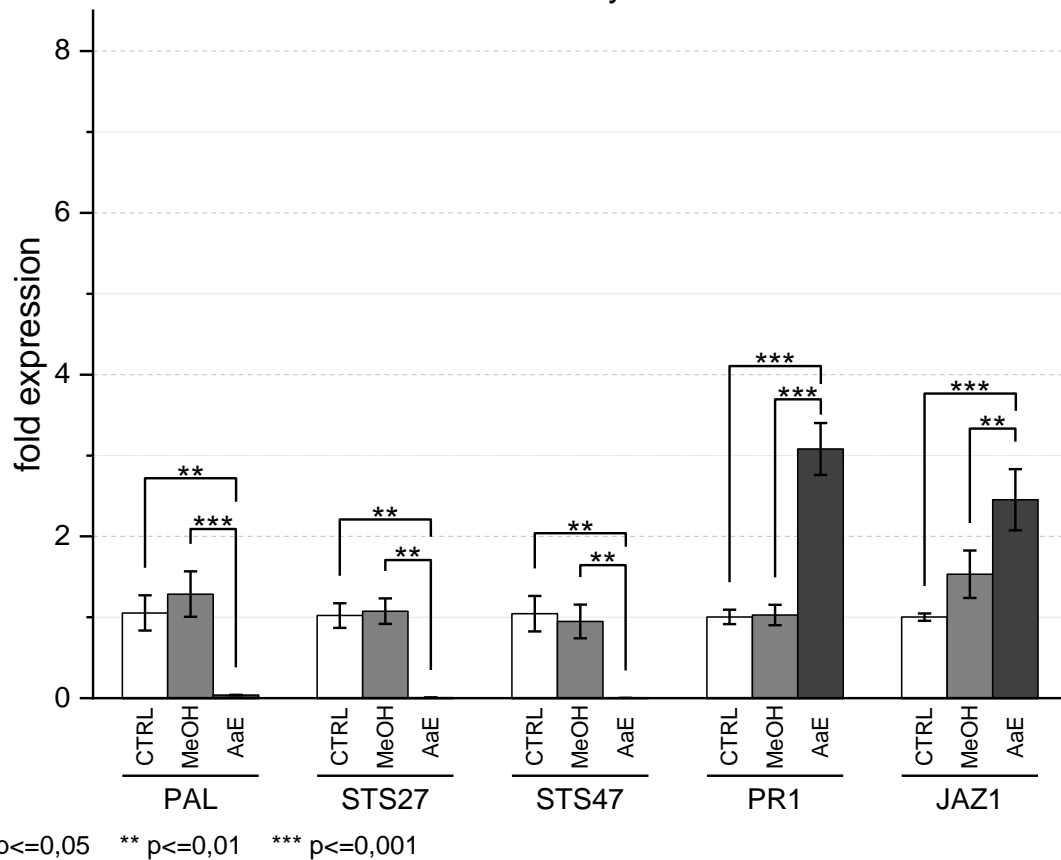
Fig. 16: Gene expression with 4 h 50 µM AaE treatment in Chardonnay: To quantify the gene expression in Chardonnay, suspension cells have been treated with 50 µM for 4 hours. The total RNA was subsequently extracted and converted to cDNA. The gene expression was quantified using an RT-qPCR. The fold induction was calculated using the expression of the housekeeping gene ubiquitin of the negative CTRL to standardize. The significance levels between the samples were calculated using the Fisher LSD ANOVA with a significance level of 0.05.

In *Vitis vinifera* cv. Chardonnay the treatment with 50 µM AaE caused a significant reduction of expression in PAL, STS27 and STS47 after 4 hours. The expression of PAL was reduced to 0.038-fold (SE $\pm$ 0.002), the expression of STS27 to 0.006-fold (SE $\pm$ 0.001) and the expression of STS47 to 0.002-fold (SE $\pm$ 0.0002). These expression levels were all significantly reduced when compared to their respective controls, whereas the solvent control of 0.5 % methanol (MeOH) did not significantly differ from the negative control (see Fig. 16). The expression level of PR1 was increased 3.08-fold (SE $\pm$ 0.32) in the 4 h AaE treatment when compared to the respective controls (see Fig. 16). The expression level of PR1 was not significantly altered from the level in the CTRL by the presence of 0.5 % MeOH. The level of JAZ1

expression was slightly but not significantly higher in the MeOH-treated samples when compared to the negative control. The treatment with 50 µM of AaE caused a significant induction of JAZ1 of 2.45-fold (SE ± 0.38). This induction was significantly different from both negative and methanol control (see Fig. 16).

4.2 Microfluidics: an abstract ecosystem

4.2.1 Plant cell cultivation

When detecting a leak in the Microfluidic BioReactors (MBR) during any sort of experimentation, the cause of the leak was identified in cooperation with the cooperation partner and subsequently, design and fabrication were improved.

To test the viability of different cell lines cultivated inside of the MBR, 800 µL of either BY2, Chardonnay, Ke15 or *Vitis rupestris* cell suspension were loaded into the cell chamber of the MBR. The cell suspension within the MBR was supplied with a steady flow of standard MS medium (see Chapter 2.2) at a pump rate of 30 µL/min for seven days. After seven days a sample of the cell suspension was taken from the cell chamber by extracting it through an opening in the MBR and cell mortality was quantified using the Evans Blue selective staining protocol (see Chapter 3.4.2). The mortality of the MBR cultivation was compared to the mortality of the respective cell suspension cultivated with an established Erlenmeyer flask cultivation (see Chapter 3.1).

* p<=0,05   ** p<=0,01   *** p<=0,001
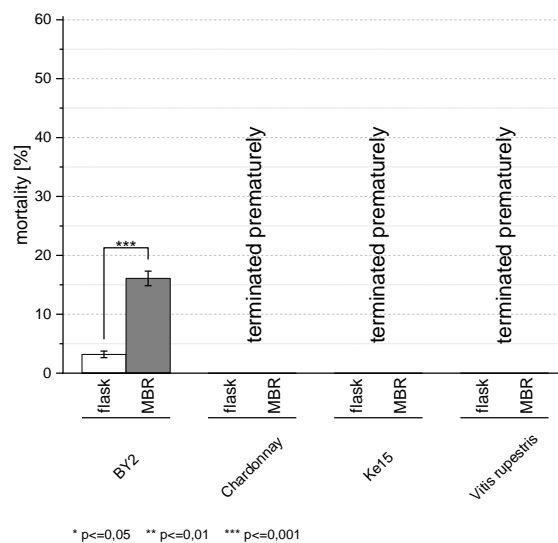
Fig. 17: Cell mortality in long-time MBR cultivation: 800 µL of cell suspension of BY2, Chardonnay, Ke15 and *Vitis rupestris* were loaded into separate MBRs and cultivated for seven days at an MS medium flow rate of 30 µL/min. Control samples were cultivated in Erlenmeyer flasks for seven days, in the dark at 26°C while shaking at 150 rpm on an orbital shaker. Cell mortality was quantified by extracting a sample after seven days and applying the Evans Blue selective staining protocol (see Chapter 3.4.2). Samples of Chardonnay, Ke15 and *V. rupestris* visibly deteriorated within a few days. Therefore the experiment was prematurely stopped and the samples were not quantified via Evans Blue. Of the BY2 samples, biological triplicates were performed. The significance of the difference in the values was calculated using a Fisher LSD ANOVA with a significance level of 0.05.

The cell suspensions of BY2, Chardonnay and Ke15 were easy to transfer into the cell chamber of the MBR using a truncated tip of a 1000 µL pipette. The tip was truncated in a way the diameter of the resulting tip opening was just smaller than the diameter of the opening of the MBR's cell chamber. Thus, closing the opening as air-tight as possible, the pipetting forced the cell suspension into the chamber with minimal pushback. The cell suspension of *Vitis rupestris* proved more difficult due to cell aggregation. The cells did not enter the cell chamber easily and mainly remained in the opening of the chamber. After closing all openings of the cell cultivation chamber, pumping was resumed and the system was checked daily. All *Vitis* line samples visually deteriorated after a few days. The colour of the cell suspension changed from greenish-yellow to a darker brownish tone, indicating that the cells were dying quickly. At this point, the experiments cultivating the lines Chardonnay, Ke15 and *V. rupestris* were terminated prematurely. After seven days the colour of the BY2 cultivation did not change but one MBR proved to be leaky. The corresponding replicate was stopped because a constant supply of fresh MS medium was not guaranteed. Samples were taken from both the remaining MBR systems and the respective flask-cultivated control and cell mortality was quantified in all biological replicates.

The cell mortality observed in the flask-cultivated samples (n=3) of BY2 was 3.19% (SE ± 0.56) and was significantly lower than the mortality observed in the MBR-cultivated cells (n=2) with a mortality rate of 16.09 % (SE ± 1.23) (see Fig. 17). Since extreme cell mortality was observable in the Chardonnay, Ke15 and *V. rupestris* samples within a few days, the experiment was stopped and the precise cell mortality was not quantified (see Fig. 17).

4.2.2 Plant cell cultivation with elicitation

To check the feasibility of the cells incubated within a Microfluidic BioReactor (MBR) system to react to a substance that is supplied via the medium flow of the system, BY2 wild-type cells were loaded into an MBR, were supplied with an MS medium containing 27 µg/mL of harpin. Harpin is a known elicitor of an Effector Triggered Immunity (ETI) response with a corresponding Hypersensitive Response (HR) cumulating in programmed cell death (PCD) (see Chapter 1.2.4). Therefore, the potential reaction of the BY2 culture was read out by quantifying the cell mortality induced by an harpin treatment of two days.
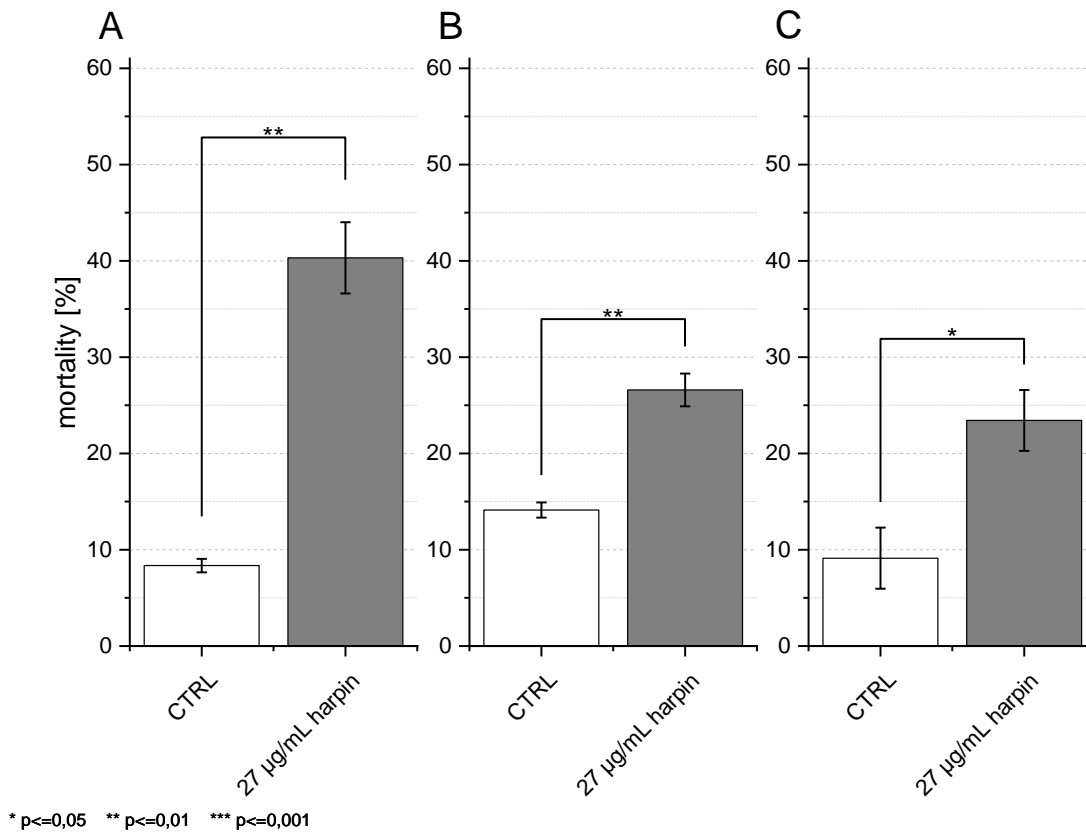
* p<=0,05   ** p<=0,01   *** p<=0,001

Fig. 18: Cell mortality in harpin-treated BY2 wild-type cells in the MBR system: 800 µL of BY2 wild-type cells were loaded into each MBR and continuously supplied with a medium via a peristaltic pump at a pump rate of 30 µL/min. Both the harpin-treated and the control (CTRL) samples were equilibrated with an untreated MS medium for 60 min. Subsequently, the harpin-treated samples were switched to an MS medium containing 27 µg/mL harpin. Cell mortality was quantified after two days of incubation via Evans Blue staining (see Chapter 3.4.2). Each set of experimentations was performed with triplicates of CTRL and harpin treatment. The entire experiment was performed thrice to observe variations in the results at different dates. The significance of differences was calculated via a Fisher LSD ANOVA with a significance level of 0.05.

In addition to three biological replicates per treatment (CTRL and harpin), the entire experiment was repeated three times on three separate dates to look at the variations. In the first set of experiments (see Fig. 18 A), the cell mortality in the CTRL MBRs was at 8.36 % (SE ± 0.7) and the mortality in the harpin-treated samples was significantly increased with a mortality rate of 40.31 % (SE ± 3.7). In the second set of experiments on a later date (see Fig. 18 B) the baseline mortality in the negative CTRL was slightly higher with a rate of 14.13 % (SE ± 0.79). The respective harpin treatment exhibited a significantly higher cell mortality of 26.59 % (SE ± 1.7). In the third and final set of experiments (see Fig. 18 C) a mortality rate of 9.12 % (SE ± 3.17) was observable in the CTRL with a significantly higher mortality of 23.43 % (SE ± 3.16) in the harpin-

treated samples. In all three technical replicates, the mortality in the control was higher than the death rate observed in the flask treatment (see Fig. 17), yet there was a significant difference observable between the respective treatments.

4.2.3 Fungal cultivation in MBR

Microfluidic BioReactors (MBR) could potentially be used to install multiple MBRs in sequence, with the single MBRs containing different kinds of cells. This could be used to cultivate similar cells that individually overexpress different enzymes to create an artificial metabolic cascade (Finkbeiner et al. 2022) or it could be used to co-cultivate cells belonging to different kingdoms like fungal and plant cells. This harbours the potential to screen the reaction of plant cells to the presence of different fungal strains and then identify communication signals in the medium, should a reaction be observed.

To test the feasibility of cultivating a cell suspension of *Neofusicoccum parvum* within the cell chamber of an MBR, 800 µL of a one-day-old cell suspension of *N. parvum* was loaded onto an MBR to conduct long-time cultivation of seven days. The MBR system was supplied with fresh MS medium using a peristaltic pump operating with a pump rate of 137 µL/min. The fungal suspension was loaded into MBRs that were constructed with both a membrane with a pore size of 5 µm or a pore size of 1 µm respectively. The system was supplied with sufficient amounts of standard MS medium (see Chapter 2.2) and checked daily. Yet, in all replicates, regardless of the membrane installed the setup broke down within two or three days: the Tygon tubing (see Table 3) connected to the inlet of the MBR popped off due to a pressure building in the inlet. After the long-time cultivation was forcefully prematurely terminated, the MBR containing *N. parvum* was observed using brightfield microscopy (see Table 4).
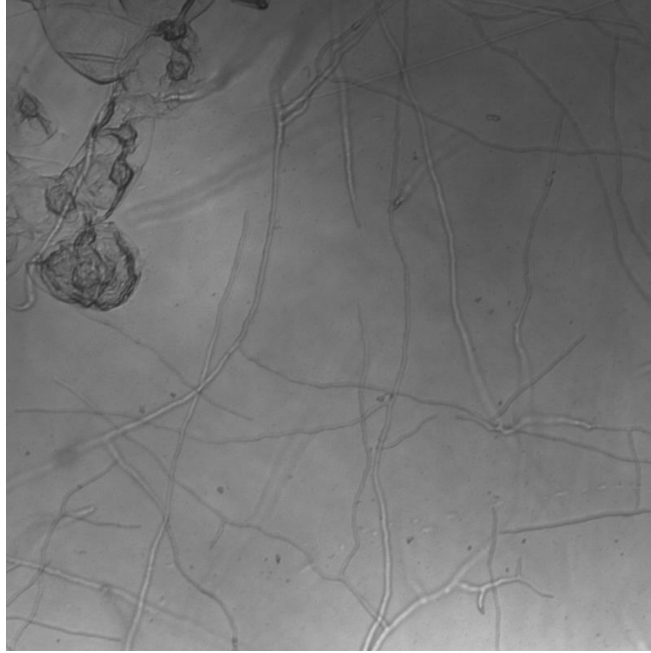
Fig. 19: Hyphae of *Neofusicoccum parvum* in the cell chamber of the MBR system: Brightfield microscopy picture of the hyphae of *N. parvum* growing in the cell chamber of an MBR system. The picture was taken with brightfield filters and an exposure time of 15 ms. The cell debris in the picture originated from an earlier cultivation of BY2 wild-type cells in the MBR that were not properly cleaned out.

The entire cell chamber of the MBR was filled with the hyphae of *N. parvum*, evenly distributed. The picture in Fig. 19 was taken near the centre of the MBR to represent the density of hyphae found throughout the cell chamber.

Fig. 20: Hyphae of *N. parvum* growing into the inlet and outlet of the MBR system: Brightfield microscopy pictures were taken of both the inlet and outlet of the MBR with an exposure time of 15 ms. An overview schematic of an MBR visualises where the pictures were taken. Hyphae of *N. parvum* grew into both inlet and outlet of the MBR with the density of hyphae being higher in the inlet. The membrane installed into the MBR observed had a pore size of 1 µm.

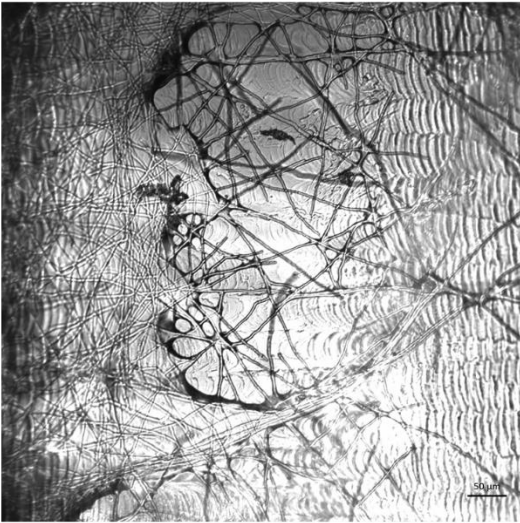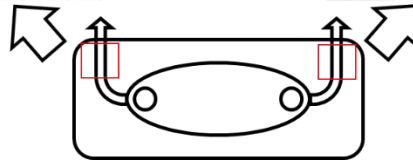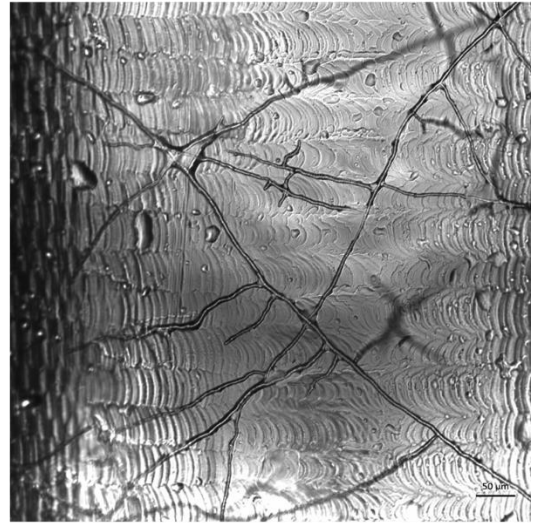First cultivation experiments with *N. parvum* were performed using MBRs that contained a membrane with a pore size of 5 µm. The fungus was easily able to grow into the inlet and outlet of the MBR, thus blocking the flow of the MS medium into the inlet. This caused pressure to build and the Tygon tube connected to the inlet to loosen. To restrict the access of the fungus to the perfusion chamber and thus the inlet, the cooperation partner installed a membrane into the MBR with a pore size of 1 µm. Yet, even in the MBRs with drastically smaller pores, the fungus was still able to grow into the inlet and outlet of the MBR (see Fig. 20). The density of hyphae in the inlet was higher than the density of hyphae in the outlet (see Fig. 20).

4.2.4 Co-Cultivation of fungus and plant

To test the feasibility of co-cultivating two cell types belonging to different species across kingdoms barriers, a co-cultivation experiment was conducted cultivating both a Microfluidic BioReactor (MBR) containing fungal cells of *Neofusicoccum parvum* and an MBR containing BY2 wild-type cells in the same system. The fungal MBR was filled with 800 µL of a one-day-old suspension cell line of *N. parvum* and the plant MBR was

filled with 800 µL of seven-day-old BY2 wild-type cells. Both MBRs were installed in sequence so the unidirectional MS medium flow generated by the peristaltic pump supplied first the cells in the fungal MBR and subsequently reached the MBR cultivating the BY2 cells (see Chapter 2.1.4). Therefore potential metabolites of the fungus were able to be transported into the MBR with the plant cells. The reaction of the BY2 cells to the presence of the prior *N. parvum* culture was quantified as the resulting mortality rate by extracting BY2 cells after two days of co-cultivation and applying the Evans Blue selective staining protocol (see Chapter 3.4.2). This was compared to a control (CTRL) group consisting of singular MBRs cultivating only BY2 wild-type cells. Both the co-cultivation and the CTRL were supplied with the same standard MS medium.

* p<=0,05   ** p<=0,01   *** p<=0,001
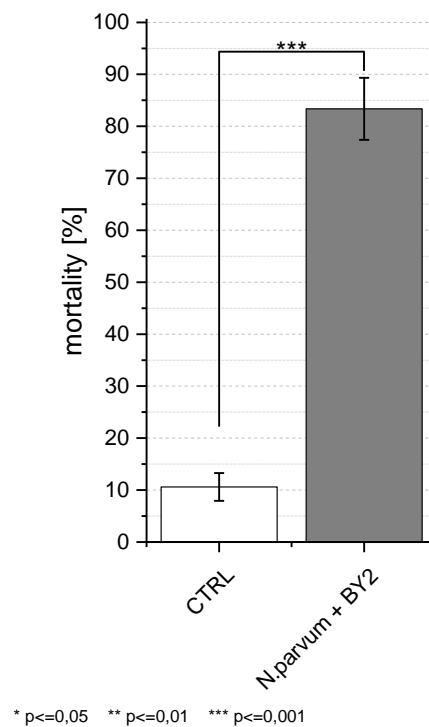
Fig. 21: Cell mortality observed in BY2 cells during co-cultivation with *N. parvum*: The co-cultivation (*N. parvum* + BY2) consisted of two MBRs installed in sequence. The first MBR contained 800 µL of one-day-old *N. parvum* culture and the latter 800 µL of seven-day-old BY2 cells. The CTRL consisted of singular MBRs with 800 µL of BY2 cells. All treatments were supplied with standard MS medium. Cell mortality was quantified after two days of cultivation via Evans Blue staining. Three biological replicates were performed each and significance levels were calculated using Fisher LSD ANOVA with a significance level of 0.05.

In the negative control (CTRL) the extracted samples of the BY2 culture exhibited cell mortality of 10.6 % (SE ± 2.67). The mortality rate of the BY2 cells grown in the co-cultivation treatment (*N. parvum* + BY2) was significantly higher with a value of

83.36 % (SE ± 5.98). All experiments were performed in biological triplicates and due to the restricted two-day period of the experiment, no sealing of the connecting tubes to the fungal MBR failed (see Fig. 21). The results described above are published in Finkbeiner et al. (2022).

4.2.5 MBR pH measurement

The observation of a shift in the extracellular pH of plant cells is an established method to detect early signalling in the defence reactions of plants. This is due to the influx of Ca^{2+} ions being an integral part of early signalling (Lecourieux et al. 2006). The transport of Ca^{2+} across the membrane causes a shift in the extracellular pH due to the effects of the depolarization of the membrane and the shift of ion balance (Jabs et al. 1997; Nürnberger and Scheel 2001; Felle 2001). To see whether it would be feasible to measure a shift in pH within the Microfluidic BioReactor (MBR) during the cultivation process, a cell suspension of BY2 wild-type was transferred into the cell chamber of an MBR. After an equilibration period, a pre-measurement of 30 minutes was performed to calculate a baseline. Subsequently, the cells were exposed to 25 µg/mL of chitosan, a known elicitor of a basal defence reaction coinciding with a shift in pH. The pH was continuously measured for 120 minutes with optic means using a pH sensor system by PreSens (see Table 4). The interface between this sensor and the MBR was designed by the cooperation partner (see Chapter 3.4.6).
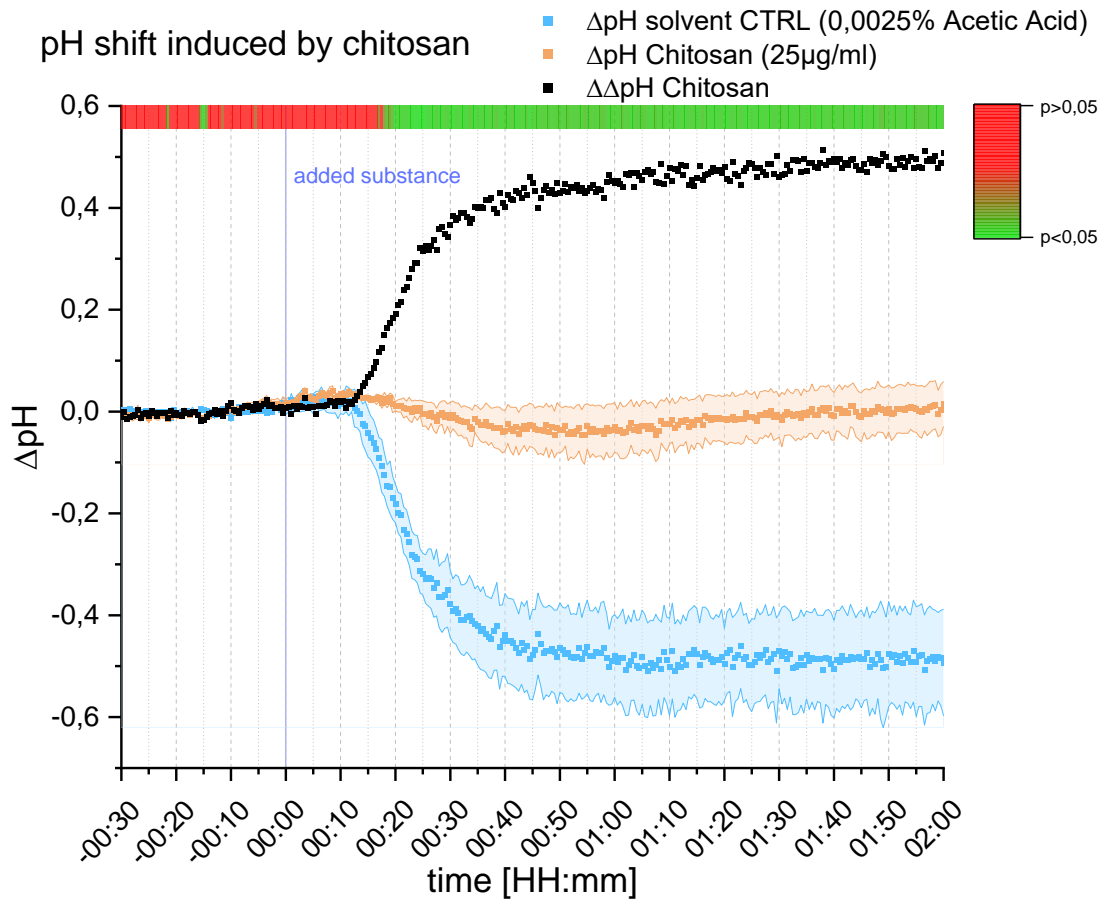
Fig. 22: Extracellular pH of BY2 cells treated with chitosan measured in the MBR system: 800 µL of seven-day-old BY2 wild-type cells was cultivated inside of the cell chamber of an MBR. The system was equilibrated for 90 minutes and a pre-measurement was done to calculate a baseline pH. The supplied medium was changed to MS medium containing 25 µg/mL chitosan and the time point was defined as 00:00. The pH was measured for 120 minutes with measurements every 30s. The graph shows the ΔpH of both the chitosan treatment, the solvent control (CTRL) and the calculated $\Delta\Delta$pH of chitosan. The significance of the difference between chitosan and the solvent control was calculated via a Student's t-test and is visualised via a heat map aligned with the time scale.

The ΔpH$_{solvent}$ decreased starting at an estimated 9 minutes after the elicitor was added to the MS medium supplied. The pH value decreased until 40 minutes after elicitation started and reached a value of -0.44 (SE ± 0.08). This value did not change severely for the remainder of the measurement. ΔpH$_{chitosan}$ only decreased slightly and stabilised near 0 (SE ± 0.05). Correcting for the ΔpH$_{solvent}$ that the solvent of chitosan caused, the $\Delta\Delta$pH$_{chitosan}$ of chitosan rises sharply at 15 minutes post elicitation, reaches a plateau at around 40 minutes post elicitation and stabilizes around 0.5. A significant difference between the ΔpH$_{chitosan}$ and ΔpH$_{solvent}$ was detectable as early as 17 minutes post elicitation (see Fig. 22).

4.2.6 MBR pH measurement - chitosan double pulse

To test whether the MBR system could be used to treat plant cells cultivated within with multiple subsequent pulses of a signal while continuously measuring the pH, BY2 cells situated in the cell chamber of an MBR were treated with pulses of 0.0025 % acetic acid and 25 µg/mL chitosan. After an equilibration period, the pH was measured for 30 minutes to calculate a baseline. To pulse a signal, the medium supplied to the MBR system was switched for 10 minutes to an MS medium containing the substance of interest. After the first treatment concluded, the pH was measured for 45 minutes after which the second treatment was started.
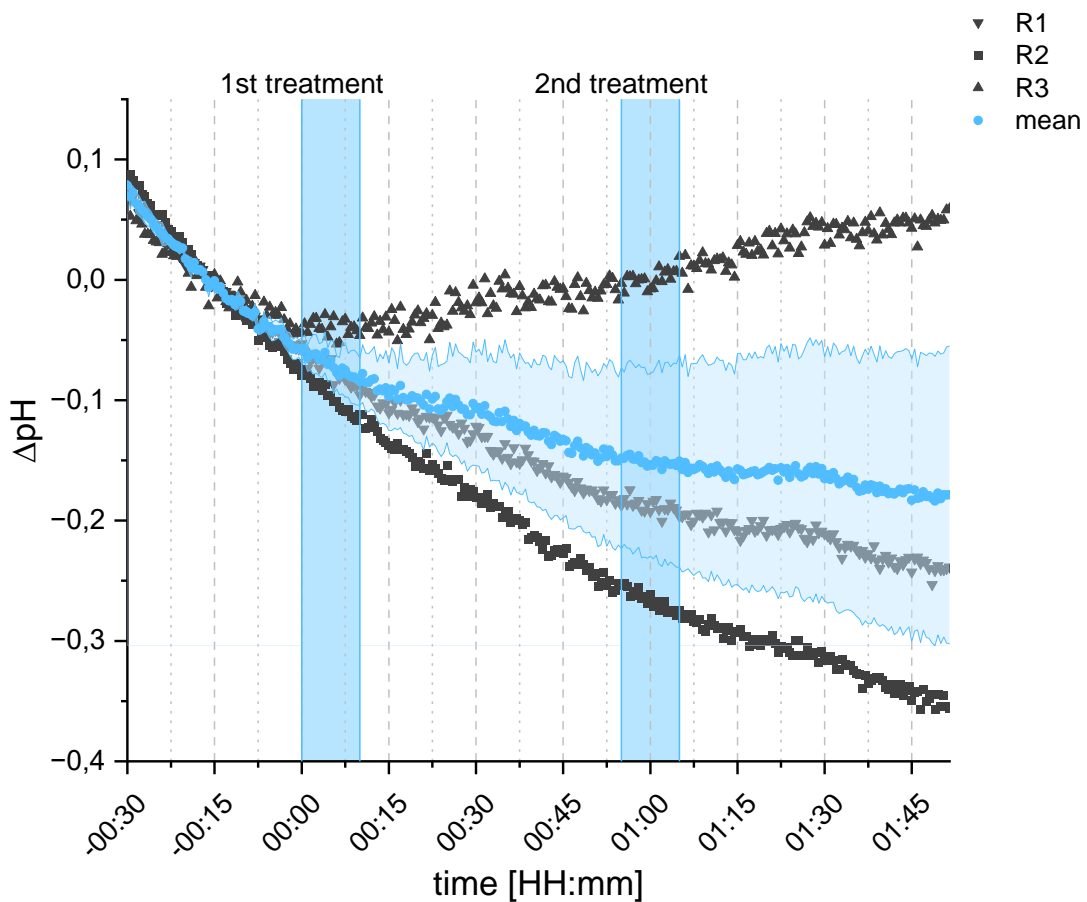
Fig. 23: Extracellular pH of BY2 cells treated with a double pulse of acetic acid: 800 µL of BY2 cells were cultivated in an MBR system supplied with standard MS medium. The system was equilibrated for 45 minutes and a pH baseline was measured for 30 minutes. For the treatments, the MS medium was switched with an MS medium containing 0.0025 % acetic acid for 10 minutes. The start of the first treatment was defined as the time point 00:00. The second treatment was started after measuring 45 minutes once the first treatment concluded. This graph shows the ΔpH of three replicates of the solvent control treatment and their mean with the respective standard error visualised as a ribbon graph.

In all three replicates of the solvent control (slvCTRL), the pH continuously decreased before the first treatment was started at 00:00. In replicate three (R3), the pH slightly increased the entire duration of the experiment after the first treatment started. In both replicate one (R1) and two (R2), the pH kept decreasing during the entirety of the measurement. After the second treatment, there appears to be a minor peak in R1 and R2 at around 01:27 (see Fig. 23). The standard error of the mean is too big to validate the peak after the second treatment.
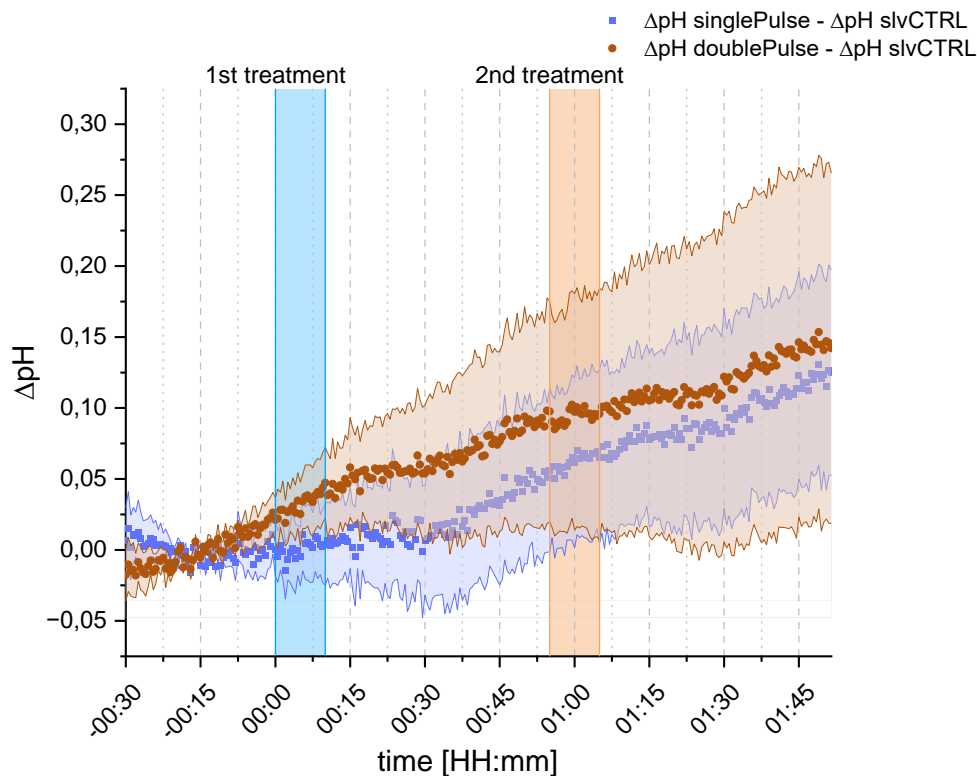
Fig. 24: Extracellular pH of BY2 cells treated with pulses of acetic acid and chitosan: 800 µL of BY2 cell suspension was introduced into the MBR system supplied with a standard MS medium. After equilibrating the system for 45 minutes a baseline was measured for 30 minutes. For the treatments, the supplied MS medium was switched for 10 minutes with an MS medium containing a substance of interest. The start time of the first treatment was defined as 00:00. The second treatment was started after measuring the pH for 45 minutes once the first treatment concluded. The singlePulse treatment was first treated with 0.0025 % acetic acid and subsequently with 25 µg/mL chitosan. In the doublePulse treatment, the cells were elicited with 25 µg/mL chitosan in both treatments. The graph shows the mean ΔpH of both singlePulse and doublePulse subtracted by the ΔpH slvCTRL. The standard error is visualised as a ribbon graph.

In Fig. 24 the ΔpH of both singlePulse and doublePulse were standardized to the slvCTRL (see Fig. 23). Starting at -00:15, the means of both treatments kept increasing during the experiment to a maximum of above ΔpH 0.10 (see Fig. 24). The ΔpH values of the singlePulse treatment were consistently below the values of the doublePulse treatment. Yet, the standard error is too wide at all times to validate any differences between and within the treatments (see Fig. 24). In the doublePulse treatment, there was no additive increase in pH caused by the second pulse of chitosan.

4.2.7 MBR H_2O_2 measurement

An increase in Reactive Oxygen Species (ROS) levels can be used as an indicator to detect stress signalling in plants. In our institute, rising ROS levels have been measured in relation to the application of salt stress (Ismail et al. 2012). To see whether a stress-related increase in ROS levels would be detectable within the Microfluidic BioReactor (MBR) system, BY2 wild-type cells cultivating in the cell chamber of the MBR were treated with 150 mM of NaCl and the H_2O_2 levels in the medium runoff have been quantified using the Amplex™ Red Hydrogen Peroxide/Peroxidase Assay Kit (see Table 6) and using a microplate reader to measure the resulting fluorescence. To quantify the H_2O_2 levels, a standard curve has also been created and measured.
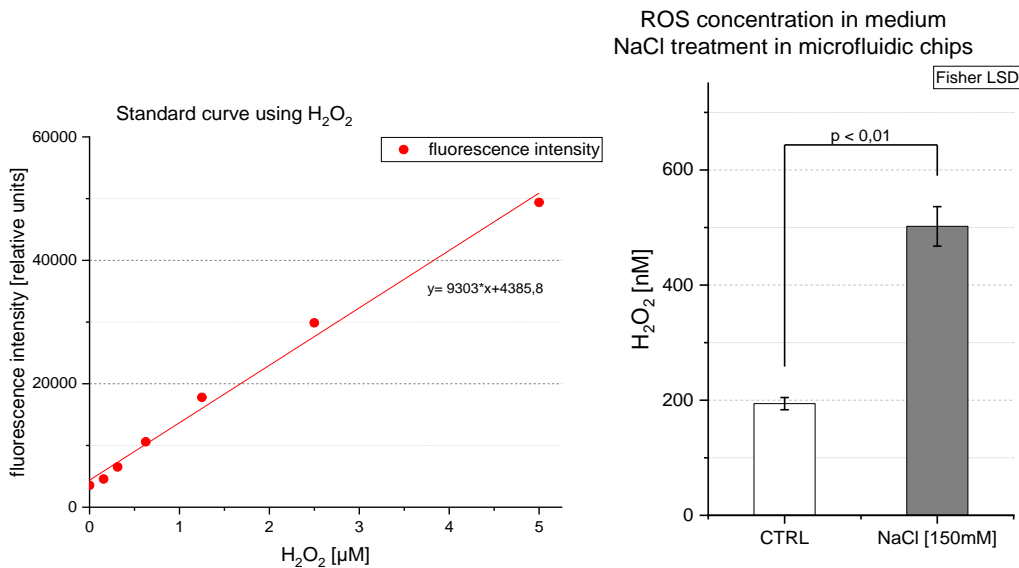
Fig. 25: H_2O_2 measurement in medium runoff of the MBR: BY2 cells cultivating inside of the cell chamber of the MBR were treated with 150 mM of NaCl added to their MS medium for 90 minutes. Afterwards, the medium transported out of the outlet of the MBR was collected and H_2O_2 levels within were quantified using the Amplex™ Red Hydrogen Peroxide/Peroxidase Assay Kit. Absolute values of the H_2O_2 concentration were calculated using a standard curve. The data represents one biological replicate for CTRL and NaCl treatment with three technical replicates each. Significance levels were calculated using a Fisher LSD ANOVA with a significance level of 0.05.

Using the standard curve (see Fig. 25) the relative fluorescence measured in the samples in the technical replicates of either CTRL and NaCl treatment was converted into a concentration of H_2O_2 in the medium runoff. In the CTRL we were able to detect a concentration of 194.11 nM (SE ± 10.64) H_2O_2. In the BY2 samples that were treated with 150 mM of NaCl the concentration of H_2O_2 was significantly increased to 502.06 nM (SE ± 34.22). The replicates analysed here were technical replicates.

5. Discussion and Outlook

5.1 *Roesleria subterranea* and the Acetonadduct of Entatrevenetinon

5.1.1 Mortality induced by *R. subterranea* compounds

To get first insights into the potential immunoactivity of the isolated metabolic compounds that the ascomycete *Roesleria subterranea* produces, Sclerodin and the AcetonAdduct of Entatrevenetinon (AaE) were tested on three *Vitis* cell lines and BY2 wild-type cells. An Effector Triggered Immunity (ETI) response oftentimes coincides with Programmed Cell Death (PCD) of cell tissues to hinder the advance of an attacking pathogen. Therefore, an easy-to-quantify method to detect potential immune reactions is to look for an increase in cell mortality when treating plant cells with a Substance of Interest (SoI). In this work, we treated cell suspension lines of *V. vinifera slyvestris* Ke15, *V. rupestris* and Chardonnay with 50 µM of either Sclerodin or AaE and quantified the mortality rate of the cells after predetermined amounts of time. The same procedure was also performed on *Nicotiana tabacum* BY2 wild-type cells as a well-established control group.

The treatment of the cell lines with 50 µM of Sclerodin for 48 h yielded no significant changes in cell mortality in all cases. In Ke15 there was a small but significant decrease in cell mortality, but this difference was not significant when compared to its respective solvent control of 0.5 % methanol (MeOH) (see Fig. 8). Additionally, this decrease, albeit significant, is negligible in comparison to the changes in mortality observed in the AaE-treated samples (see Fig. 9). In *Vitis rupestris*, 50 µM of Sclerodin did not induce cell mortality, but the MeOH control showed increased levels of cell mortality. Combining this with findings in the gene expression (see Fig. 14) methanol seems to activate immunity signalling in *V. rupestris*. Munnik et al. (1995) showed that methanol could activate the phospholipase D. *V. rupestris* likely relies on this signalling pathway during its defence response more than the other *Vitis* lines observed do. In BY2 the treatment with Sclerodin slightly but significantly increased the mortality when compared to the negative CTRL, but not compared to the MeOH control (see Fig. 8). In Chardonnay, there were no changes in mortality regardless of the treatment (see Fig. 8). We can confidently say, that 50 µM of Sclerodin did not cause cell death, nor an ETI-associated PCD in the lines Ke15, *V. rupestris*, Chardonnay and BY2.

Treating these cell lines with 50 µM of AaE, on the other hand, caused drastic and significant increases in the mortality rates in Ke15, Chardonnay and BY2, but

surprisingly did not so in *Vitis rupestris* (see Fig. 9). After 48 hours of incubation, BY2 exhibited an extreme mortality rate of 94.45 % (SE ± 4.22) while the *V. rupestris* samples treated alike showed no significant increase in mortality when compared to the respective MeOH control (see Fig. 9). This was surprising since in our lab we consider BY2 cells to be rather inactive regarding the speed and intensity of the defence reaction, while *V. rupestris* is generally accepted as a cell line that reacts rather quickly and intensely, when faced with a challenge to the immune system, especially regarding PCD. In the two European lines of *Vitis*, Ke15 and Chardonnay, the treatment with 50 µM AaE caused a significant increase in mortality levels after 48 hours when compared to the controls (see Fig. 9). The cell lines are relatively closely related, yet exhibited differing mortality rates. Ke15 showed a mortality of 39.63 % (SE ± 5.43) and Chardonnay died at a rate of 21.77 % (SE ± 0.51).

A time course was created to get insight into the rate at which mortality increases. In BY2 the significant increase in mortality already set in at 4 hours with 41.39 % (SE ± 6.85). At 8 h post-elicitation, the rate of mortality was at 76.57 % (SE ± 2.53) and at 48 h reached 94.45 % (SE ± 4.22) (see Fig. 10). In all *Vitis* lines, there was no mortality observable at 4 hours. In *Vitis rupestris,* general mortality increased in all treatments at 48 h, yet AaE had no significantly different effect (see Fig. 10). In Ke15 and Chardonnay, the increase in mortality set in at 8 h post-elicitation and increased even further at 48 h of incubation (see Fig. 10). The PCD set in late and increased further at later time points.

We believe the AcetonAdduct of Entatrevenetinon (AaE) to be a specific signal, that is recognized by some cell lines. These subsequently engage PCD upon detection of AaE. For one, the mortality observed is likely caused by deliberate mechanisms and signal transduction that need time to be engaged since, with the exception of BY2, the onset of cell mortality is delayed (see Fig. 10). If the mortality was caused by general toxicity, we would assume the cells start dying quicker. Additionally, cell lines that are closely related differ in the intensity of their reaction, like Ke15 and Chardonnay. Ke15 is a wild relative of the local cultivar *Vitis vinifera* cv. Chardonnay. More striking, the North American relative *Vitis rupestris* seems entirely unreactive concerning cell mortality. These differences between close relatives imply a signal specificity of AaE and the underlying signalling pathways to differ between the species.

5.1.2 Cytoskeletal effects induced by *R. subterranea* compound AaE

Changes in the integrity and composition of the cytoskeleton can be signs of a defence reaction (Wang et al. 2022b; Sofi et al. 2023) or cell death. To see whether the detection of AaE engages signalling pathways that include effects on the cytoskeleton, we treated cells of the lines Chardonnay FABD$_2$-GFP and BY2 TuA3:GFP with 50 µM of AaE for 60 minutes. These cell lines are marker lines for the actin filaments and microtubules respectively (see Chapters 2.1.6 and 2.1.7).

After 60 minutes of treatment, AaE did not affect the actin filament or the microtubules of the respective cell lines (see Fig. 11 and Fig. 12). To be able to compare the effect to a positive control that disintegrates the respective cytoskeletal element controls with latrunculin B and oryzalin were included. AaE-treated cells resembled cells of the untreated CTRL in both cell lines. Additionally, the solvent controls for AaE had little effect on the cell lines (see sFig. 1 and sFig. 2). Therefore we propose that AaE signalling does not engage the reorientation or disintegration of both actin filament and microtubules within one hour of treatment. This would imply that the signalling pathways triggered would not involve the cytoskeleton. Yet, to make sure, it might be necessary to look at later time points once sufficient amounts of AaE would be available.

5.1.3 Effect of AaE on the expression of defence-related genes

To get insight into the mode of action, the reaction of plant cells to the detection of AaE applies, we treated cell suspension lines of *Vitis vinifera sylvestris* Ke15, *V. rupestris*, and *V. vinifera* cv. Chardonnay with 50 µM of AaE and quantified gene expression 4 hours after elicitation. The same procedure was performed on cells of BY2 as a well-established control group within our institute. The 4-hour time point was chosen, because the cell mortality, which was potentially caused by a defence reaction of the plant was observed at 8 hours post-elicitation (see Fig. 10). Therefore, the respective signalling processes must have necessarily been taking place before. We observed the expression patterns of PAL, STS27 and STS47 to get insight into the metabolic processes generating the so-called phytoalexins, secondary metabolites the plants synthesize to defend themselves. Additionally, we quantified the expression of both PR1 and JAZ1 as marker genes for the salicylic acid and jasmonate signalling pathways, respectively.

In all *Vitis* lines, the treatment with 50 µM AaE for 4 hours did inhibit the expression of genes associated with the synthesis of phytoalexins. In both Ke15 and Chardonnay, the expression of STS27 and STS47 was downregulated from the baseline of negative and solvent control (see Fig. 13 and Fig. 16). In *V. rupestris* the expression of STS47 was induced by the solvent of AaE, 0.5 % methanol. The AaE-treated sample of this line, on the other hand, was significantly downregulated when compared to the solvent control. Therefore, it seems as though AaE downregulated the expression of STS47 that was caused by the solvent it was in (see Fig. 14). PAL, the enzyme committing phenylalanine into the phenylpropanoid pathway and thus towards the generation of phytoalexins, was also downregulated by AaE in *V. rupestris* and Chardonnay. In Ke15, the genes seemed to be unaffected (see Fig. 13). In BY2 the expression of PAL was downregulated when compared to the level that the solvent of AaE induced. Due to the expression levels in PR1 and JAZ1, it seemed as if the salicylic acid and the jasmonate signalling pathways were engaged in Ke15 and Chardonnay (see Fig. 13 and Fig. 16). This was juxtaposed with negative regulation of these signalling pathways in BY2 and *V. rupestris*. Whereas the expression of JAZ1 in *V. rupestris* only hints at inhibition and fails the significance test (see Fig. 14). Here, repetition of the experiment might produce more reliable results.

AaE seems to have been able to inhibit the expression of genes that are involved in the synthesis of phytoalexins in Ke15 and Chardonnay, while the signalling pathways of salicylic acid and jasmonate were engaged. While *Vitis rupestris* is relatively closely related to these species, it starkly differed in the expression levels of PR1 and JAZ1. While AaE seemed to induce signalling in both pathways in Ke15 and Chardonnay, it inhibited them in *V. rupestris*. This might imply a certain signal specificity in the signalling of the detection of AaE. The notion, that the signalling between the species differs is also supported by the fact that in *Vitis rupestris* the expression of PAL and STS47 was induced by MeOH. This might be caused by the possible involvement of phospholipase D (Munnik et al. 1995) in the signalling in *V. rupestris*, and the lack thereof in the European species.

5.1.4 Resumé and Outlook

Looking at both the results of the mortality assay and the observation of the gene expression in the *Vitis* lines, an interesting pattern emerges. 50 µM of AaE induced an increase in cell death in both *Vitis vinifera sylvestris* Ke15 and *Vitis vinifera* cv. Chardonnay starting at 8 hours post-elicitation and increasing even further until 48 hours post-elicitation (see Fig. 10). This coincided with a decrease in the expression of PAL, STS27 and STS47 involved in the synthesis of the defence compounds phytoalexins (see Fig. 13 and Fig. 16), while characteristic genes for stress signalling involving salicylic acid and jasmonate were induced. The closely related species, *Vitis rupestris*, exhibited no significant increase in mortality when treated with AaE, yet was also inhibited in the expression of PAL and STS47 (see Fig. 10 and Fig. 14). Contrasting the pattern in Ke15 and Chardonnay, the expression of PR1 was downregulated, with JAZ1 hinting at a similar pattern while failing the significance test (see Fig. 14), implying both the salicylic acid and jasmonate signalling pathway were inhibited by AaE in *V. rupestris*. We believe the cell mortality we observed to be Programmed Cell Death (PCD) normally inherent to a successful defence reaction of the plant. This claim is supported by the late onset of mortality at 8 hours post-elicitation(see Fig. 10), implying the involvement of deliberate mechanisms to induce cell death and signalling. The fact that the European Chardonnay and Ke15 differed so starkly from their close relative *V. rupestris* in both cell death and gene expression also supports the claim of the involvement of signal detection and transduction. The molecular structures of Sclerodin and AaE are quite similar (see Fig. 1), but they had contrasting effects on the cell lines, also hinting at a signal specificity. Additionally, the expression of the stress-signalling genes PR1 and JAZ1 hints at the cell death occurring to be PCD, especially with PR1 and its association with salicylic acid being a marker gene for PCD (Brodersen et al. 2005). With the mortality observed likely caused by PCD inherent to defence reactions, the inhibition of synthesis genes of phytoalexins in Ke15 and Chardonnay (see Fig. 13 and Fig. 16) is remarkable! *Roesleria subterranea* might be able to uncouple the expression of certain defence genes from the PCD of a defence reaction using AaE as a signal and effector, thus using inherent defence mechanisms of the plant to kill its tissue to generate dead material to nourish the parasitic fungus.

It would be interesting to see whether AaE treatment can downregulate an induction of defence genes caused by other elicitors.

5.2 Microfluidics: an abstract ecosystem

5.2.1 Plant cell cultivation

To test the feasibility to cultivate different established cell lines inside of the Microfluidic BioReactor (MBR), cell suspensions of BY2, Chardonnay, Ke15 and *Vitis rupestris* were cultivated inside the cell chamber of the MBR. The aim was to compare the general cell mortality observed after seven days of the established flask-based cultivation in our lab to the seven-day cultivation within the MBR. Therefore 800 µL of each cell suspension were loaded into separate MBRs, supplied with fresh MS medium (see Chapter 2.2) at a pump rate of 30 µL/min (see Chapter 3.4.3). The systems were checked daily and the samples for the comparative quantification of cell mortality were taken after seven days of incubation in either MBR or the flask-based control groups (see Chapter 3.1).

As described in Chapter 4.2.1, all *Vitis* lines observed quickly deteriorated when cultivated inside of the MBR. The colour of the cell suspension quickly changed from a greenish-whitish-yellow to a darker brownish tone. This can also be observed in flask-based cultivation if the culture ages way beyond its point of subcultivation and is a clear sign of the culture dying. Since all the *Vitis* lines showed this indication of massive cell death occurring within a few days, the experiments with the lines Chardonnay, Ke15 and *V. rupestris* were prematurely stopped and the cell mortality in neither flask-based control nor the MBR cultivation was quantified for these samples (see Fig. 17). The cells of the *V. rupestris* suspension line tend to form small aggregates in suspension. Generally, this does little to negatively affect experiments done with the line, yet proved detrimental to the cultivation of the line in the current iteration of the MBR system. Due to the size of the cell clumps, the cell line was not able to easily enter the cell chamber of the MBR while transferring the liquid culture into the system. The vast majority of the *V. rupestris* cells aggregated in the cell chamber opening, thus rendering an equal distribution of nutrients to the cells of the culture improbable. Additionally, it appeared as though the cultivation within the MBR proved inherently stressful to the *Vitis* lines, as all samples of Chardonnay, Ke15 and *V. rupestris* exhibited extreme mortality within a few days.

On the other hand, the cultivation of BY2 wild-type cells within the MBR proved uncomplicated. The cell suspension was of an agreeable viscosity to enter the cell chamber easily and did not change its colour during the long-time cultivation

experiment. Yet, one replicate of the MBR system was leaky and was terminated, since it was not guaranteed the cells were sufficiently supplied with MS medium. After seven days, samples of the remaining MBR systems were taken, as well as samples of a respective flask-based control (see Chapter 3.1). Cell mortality in all samples taken was quantified and compared. The cell mortality in the MBR system proved to be significantly higher at 16.09 % (SE ± 1.23) when compared to the mortality rate of 3.19% (SE ± 0.56) in the Erlenmeyer flask cultivated control group (see Fig. 17). Yet, the increased mortality in the MBR treatment was still well within an acceptable range of cell mortality to experiment with. Thus, BY2 wild-type suspension cells were deemed compatible with the cultivation within this MBR setup. Therefore, the majority of the MBR experimentation in this work was done with suspension cells of BY2 wild-type.

For future applications, it would be important to reevaluate the feasibility of the MBR cultivation of different species and to expand the efforts for *Vitis* cultivation. It would be interesting to check, whether cell suspension cells of *Arabidopsis thaliana* are compatible with the MBR system. As an extremely well-established and widespread model organism, work with *A. thaliana* harbours great potential for transferring results from and to the work with the MBR to different fields. Additionally, a lot of transformants of *A. thaliana* already exist and the transformation of the organism is very streamlined.

5.2.2 Plant cell cultivation with elicitation

To perform a proof of concept experiment, BY2 cells cultivated within the cell chamber of a Microfluidic BioReactor (MBR) were treated with 27 μg/mL of harpin, a known elicitor of immunity-related Programmed Cell Death (PCD). The experiment was designed to see whether a cell suspension in the MBR would react to a substance of interest mixed into the medium supplied to the system. The reaction of the cell line was quantified by observing the mortality rate of the suspension cells after two days of incubation with the elicitor (see Chapter 3.4.2).

The experiment has been repeated on three separate dates with three replicates per treatment. In all three instances, there was a significant difference observable between the CTRL group and the respective harpin treatment (see Fig. 18 A, B and C). The considerable variation between the absolute values between the different sets of experiments was likely caused by differences in the handling of the MBR system. In early experiments with the system, ideal placements of the MBR itself and the tubing used were still uncertain. This may have also been amplified by naturally occurring

shifts in the state of the BY2 wild-type cell culture. While BY2 is quite stable, it still can underly slight variations in vigour at different times of the year.

Since the harpin treatment proved to exhibit significantly higher mortality than its control in all cases, the proof of concept was deemed successful. The MBR system can be used to treat BY2 cells cultivated in the presence of the substances of interest in the supplied medium.

5.2.3 MBR fungal cell cultivation and co-cultivation:

5.2.3.1 Fungal cultivation

To co-cultivate different cell types belonging to different species, even kingdoms, this work tested the feasibility to cultivate fungal cells in the Microfluidic BioReactor (MBR) system. A suspension cell line of *Neofusicoccum parvum* was transferred into the cell chamber and attempted to be cultivated for longer periods (see Chapter 3.4.4). The transferal of the *N. parvum* cells into the MBR via pipetting through an opening of the MBR cell chamber proved easy enough. The ascomycete entered the cell chamber easily and grew throughout the chamber (see Fig. 19). The fungus was first cultivated in MBRs that were constructed using a membrane with a pore size of 5 µm to separate the cell- and perfusion chamber. *N. parvum* was easily able to grow through the membrane and into the perfusion chamber. There it grew into the inlet and the outlet of the MBR, progressively blocking the flow of medium into the perfusion chamber. This caused pressure to build within the inlet and finally, the tube sealing connecting the peristaltic pump to the MBR to fail. This caused the system to break down after two to three days. To restrict the access of the hyphae to the perfusion chamber, the project partner installed membranes into the MBR system with a pore size of 1 µm. Yet, even in the MBRs with a pore size of 1 µm, the hyphae of *N. parvum* were able to grow into the perfusion chamber and thus inlet and outlet (see Fig. 20) and finally blocking the inlet, causing the sealing to fail. Notably, the density of hyphae seems to be higher in the inlet when compared to the outlet of the same MBR (see Fig. 20). This is likely due to the fungus growing along the gradient of nutrients and thus towards the inlet of the MBR, where fresh MS medium is introduced into the chamber. The hyphae of *N. parvum* should grow at a minimal diameter of 2 µm and should not be able to fit through the pores. Yet, possible explanations for that might be tears in the membrane due to the fabrication process of the MBR. Additionally, in the production process of the membrane, multiple single 1 µm pores might happen to be placed too narrowly,

thus creating a bigger combined pore, through which the hyphae could easily pass (personal correspondence with cooperation partner).

The cultivation of *N. parvum* in the cell chamber has caused the MBR system to break after two to three days but the cultivation in principle is possible for shorter periods. Therefore, the MBR with a pore size of 5 µm was used to cultivate the fungus in the co-cultivation experiments and the co-cultivation period was restricted to two days (see Chapter 3.4.4).

5.2.3.2 Co-cultivation

In the co-cultivation experiment, a significantly higher and extreme mortality rate was observed in the BY2 wild-type culture growing in the MBR that was installed behind the MBR containing an *N. parvum* culture (see Chapter 2.8.2). This implies that a bioactive substance has been transported from the *N. parvum* culture via the unidirectional MS medium flow into the MBR containing the BY2 wild-type cells. The plant cells reacted to or were affected by the presence of this substance and died at a significantly higher rate when compared to the respective CTRL (see Fig. 21). Whether the observed mortality was caused by Programmed Cell Death (PCD) inherent to a defence reaction mounted in response to the detection of a fungal metabolite or whether it was caused by a phytotoxin produced by *N. parvum* cannot be deduced with the present results and requires further investigation. To elucidate the nature of the mortality the plant culture could be tested for characteristic signs of defence, i.e. the expression of defence-related genes or DNA laddering inherent to PCD. These results achieve the proof of concept, that the MBR system can be used to co-cultivate differing cell types and observe the reaction of the cell to the presence of one another. The component responsible for the reaction of the cells in a latter MBR must have necessarily been transported via the medium flow. Therefore analytical methods to identify the substance can be concentrated onto the medium. Given that streamlined methods to quickly detect the defence reaction of a cultivated plant cell line in the MBR are established, this system can potentially be used to perform high-throughput screening of cultivated fungal strains or other plant cells that were cultivated previously in the sequence of MBRs installed in a system. This could be used to quickly screen for bioactive molecules or metabolites that trigger a plant's immune system.

5.2.4 MBR pH measurement

Efficient use of the Microfluidic BioReactor (MBR) system requires the ability to monitor the physical reaction of cell cultures cultivated within. Early signalling of a defence reaction relies on the transport of Ca^{2+} from the apoplast into the cytoplasm of the plant cell. This transport across the plasma membrane coincides with a shift in the extracellular pH due to the depolarization of the membrane and the movement of ions across it (Jabs et al. 1997; Nürnberger and Scheel 2001; Felle 2001). To detect a basal defence reaction of plant cells within the MBR a system was designed by a cooperation partner to interface optic means of measuring the pH with the MBR system (see Chapter 3.4.6).

The connector screw designed by the project partner in the IMT was installed into an opening of the cell chamber of the MBR, thus situating an SP-HP5-SA sensor spot inside the cell chamber. This allowed for a non-invasive pH measurement during cell cultivation. BY2 wild-type cells cultivated in the MBR were treated with 25 µg/mL of chitosan added to the MS medium supplied while the pH was measured every 30 seconds. Correcting for the ΔpH that 0.0025 % acetic acid caused, a significant increase in the extracellular pH was measurable 17 minutes after adding chitosan to the medium. While the peristaltic pump was operated at a flow rate of 137 µL/min, the elicitor added to the medium reached the MBR with a considerable delay, since it was transported through a length of tubing before it reached the cells (see Fig. 22). In previous work, Sofi et al. (2023) showed that a drastic increase in pH starts within a minute, but this discrepancy is easily explained by the delay in transportation. Additionally, the pH in the MBR does not spike, but increases after a delay and subsequently plateaus. This is likely due to the diffusion of the elicitor throughout the cell chamber of the MBR. In established measurement methods, a cell suspension is elicited by adding the chitosan into the suspension and mixing the suspension by shaking the vessel on an orbital shaker while the pH is continuously measured by a pH electrode (see Table 4). Due to the immediate mixing of the elicitor and cell suspension, all cells are triggered simultaneously, causing an instant increase and subsequent decrease in pH. In the MBR, the elicitor slowly diffuses throughout the cell chamber, causing a wave of elicitations of cells dispersing in the MBR. This culminates in an increase in pH that does not decrease quickly, since at every given moment during this measurement period some new cells are mounting defence signalling and initiate an influx of Ca^{2+}.

The aim to prove whether this method is applicable was achieved successfully. The connector screw can be used to place a sensor spot within the cell chamber of an MBR and seals the system without creating leaks. We were able to continuously and non-invasively measure the pH of the cell suspension in the MBR for a period of 2.5 hours. Longer periods should not pose additional challenges but were not yet attempted. The pH shift measured due to a continuous elicitation with 25 µg/mL chitosan was observed to be significant, therefore the method proved to be precise enough to generate quantifiable results. An elicitation with other substances of interest is likely to work as well but has not yet been attempted. Arguably, there are already well-established methods to measure the reactive change in extracellular pH of plant cell suspensions, that are more streamlined at this point. Yet, the treatment in the MBR offers the novel option to treat the cell suspension with pulses of an elicitor. In classical approaches, the elicitor is added to the cell suspension and then the reaction is quantified. There it is cumbersome to rid the cell suspension of the elicitor. With the MBR system, the medium supplied can easily be switched to a medium containing a substance of interest for a defined period and then returned to the baseline medium, effectively creating a "pulse" treatment of the plant cells in the MBR.

5.2.5 MBR pH measurement - chitosan double pulse

It has been shown, that plants react quicker and more intensely to the presence of a pathogen if an immunoactive stimulus was preceding (Mauch-Mani et al. 2017). We wanted to see, whether we would be able to use the MBR system with the integrated pH measurement to treat plant cells within with two separate stimuli of chitosan and continuously measure the pH. The aim was to establish the parameters of an appropriate experiment and evaluate whether the system would be able to measure a difference in a secondary reaction if a stimulus was preceding.

As can be seen in Fig. 23, after 45 minutes of equilibration, the baseline pH did not yet settle. Additionally, there was a considerable standard error in the solvent control (slvCTRL) already, due to a difference in replicate 3. The slvCTRL was used to standardize both experiments, evaluating the shift in pH due to a single stimulus of chitosan (singlePulse) and to two subsequent stimuli of chitosan separated by 45 minutes (doublePulse). Replications within each treatment created a wide margin of error in both treatments (see Fig. 24). While both singlePuls and doublePuls continuously increased in pH during the experiment and the doublePulse values were

consistently above the values for singlePulse, the standard error prevents any validation of differences between and within the treatments (see Fig. 24). In the doublePulse treatment, the second pulse of chitosan did not cause an additive increase in pH. A second elicitor stimulus could have caused a second movement of Ca^{2+} across the membrane, further shifting the pH. Due to the size of the error margins and the slow diffusion of chitosan described in Chapter 5.2.4, we cannot determine whether this might be due to a potential refractory period, a lacking separation of chitosan signals or due to variance in the replications.

During the introduction of the cell suspension into the cell chamber of the MBR, the random folding of the membrane separating perfusion and cell chamber can gravely affect the ability of the cell chamber to receive the cells. While we were able to transfer the cell suspension evenly distributed into the cell chamber in slvCTRL R1 and R2, starting at slvCTRL R3, the membrane shifted and blocked easy access. The cells remained mainly within the opening of the cell chamber, creating a higher density of cells at the site of the SP-HP5-SA sensor spot (see Table 3). The difference in the ΔpH values between R1, R2 and R3 of the slvCTRL illustrates the importance of the local cell density during the measurement. Yet, this parameter was hard to control, with the random warping of the dividing membrane.

Additionally, the time between pulses of treatment would need to be increased. In Fig. 22, the pH shift caused by the presence of chitosan subsisted and did not exhibit a transient nature, implying a slow diffusion of chitosan throughout the cell chamber (see Chapter 5.2.4). This would suggest, that a long time would be necessary to treat the cell suspension in the MBR with standard MS medium to rid the suspension of remaining chitosan before a second stimulus could be applied. We would suggest separating the second pulse from the first by overnight incubation with an elicitor-free MS medium.

The decreasing pH values of the slvCTRL between -00:30 and 00:00 (see Fig. 23) suggest, that the 45 minutes of equilibration did not suffice and should be increased to 90 minutes, as was the case in Chapter 3.4.6.

5.2.6 MBR H_2O_2 measurement

Reactive Oxygen Species (ROS) are involved in the mechanism of plant defence and the signalling thereof in addition to the signalling to abiotic stresses (Lamb and Dixon 1997; Lee et al. 2020). This work aimed to check whether it is possible to detect an

increase in extracellular ROS levels in the runoff of the MBR system. BY2 wild-type cells cultivated in a Microfluidic BioReactor (MBR) were treated with 150 mM of NaCl, a known elicitor of an increase in H_2O_2 levels (Ismail et al. 2012) for 90 minutes. The MS medium leaving the outlet of the MBR was collected after the treatment period and H_2O_2 levels within were quantified using the Amplex™ Red Hydrogen Peroxide/Peroxidase Assay Kit (see Table 6) according to the respective protocol. Measurement of the resulting fluorescence was performed with a Spark Multimode Microplate reader (see Table 4).

After 60 minutes of salt stress treatment, the BY2 wild-type cell suspension in the MBR produced enough H_2O_2 that a concentration of 502.06 nM (SE ± 34.22) was measurable. Additionally, this result was significantly higher than the 194.11 nM (SE ± 10.64) H_2O_2 that was observed in the respective negative CTRL (see Fig. 25). These results were achieved using only one biological replicate per treatment with three technical replicates each. Yet, with these technical replicates, we were able to detect a significant difference between treatment and CTRL and thereby prove, that it would be technically feasible to detect ROS levels in the outgoing medium of the MBR system.

The procedure of the measurement itself needs streamlining. To use the MBR for high-throughput screening, a method is needed to measure the H_2O_2 levels within the system. To achieve efficiency it would be beneficial to be able to continuously measure fluorescent signals in the medium flow and be able to add necessary reagents into the medium supplied. An option found would be a "mikron 17 fluorimeter" by the company F. F. Runge GmbH in Berlin, Germany. These could potentially be designed to continuously observe the unidirectional medium flow generated by the peristaltic pump that supplies the MBR system. The reagents of the Amplex™ Red Hydrogen Peroxide/Peroxidase Assay Kit would be unsuitable to use in the given system. The reagents are too expensive and too unstable for long-time storage, once the reagents are prepared. Yet, the fact remains, that the levels of ROS generated due to stress experienced by plant cells within the MBR are reliably detectable in the medium runoff and the methods for the detection thereof is subject to change and improvement.

6. Summary and outlook

In this work, we aimed to investigate the mode of action of the isolated *Roesleria subterranea* metabolites Sclerodin and the AcetonAdduct of Entatrevenetinon (AaE) to see whether they act as signals that manipulate the host's immune response. While the metabolite Sclerodin proved unremarkable, AaE was identified as a potential effector able to uncouple the synthesis of important phytoalexins from the Programmed Cell Death (PCD) inherent to a successful defence reaction. Surprisingly, even though AaE induced an increase in cell mortality in Ke15 and Chardonnay while engaging the jasmonate and salicylic acid signalling pathways, it inhibited the expression of STS27, STS47 and PAL. *R. subterranea* may be able to exploit the plant's hypersensitive PCD to generate dead tissue for its nourishment combined with the repression of the generation of defence compounds. To get further insight into the possible function of AaE, we need to look at further defence genes and quantify the plant's reaction while blocking specific signalling pathways. This interaction of *Roesleria subterranea* with its host plant highlights the importance of signals for the outcome of a pathogen invasion. Both defending host and attacking microbe deploy many signals during an invasion, essentially waging warfare with chemical signals. The host sends signals to engage defensive reactions in the affected and neighbouring tissues while the pathogen injects effectors into the host cells to act as signals either quenching an immune response or to manipulate the host's signalling to induce beneficial effects for the pathogen. In this work we were able to use an isolated compound to act as a signal and drastically change the plant's immune response, lending credence to the possibility to use such components to manipulate the defence capabilities of crop plants.

Such immunoactive substances have potential use in plant protection by using them to prime the defence capabilities of crop plants (see Chapter 1.2.6). Searching for and identifying such compounds is a time and labour-intensive procedure. In this work, we took exploratory steps in using Microfluidic BioReactors (MBR) to non-invasively quantify the immune responses of plant cells cultivated within. This would enable high-throughput screening for immunoactivity of substances of interest contained in the medium transported to the plant cell containing MBR. These compounds could originate from cells cultivated in a preceding MBR or substances of interest could be solved to a desired concentration into the medium supplied to the system. Immunoactive compounds identified with the given setup could potentially be used in plant protection by priming the plant's immune system. To efficiently screen the

reaction of plant cells to the presence of fungal strains, we tested the feasibility to co-cultivate plant and fungal cells in separate MBRs. We were able to illustrate the possibility of using optical means to continuously measure the pH in the cell chamber of the MBR. The resolution of the measurement was sufficient to detect the defence-related shift in extracellular pH induced by the detection of the fungal elicitor chitosan. Additionally, we were able to detect significant differences in the concentration of H_2O_2 in the outgoing medium of the MBR, representing Reactive Oxygen Species (ROS) produced due to the application of salt stress. Therefore, it is possible to detect biotic and abiotic stress responses of the plant cells during MBR cultivation. Yet, to perform high-throughput screenings, these methods need to be streamlined. For a potential co-cultivation of fungal and plant cells within separate MBRs in the same system, the MBR design needs to be adjusted for the appropriate containment of fungal cells. In this work, we were able to co-cultivate BY2 cells and *Neofusicoccum parvum* suspension cells for two days and detect increased mortality in the BY2 cells, proving that co-cultivation enables substances to be transported from one cell type to the other. After two days, the fungal hyphae, able to penetrate the separating membrane of the MBR, blocked the inlet of the MBR, causing a breakdown of the system. To enable long-time co-cultivation, the MBR design needs to be adjusted to restrict the access of fungal hyphae to the perfusion chamber.

In summary, we were able to identify AaE as an important signal in the "chemical warfare" taking place between *Roesleria subterranea* and the host plant being invaded, giving a striking example of the concept, that single signal molecules can drastically alter the nature of a symbiosis. AaE proved a potential effector uncoupling the hypersensitive PCD from the synthesis of phytoalexins inherent to a successful defence reaction, effectively exploiting the plant's own immune system by initiating PCD to create dead tissue for nourishment while repressing genes that would synthesise defensive compounds. Additionally, this sheds light on the relationship between *Roesleria subterranea* and its host plant the grapevine. The research into AaE requires further experiments to elucidate the mode of action by blocking certain signalling pathways and looking at the expression of further genes. New experiments need precise planning since the fermentation of *R. subterranea* and the isolation of its metabolites is very time intensive. The preliminary experiments into the on-chip quantification of immune responses in the MBR system showed promising results. We were able to successfully quantify the pH shift and ROS generation, both important

indicators for stress signalling. With further improvements to MBR design, detection systems and handling, these quantification methods could be streamlined to surpass established methods and enable high throughput screening for immunoactive substances. Additionally, we performed preliminary experiments in a novel double-exposure treatment in the MBR (see Chapter 4.2.6) and the generation of a potential reporter line, generating a green fluorescent signal upon elicitation of the basal defence reaction (see supplementary Chapter 8.1).

7. Publication bibliography

Aftab, Tariq; Yusuf, Mohammad (Eds.) (2021): Jasmonates and Salicylates Signaling in Plants. 1st ed. 2021. Cham: Springer International Publishing; Imprint Springer (Signaling and Communication in Plants).

Agudelo, Carlos G.; Sanati Nezhad, Amir; Ghanbari, Mahmood; Naghavi, Mahsa; Packirisamy, Muthukumaran; Geitmann, Anja (2013): TipChip: a modular, MEMS-based platform for experimentation and phenotyping of tip-growing cells. In *Plant J* 73 (6), pp. 1057–1068. DOI: 10.1111/tpj.12093.

Allan, Claudia; Tayagui, Ayelen; Hornung, Rainer; Nock, Volker; Meisrimler, Claudia-Nicole (2022): A dual-flow RootChip enables quantification of bi-directional calcium signaling in primary roots. In *Frontiers in plant science* 13, p. 1040117. DOI: 10.3389/fpls.2022.1040117.

Atkinson, M. M.; Keppler, L. D.; Orlandi, E. W.; Baker, C. J.; Mischke, C. F. (1990): Involvement of plasma membrane calcium influx in bacterial induction of the k/h and hypersensitive responses in tobacco. In *Plant physiology* 92 (1), pp. 215–221. DOI: 10.1104/pp.92.1.215.

Balint-Kurti, Peter (2019): The plant hypersensitive response: concepts, control and consequences. In *Molecular plant pathology* 20 (8), pp. 1163–1178. DOI: 10.1111/mpp.12821.

Bao Do, C.; Cormier, F. (1991): Effects of low nitrate and high sugar concentrations on anthocyanin content and composition of grape (Vitis vinifera L.) cell suspension. In *Plant cell reports* 9 (9), pp. 500–504. DOI: 10.1007/BF00232105.

Baral, Hans-Otto; Queloz, Valentin; Hosoya, Tsuyoshi (2014): Hymenoscyphus fraxineus, the correct scientific name for the fungus causing ash dieback in Europe. In *IMA fungus* 5 (1), pp. 79–80. DOI: 10.5598/imafungus.2014.05.01.09.

Beckwith, Angie M. (1924): The Life History of the Grape Rootrot Fungus Roesleria hypogaea Thum et Pass. Available online at https://naldc.nal.usda.gov/catalog/ind43966780.

Beris, Evangelos; Selim, Moustafa; Kechagia, Despoina; Evangelou, Alexandra (2023): Overview of the Esca Complex as an Increasing Threat in Vineyards Worldwide: Climate Change, Control Approaches and Impact on Grape and Wine Quality. In António M. Jordão, Renato Botelho, Uroš Miljić (Eds.): Recent Advances in Grapes and Wine Production - New Perspectives for Quality Improvement: IntechOpen.

Block, Anna; Li, Guangyong; Fu, Zheng Qing; Alfano, James R. (2008): Phytopathogen type III effector weaponry and their plant targets. In *Current opinion in plant biology* 11 (4), pp. 396–403. DOI: 10.1016/j.jbi.2008.06.007.

Boller, Thomas; He, Sheng Yang (2009): Innate immunity in plants: an arms race between pattern recognition receptors in plants and effectors in microbial pathogens. In *Science (New York, N.Y.)* 324 (5928), pp. 742–744.

Boutrot, Freddy; Zipfel, Cyril (2017): Function, Discovery, and Exploitation of Plant Pattern Recognition Receptors for Broad-Spectrum Disease Resistance. In *Annual review of phytopathology* 55, pp. 257–286.

Brodersen, Peter; Malinovsky, Frederikke Gro; Hématy, Kian; Newman, Mari-Anne; Mundy, John (2005): The Role of Salicylic Acid in the Induction of Cell Death in Arabidopsis acd111. In *Plant physiology* 138 (2), pp. 1037–1045. DOI: 10.1104/pp.105.059303.

Busch, Wolfgang; Moore, Brad T.; Martsberger, Bradley; Mace, Daniel L.; Twigg, Richard W.; Jung, Jee et al. (2012): A microfluidic device and computational platform for high throughput live imaging of gene expression. In *Nature methods* 9 (11), pp. 1101–1106. DOI: 10.1038/nmeth.2185.

Cameron, Robin K.; PAIVA, NANCY L.; LAMB, CHRIS J.; Dixon, Richard A. (1999): Accumulation of salicylic acid and PR-1 gene transcripts in relation to the systemic acquired resistance (SAR) response induced by Pseudomonas syringae pv. tomato in Arabidopsis. In *Physiological and Molecular Plant Pathology* 55 (2), pp. 121–130. DOI: 10.1006/pmpp.1999.0214.

Publication bibliography

Cao, Lingyan; Wang, Wenyi; Zhang, Weiwei; Staiger, Christopher J. (2022): Lipid Signaling Requires ROS Production to Elicit Actin Cytoskeleton Remodeling during Plant Innate Immunity. In *International journal of molecular sciences* 23 (5). DOI: 10.3390/ijms23052447.

Carlucci, Antonia; Cibelli, Francesca; Lops, Francesco; Raimondo, Maria Luisa (2015): Characterization of Botryosphaeriaceae Species as Causal Agents of Trunk Diseases on Grapevines. In *Plant disease* 99 (12), pp. 1678–1688. DOI: 10.1094/PDIS-03-15-0286-RE.

Catalgol, Betul; Batirel, Saime; Taga, Yavuz; Ozer, Nesrin Kartal (2012): Resveratrol: French Paradox Revisited. In *Frontiers in Pharmacology* 3. DOI: 10.3389/fphar.2012.00141.

Chang, Xiaoli; Nick, Peter (2012): Defence signalling triggered by Flg22 and Harpin is integrated into a different stilbene output in Vitis cells. In *PloS one* 7 (7), e40446. DOI: 10.1371/journal.pone.0040446.

Chico, Jose M.; Chini, Andrea; Fonseca, Sandra; Solano, Roberto (2008): JAZ repressors set the rhythm in jasmonate signaling. In *Current opinion in plant biology* 11 (5), pp. 486–494. DOI: 10.1016/j.pbi.2008.06.003.

Chini, A.; Fonseca, S.; Fernández, G.; Adie, B.; Chico, J. M.; Lorenzo, O. et al. (2007): The JAZ family of repressors is the missing link in jasmonate signalling. In *Nature* 448 (7154), pp. 666–671. DOI: 10.1038/nature06006.

Chung, Hoo Sun; Koo, Abraham J. K.; Gao, Xiaoli; Jayanty, Sastry; Thines, Bryan; Jones, A. Daniel; Howe, Gregg A. (2008): Regulation and function of Arabidopsis JASMONATE ZIM-domain genes in response to wounding and herbivory. In *Plant physiology* 146 (3), pp. 952–964. DOI: 10.1104/pp.107.115691.

Cooper, Geoffrey M.; Hausman, Robert E. (2016): The cell. A molecular approach. Seventh edition. Sunderland, Massachusetts U.S.A.: Sinauer Associates Inc. Available online at http://sites.sinauer.com/cooper7e/.

Crocq, Marc-Antoine (2007): Historical and cultural aspects of man's relationship with addictive drugs. In *Dialogues in clinical neuroscience* 9 (4), pp. 355–361. DOI: 10.31887/DCNS.2007.9.4/macrocq.

Crous, Pedro W.; Slippers, Bernard; Wingfield, Michael J.; Rheeder, John; Marasas, Walter F.O.; Philips, Alan J.L. et al. (2006): Phylogenetic lineages in the Botryosphaeriaceae. In *Studies in Mycology* 55, pp. 235–253.

Czemmel, Stefan; Stracke, Ralf; Weisshaar, Bernd; Cordon, Nicole; Harris, Nilangani N.; Walker, Amanda R. et al. (2009): The grapevine R2R3-MYB transcription factor VvMYBF1 regulates flavonol synthesis in developing grape berries. In *Plant physiology* 151 (3), pp. 1513–1530. DOI: 10.1104/pp.109.142059.

Database | OIV (2023). Available online at https://www.oiv.int/what-we-do/data-discovery-report?oiv, updated on 4/3/2023, checked on 4/3/2023.

Degawa, Yousuke; Hosoya, Tsuyoshi; Hosaka, Kentaro; Hirayama, Yumiko; Saito, Yukiko; Zhao, Yan-Jie (2015): Rediscovery of Roesleria subterranea from Japan with a discussion of its infraspecific relationships detected using molecular analysis. In *MC* 9, pp. 1–9. DOI: 10.3897/mycokeys.9.6564.

Demidchik, Vadim; Shabala, Sergey; Isayenkov, Stanislav; Cuin, Tracey A.; Pottosin, Igor (2018): Calcium transport across plant membranes: mechanisms and functions. In *The New phytologist* 220 (1), pp. 49–69. DOI: 10.1111/nph.15266.

Dittrich, Georg (2015): Wein und Weinbau im Heiligen Land. [eine kleine Kulturgeschichte]. 3., erneut überarb. und noch einmal erw. Aufl. Pleinfeld: Maaruf-Verl.

Dong, Yang; Duan, Shengchang; Xia, Qiuju; Liang, Zhenchang; Dong, Xiao; Margaryan, Kristine et al. (2023): Dual domestications and origin of traits in grapevine evolution. In *Science (New York, N.Y.)* 379 (6635), pp. 892–901. DOI: 10.1126/science.add8655.

Drew, Georgia C.; Stevens, Emily J.; King, Kayla C. (2021): Microbial evolution and transitions along the parasite–mutualist continuum. In *Nat Rev Microbiol*. DOI: 10.1038/s41579-021-00550-7.

Duan, Dong; Fischer, Sabine; Merz, Patrick; Bogs, Jochen; Riemann, Michael; Nick, Peter (2016): An ancestral allele of grapevine transcription factor MYB14 promotes plant defence. In *Journal of experimental botany* 67 (6), pp. 1795–1804. DOI: 10.1093/jxb/erv569.

Duan, Dong; Halter, David; Baltenweck, Raymonde; Tisch, Christine; Tröster, Viktoria; Kortekamp, Andreas et al. (2015): Genetic diversity of stilbene metabolism in Vitis sylvestris. In *J Exp Bot* 66 (11), pp. 3243–3257. DOI: 10.1093/jxb/erv137.

Elad, Yigal; Pertot, Ilaria (2014): Climate Change Impacts on Plant Pathogens and Plant Diseases. In *Journal of Crop Improvement* 28 (1), pp. 99–139. DOI: 10.1080/15427528.2014.865412.

F. F. Runge GmbH: Runge mikron. Available online at https://www.ff-runge.de/dokumente/31.6B0.1701.de-Runge-mikron.pdf#zoom=page-height, checked on 3/13/2023.

Felix, Georg; Regenass, Martin; Boller, Thomas (1993): Specific perception of subnanomolar concentrations of chitin fragments by tomato cells: induction of extracellular alkalinization, changes in protein phosphorylation, and establishment of a refractory state. In *Plant J* 4 (2), pp. 307–316. DOI: 10.1046/j.1365-313X.1993.04020307.x.

Felle, H. H. (2001): pH: Signal and Messenger in Plant Cells. In *Plant Biology* 3 (6), pp. 577–591. DOI: 10.1055/s-2001-19372.

Felle, H. H.; Kondorosi, E.; Kondorosi, A.; Schultze, M. (2000): How alfalfa root hairs discriminate between Nod factors and oligochitin elicitors. In *Plant physiology* 124 (3), pp. 1373–1380. DOI: 10.1104/pp.124.3.1373.

Finkbeiner, T.; Manz, C.; Raorane, M. L.; Metzger, C.; Schmidt-Speicher, L.; Shen, N. et al. (2022): A modular microfluidic bioreactor to investigate plant cell-cell interactions. In *Protoplasma* 259 (1), pp. 173–186. DOI: 10.1007/s00709-021-01650-0.

Finkbeiner, Tim (2019): Entwicklung eines mikrofluidischen Bioreaktors für die Kultivierung von Pflanzenzellen. Karlsruher Institut für Technologie, Karlsruhe. Institut für Mikrostrukturtechnik (IMT).

Foyer, Christine H. (2018): Reactive oxygen species, oxidative signaling and the regulation of photosynthesis. In *Environmental and experimental botany* 154, pp. 134–142. DOI: 10.1016/j.envexpbot.2018.05.003.

Frei dit Frey, Nicolas; Mbengue, Malick; Kwaaitaal, Mark; Nitsch, Lisette; Altenbach, Denise; Häweker, Heidrun et al. (2012): Plasma membrane calcium ATPases are important components of receptor-mediated signaling in plant immune responses and development. In *Plant physiology* 159 (2), pp. 798–809. DOI: 10.1104/pp.111.192575.

Frey, Nolan; Sönmez, Utku M.; Minden, Jonathan; LeDuc, Philip (2022): Microfluidics for understanding model organisms. In *Nat Commun* 13 (1). DOI: 10.1038/s41467-022-30814-6.

Gamir, Jordi; Darwiche, Rabih; Van't Hof, Pieter; Choudhary, Vineet; Stumpe, Michael; Schneiter, Roger; Mauch, Felix (2017): The sterol-binding activity of PATHOGENESIS-RELATED PROTEIN 1 reveals the mode of action of an antimicrobial protein. In *Plant J* 89 (3), pp. 502–509. DOI: 10.1111/tpj.13398.

Gill, Sarvajeet Singh; Tuteja, Narendra (2010): Reactive oxygen species and antioxidant machinery in abiotic stress tolerance in crop plants. In *Plant physiology and biochemistry : PPB* 48 (12), pp. 909–930. DOI: 10.1016/j.plaphy.2010.08.016.

Glazebrook, Jane (2005): Contrasting mechanisms of defense against biotrophic and necrotrophic pathogens. In *Annual review of phytopathology* 43, pp. 205–227. DOI: 10.1146/annurev.phyto.43.040204.135923.

Granett, J.; Walker, M. A.; Kocsis, L.; Omer, A. D. (2001): Biology and management of grape phylloxera. In *Annual review of entomology* 46, pp. 387–412. DOI: 10.1146/annurev.ento.46.1.387.

Gross, Andrin; Holdenrieder, Ottmar; Pautasso, Marco; Queloz, Valentin; Sieber, Thomas Niklaus (2014): Hymenoscyphus pseudoalbidus, the causal agent of European ash dieback. In *Molecular plant pathology* 15 (1), pp. 5–21. DOI: 10.1111/mpp.12073.

Guan, Pingyin; Shi, Wenjing; Riemann, Michael; Nick, Peter (2021): Dissecting the membrane-microtubule sensor in grapevine defence. In *Hortic Res* 8 (1), p. 260. DOI: 10.1038/s41438-021-00703-y.

Guan, Xin; Buchholz, Günther; Nick, Peter (2013): The cytoskeleton is disrupted by the bacterial effector HrpZ, but not by the bacterial PAMP flg22, in tobacco BY-2 cells. In *J Exp Bot* 64 (7), pp. 1805–1816. DOI: 10.1093/jxb/ert042.

Guan, Xin; Buchholz, Günther; Nick, Peter (2014): Actin marker lines in grapevine reveal a gatekeeper function of guard cells. In *Journal of plant physiology* 171 (13), pp. 1164–1173. DOI: 10.1016/j.jplph.2014.03.019.

Hashimoto, Kenji; Kudla, Jörg (2011): Calcium decoding mechanisms in plants. In *Biochimie* 93 (12), pp. 2054–2059. DOI: 10.1016/j.biochi.2011.05.019.

Hilleary, Richard; Paez-Valencia, Julio; Vens, Cullen; Toyota, Masatsugu; Palmgren, Michael; Gilroy, Simon (2020): Tonoplast-localized Ca2+ pumps regulate Ca2+ signals during pattern-triggered immunity in Arabidopsis thaliana. In *Proceedings of the National Academy of Sciences of the United States of America* 117 (31), pp. 18849–18857. DOI: 10.1073/pnas.2004183117.

Höll, Janine; Vannozzi, Alessandro; Czemmel, Stefan; D'Onofrio, Claudio; Walker, Amanda R.; Rausch, Thomas et al. (2013): The R2R3-MYB Transcription Factors MYB14 and MYB15 Regulate Stilbene Biosynthesis in Vitis vinifera. In *The Plant Cell* 25 (10), pp. 4135–4149. DOI: 10.1105/tpc.113.117127.

Iftikhar, Sehrish; Vigne, Aurélie; Sepulveda-Diaz, Julia Elisa (2021): Droplet-based microfluidics platform for antifungal analysis against filamentous fungi. In *Sci Rep* 11 (1), p. 22998. DOI: 10.1038/s41598-021-02350-8.

Ismail, Ahmed; Riemann, Michael; Nick, Peter (2012): The jasmonate pathway mediates salt tolerance in grapevines. In *J Exp Bot* 63 (5), pp. 2127–2139. DOI: 10.1093/jxb/err426.

Jabs, T.; Tschope, M.; Colling, C.; Hahlbrock, K.; Scheel, D. (1997): Elicitor-stimulated ion fluxes and O2- from the oxidative burst are essential components in triggering defense gene activation and phytoalexin synthesis in parsley. In *Proceedings of the National Academy of Sciences of the United States of America* 94 (9), pp. 4800–4805. DOI: 10.1073/pnas.94.9.4800.

Jiang, Huawei; Xu, Zhen; Aluru, Maneesha R.; Dong, Liang (2014): Plant chip for high-throughput phenotyping of Arabidopsis. In *Lab on a chip* 14 (7), pp. 1281–1293. DOI: 10.1039/C3LC51326B.

Jiang, Yuxiang; Ding, Pingtao (2022): Calcium signaling in plant immunity: a spatiotemporally controlled symphony. In *Trends in Plant Science*.

Jones, Jonathan D. G.; Dangl, Jeffery L. (2006): The plant immune system. In *Nature* 444 (7117), pp. 323–329. DOI: 10.1038/nature05286.

Jones, Jonathan D. G.; Vance, Russell E.; Dangl, Jeffery L. (2016): Intracellular innate immune surveillance devices in plants and animals. In *Science (New York, N.Y.)* 354 (6316). DOI: 10.1126/science.aaf6395.

Kadota, Yasuhiro; Shirasu, Ken; Zipfel, Cyril (2015): Regulation of the NADPH Oxidase RBOHD During Plant Immunity. In *Plant & cell physiology* 56 (8), pp. 1472–1480. DOI: 10.1093/pcp/pcv063.

Keppler, L. Dale (1989): Active Oxygen Production During a Bacteria-Induced Hypersensitive Reaction in Tobacco Suspension Cells. In *Phytopathology* 79 (9), p. 974. DOI: 10.1094/Phyto-79-974.

Khattab, Islam M.; Fischer, Jochen; Kaźmierczak, Andrzej; Thines, Eckhard; Nick, Peter (2022): Ferulic acid is a putative surrender signal to stimulate programmed cell death in grapevines after infection with Neofusicoccum parvum. In *Plant, cell & environment*.

Khattab, Islam M.; Sahi, Vaidurya P.; Baltenweck, Raymonde; Maia-Grondard, Alessandra; Hugueney, Philippe; Bieler, Eva et al. (2021): Ancestral chemotypes of cultivated grapevine with resistance to

Botryosphaeriaceae-related dieback allocate metabolism towards bioactive stilbenes. In *The New phytologist* 229 (2), pp. 1133–1146. DOI: 10.1111/nph.16919.

Kirchmair, Martin; Neuhauser, Sigrid; Buzina, Walter; Huber, Lars (2008): The taxonomic position of Roesleria subterranea. In *Mycological research* 112 (Pt 10), pp. 1210–1219.

Kumagai, F.; Yoneda, A.; Tomida, T.; Sano, T.; Nagata, T.; Hasezawa, S. (2001): Fate of nascent microtubules organized at the M/G1 interface, as visualized by synchronized tobacco BY-2 cells stably expressing GFP-tubulin: time-sequence observations of the reorganization of cortical microtubules in living plant cells. In *Plant & cell physiology* 42 (7), pp. 723–732. DOI: 10.1093/pcp/pce091.

Lagoy, Ross C.; Albrecht, Dirk R. (2015): Microfluidic Devices for Behavioral Analysis, Microscopy, and Neuronal Imaging in Caenorhabditis elegans. In *Methods in molecular biology (Clifton, N.J.)* 1327, pp. 159–179. DOI: 10.1007/978-1-4939-2842-2_12.

Lamb, Chris; Dixon, Richard A. (1997): THE OXIDATIVE BURST IN PLANT DISEASE RESISTANCE. In *Annual review of plant physiology and plant molecular biology* 48, pp. 251–275. DOI: 10.1146/annurev.arplant.48.1.251.

Lecourieux, David; Ranjeva, Raoul; Pugin, Alain (2006): Calcium in plant defence-signalling pathways. In *The New phytologist* 171 (2), pp. 249–269. DOI: 10.1111/j.1469-8137.2006.01777.x.

Lee, DongHyuk; Lal, Neeraj K.; Lin, Zuh-Jyh Daniel; Ma, Shisong; Liu, Jun; Castro, Bardo et al. (2020): Regulation of reactive oxygen species during plant immunity through phosphorylation and ubiquitination of RBOHD. In *Nat Commun* 11 (1). DOI: 10.1038/s41467-020-15601-5.

Li, Lei; Li, Meng; Yu, Liping; Zhou, Zhaoyang; Liang, Xiangxiu; Liu, Zixu et al. (2014): The FLS2-associated kinase BIK1 directly phosphorylates the NADPH oxidase RbohD to control plant immunity. In *Cell host & microbe* 15 (3), pp. 329–338. DOI: 10.1016/j.chom.2014.02.009.

Livak, K. J.; Schmittgen, T. D. (2001): Analysis of relative gene expression data using real-time quantitative PCR and the 2(-Delta Delta C(T)) Method. In *Methods (San Diego, Calif.)* 25 (4), pp. 402–408. DOI: 10.1006/meth.2001.1262.

Mauch-Mani, Brigitte; Baccelli, Ivan; Luna, Estrella; Flors, Victor (2017): Defense Priming: An Adaptive Part of Induced Resistance. In *Annual review of plant biology* 68, pp. 485–512. DOI: 10.1146/annurev-arplant-042916-041132.

McGovern, Patrick; Jalabadze, Mindia; Batiuk, Stephen; Callahan, Michael P.; Smith, Karen E.; Hall, Gretchen R. et al. (2017): Early Neolithic wine of Georgia in the South Caucasus. In *Proceedings of the National Academy of Sciences of the United States of America* 114 (48), E10309-E10318. DOI: 10.1073/pnas.1714728114.

Miles, T. D.; Schilder, A. M. C. (2009): First Report of Grape Root Rot Caused by Roesleria subterranea in Michigan. In *Plant disease* 93 (7), p. 765. DOI: 10.1094/PDIS-93-7-0765C.

Miller, Gad; Schlauch, Karen; Tam, Rachel; Cortes, Diego; Torres, Miguel A.; Shulaev, Vladimir et al. (2009): The plant NADPH oxidase RBOHD mediates rapid systemic signaling in response to diverse stimuli. In *Science signaling* 2 (84), ra45.

Munnik, T.; Arisz, S. A.; Vrije, T. de; Musgrave, A. (1995): G Protein Activation Stimulates Phospholipase D Signaling in Plants. In *The Plant Cell* 7 (12), pp. 2197–2210. DOI: 10.1105/tpc.7.12.2197.

Nagata, Toshiyuki; Nemoto, Yasuyuki; Hasezawa, Seiichiro (1992): Tobacco BY-2 Cell Line as the "HeLa" Cell in the Cell Biology of Higher Plants. In, vol. 132: Elsevier (International Review of Cytology), pp. 1–30.

Neuhauser, Sigrid; Huber, Lars; Kirchmair, Martin (2009): A DNA based method to detect the grapevine root-rotting fungus Roesleria subterranea in soil and root samples. In *Phytopathol. Mediterr.* 48 (1), pp. 59–72.

Neuhauser, Sigrid; Huber, Lars; Kirchmair, Martin (2011): Is Roesleria subterranea a primary pathogen or a minor parasite of grapevines? Risk assessment and a diagnostic decision scheme.

In *European journal of plant pathology / European Foundation for Plant Pathology* 130 (4), pp. 503–510. DOI: 10.1007/s10658-011-9769-3.

Nürnberger, Thorsten; Brunner, Frédéric; Kemmerling, Birgit; Piater, Lizelle (2004): Innate immunity in plants and animals: striking similarities and obvious differences. In *Immunological reviews* 198, pp. 249–266.

Nürnberger, Thorsten; Scheel, Dierk (2001): Signal transmission in the plant immune response. In *Trends in Plant Science* 6 (8), pp. 372–379.

Page, Mike T.; Parry, Martin A. J.; Carmo-Silva, Elizabete (2019): A high-throughput transient expression system for rice. In *Plant, cell & environment* 42 (7), pp. 2057–2064. DOI: 10.1111/pce.13542.

Parage, Claire; Tavares, Raquel; Réty, Stéphane; Baltenweck-Guyot, Raymonde; Poutaraud, Anne; Renault, Lauriane et al. (2012): Structural, functional, and evolutionary analysis of the unusually large stilbene synthase gene family in grapevine. In *Plant physiology* 160 (3), pp. 1407–1419. DOI: 10.1104/pp.112.202705.

Parida, Asish Kumar; Das, Anath Bandhu (2005): Salt tolerance and salinity effects on plants: a review. In *Ecotoxicology and environmental safety* 60 (3), pp. 324–349. DOI: 10.1016/j.ecoenv.2004.06.010.

Peng, M. (1992): Peroxidase-Generated Hydrogen Peroxide as a Source of Antifungal Activity In Vitro and on Tobacco Leaf Disks. In *Phytopathology* 82 (6), p. 696. DOI: 10.1094/Phyto-82-696.

Qiao, Fei; Chang, Xiao-Li; Nick, Peter (2010): The cytoskeleton enhances gene expression in the response to the Harpin elicitor in grapevine. In *J Exp Bot* 61 (14), pp. 4021–4031. DOI: 10.1093/jxb/erq221.

Sanati Nezhad, A. (2014): Microfluidic platforms for plant cells studies. In *Lab on a chip* 14 (17), pp. 3262–3274. DOI: 10.1039/C4LC00495G.

Seibicke, Tobias (2002): Untersuchungen zur induzierten Resistenz an Vitis spec. Dissertation. Albert-Ludwigs-Universtität, Freiburg im Breisgau. Available online at http://biocrop.de/site/images/dissertation%20tobias%20seibicke.pdf.

Shorr, Ardon Z.; Sönmez, Utku M.; Minden, Jonathan S.; LeDuc, Philip R. (2019): High-throughput mechanotransduction in Drosophila embryos with mesofluidics. In *Lab on a chip* 19 (7), pp. 1141–1152. DOI: 10.1039/C8LC01055B.

Slippers, Bernard; Wingfield, Michael J. (2007): Botryosphaeriaceae as endophytes and latent pathogens of woody plants: diversity, ecology and impact. In *Fungal Biology Reviews* 21 (2-3), pp. 90–106. DOI: 10.1016/j.fbr.2007.06.002.

Sofi, Karwan Gafoor; Metzger, Christian; Riemann, Michael; Nick, Peter (2023): Chitosan triggers actin remodelling and activation of defence genes that is repressed by calcium influx in grapevine cells. In *Plant science : an international journal of experimental plant biology* 326, p. 111527. DOI: 10.1016/j.plantsci.2022.111527.

Subendran, Satishkumar; Kang, Chun-Wei; Chen, Chia-Yuan (2021): Comprehensive Hydrodynamic Investigation of Zebrafish Tail Beats in a Microfluidic Device with a Shape Memory Alloy. In *Micromachines* 12 (1). DOI: 10.3390/mi12010068.

Svyatyna, Katharina; Jikumaru, Yusuke; Brendel, Rita; Reichelt, Michael; Mithöfer, Axel; Takano, Makoto et al. (2014): Light induces jasmonate-isoleucine conjugation via OsJAR1-dependent and -independent pathways in rice. In *Plant, cell & environment* 37 (4), pp. 827–839. DOI: 10.1111/pce.12201.

Takken, F. L. W.; Tameling, W. I. L. (2009): To nibble at plant resistance proteins. In *Science (New York, N.Y.)* 324 (5928), pp. 744–746. DOI: 10.1126/science.1171666.

Thaler, Jennifer S.; Humphrey, Parris T.; Whiteman, Noah K. (2012): Evolution of jasmonate and salicylate signal crosstalk. In *Trends in Plant Science* 17 (5), pp. 260–270.

Thines, Bryan; Katsir, Leron; Melotto, Maeli; Niu, Yajie; Mandaokar, Ajin; Liu, Guanghui et al. (2007): JAZ repressor proteins are targets of the SCF(COI1) complex during jasmonate signalling. In *Nature* 448 (7154), pp. 661–665. DOI: 10.1038/nature05960.

Thomma, Bart P. H. J.; Nürnberger, Thorsten; Joosten, Matthieu H. A. J. (2011): Of PAMPs and effectors: the blurred PTI-ETI dichotomy. In *The Plant Cell* 23 (1), pp. 4–15. DOI: 10.1105/tpc.110.082602.

Tripathi, Diwaker; Raikhy, Gaurav; Kumar, Dhirendra (2019): Chemical elicitors of systemic acquired resistance—Salicylic acid and its functional analogs. In *Current Plant Biology* 17, pp. 48–59. DOI: 10.1016/j.cpb.2019.03.002.

Tsuda, Kenichi; Katagiri, Fumiaki (2010): Comparing signaling mechanisms engaged in pattern-triggered and effector-triggered immunity. In *Current opinion in plant biology* 13 (4), pp. 459–465.

van Treuren, Will; Brower, Kara K.; Labanieh, Louai; Hunt, Daniel; Lensch, Sarah; Cruz, Bianca et al. (2019): Live imaging of Aiptasia larvae, a model system for coral and anemone bleaching, using a simple microfluidic device. In *Sci Rep* 9 (1), p. 9275. DOI: 10.1038/s41598-019-45167-2.

Vannozzi, Alessandro; Dry, Ian B.; Fasoli, Marianna; Zenoni, Sara; Lucchin, Margherita (2012): Genome-wide analysis of the grapevine stilbene synthase multigenic family: genomic organization and expression profiles upon biotic and abiotic stresses. In *BMC plant biology* 12, p. 130. DOI: 10.1186/1471-2229-12-130.

Wang, Jingyi; Lian, Na; Zhang, Yue; Man, Yi; Chen, Lulu; Yang, Haobo et al. (2022a): The Cytoskeleton in Plant Immunity: Dynamics, Regulation, and Function. In *International journal of molecular sciences* 23 (24). DOI: 10.3390/ijms232415553.

Wang, Lixin; Sadeghnezhad, Ehsan; Riemann, Michael; Nick, Peter (2019): Microtubule dynamics modulate sensing during cold acclimation in grapevine suspension cells. In *Plant science : an international journal of experimental plant biology* 280, pp. 18–30. DOI: 10.1016/j.plantsci.2018.11.008.

Wang, Ruipu; Duan, Dong; Metzger, Christian; Zhu, Xin; Riemann, Michael; Pla, Maria; Nick, Peter (2022b): Aluminum can activate grapevine defense through actin remodeling. In *Hortic Res* 9. DOI: 10.1093/hr/uhab016.

Wong, Darren Chern Jan; Schlechter, Rudolf; Vannozzi, Alessandro; Höll, Janine; Hmmam, Ibrahim; Bogs, Jochen et al. (2016): A systems-oriented analysis of the grapevine R2R3-MYB transcription factor family uncovers new insights into the regulation of stilbene accumulation. In *DNA research : an international journal for rapid publication of reports on genes and genomes* 23 (5), pp. 451–466. DOI: 10.1093/dnares/dsw028.

Xiang, Jiang; Li, Xinlong; Wu, Jiao; Yin, Ling; Zhang, Yali; Lu, Jiang (2016): Studying the Mechanism of Plasmopara viticola RxLR Effectors on Suppressing Plant Immunity. In *Frontiers in microbiology* 7, p. 709. DOI: 10.3389/fmicb.2016.00709.

Xie, D. X.; Feys, B. F.; James, S.; Nieto-Rostro, M.; Turner, J. G. (1998): COI1: an Arabidopsis gene required for jasmonate-regulated defense and fertility. In *Science (New York, N.Y.)* 280 (5366), pp. 1091–1094. DOI: 10.1126/science.280.5366.1091.

Yao, Y.-J.; Spooner, B. M. (1999): Roesleriaceae, a New Family of Ascomycota, and a New Species of Roeslerina. In *Kew Bulletin* 54 (3), p. 683. DOI: 10.2307/4110864.

Zhang, Jie; Shao, Feng; Li, Yan; Cui, Haitao; Chen, Linjie; Li, Hongtao et al. (2007): A Pseudomonas syringae effector inactivates MAPKs to suppress PAMP-induced immunity in plants. In *Cell host & microbe* 1 (3), pp. 175–185. DOI: 10.1016/j.chom.2007.03.006.

Zipfel, Cyril; Felix, Georg (2005): Plants and animals: a different taste for microbes? In *Current opinion in plant biology* 8 (4), pp. 353–360.

8. Supplementary

CTRL   DMSO CTRL – 60 min   MeOH CTRL – 60 min
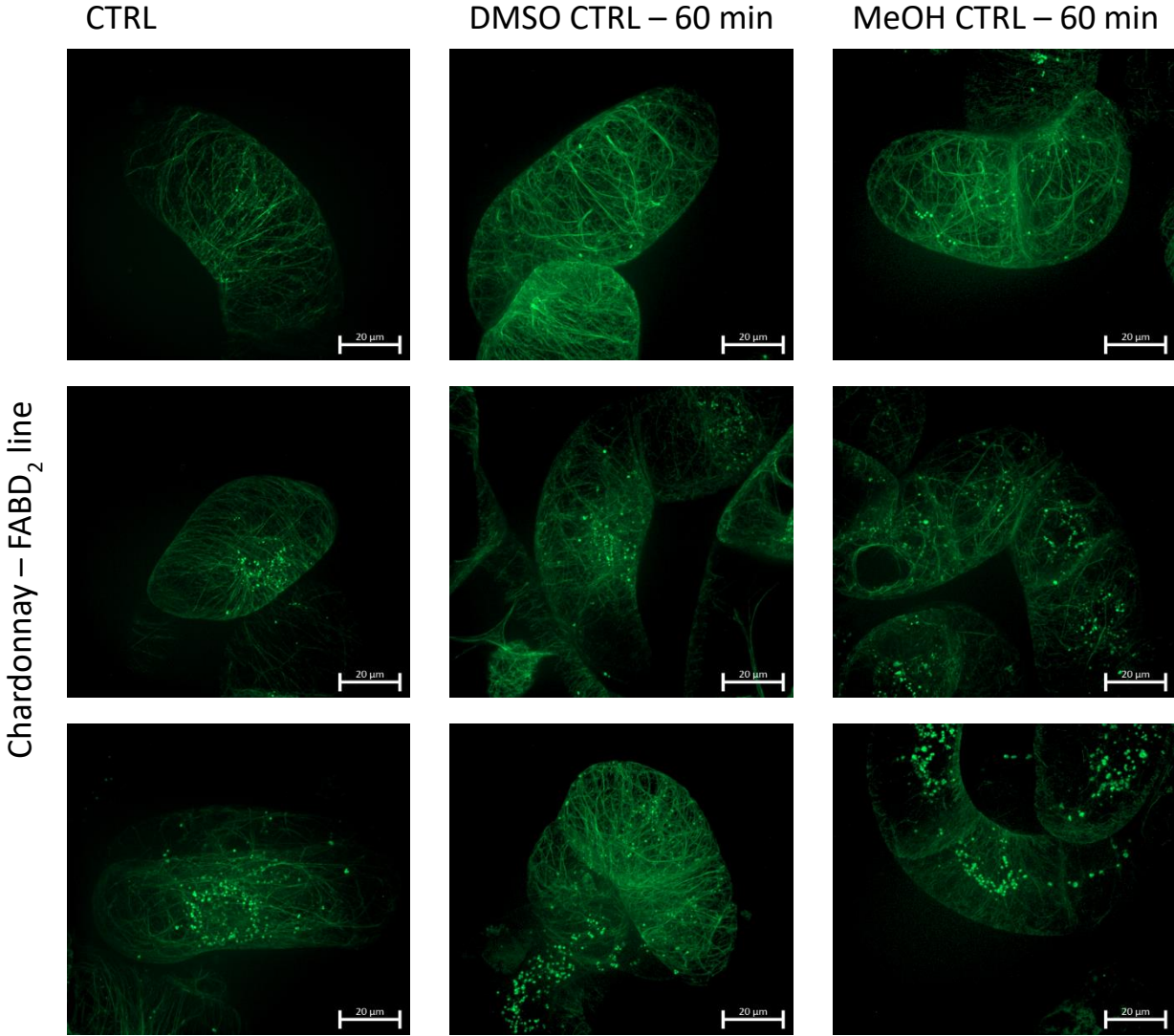
sFig. 1: Effects of solvents on the actin filament of Chardonnay – FABD$_2$-GFP: Suspension cells of Chardonnay – FABD2-GFP were treated with either 0.5 % methanol or 0.1 % DMSO for 60 minutes and subsequently observed using fluorescent microscopy. Pictures were taken using an excitation filter with a 488 nm wavelength and an emission filter with 509 nm of wavelength and an exposure time of 500 ms.

| CTRL	DMSO CTRL – 60 min	MeOH CTRL – 60 min
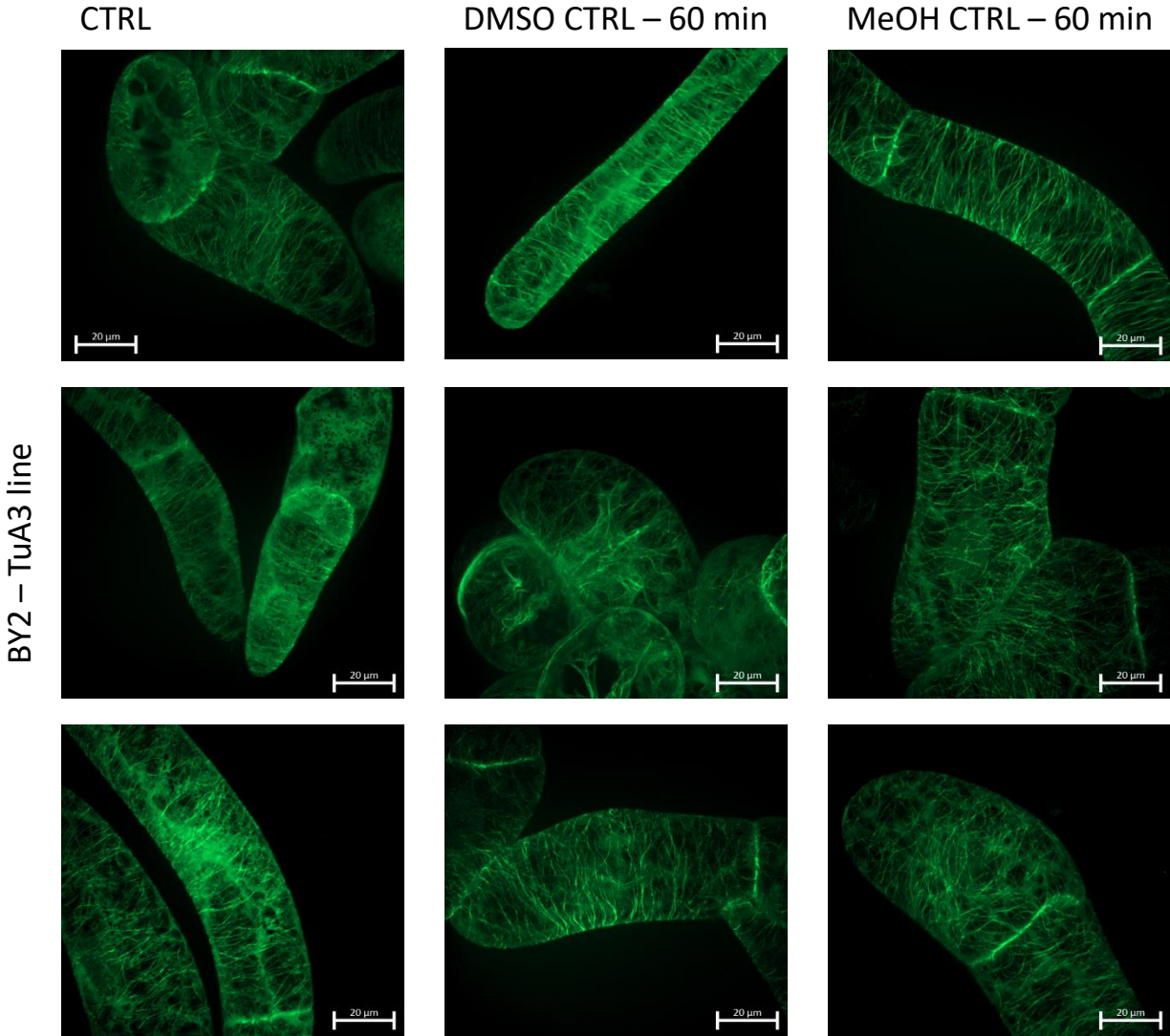
sFig. 2: Effects of solvents on the microtubules of BY2 TuA3:GFP: Cells of BY2 TuA3:GFP were treated for 60 minutes with either 0.5 % methanol or 0.1 % DMSO. Subsequently, fluorescence microscopy pictures were taken using an excitation filter with a 488 nm wavelength and an emission filter with a 509 nm wavelength and an exposure time of 500 ms.
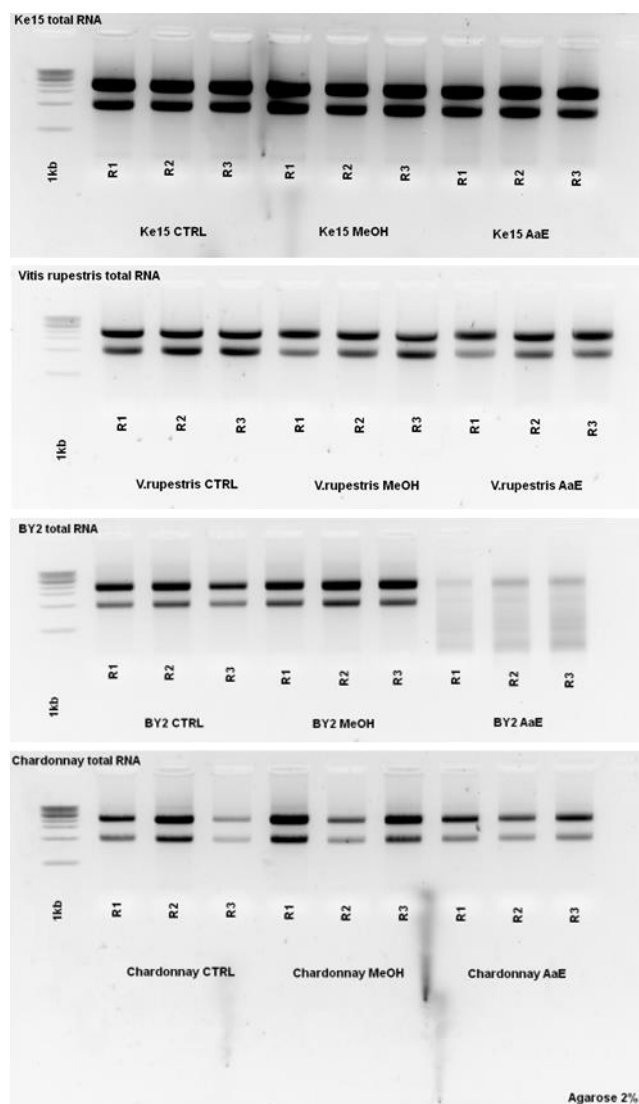
sFig. 3: Total RNA extracted from Ke15, *V. rupestris*, BY2 and Chardonnay: Total RNA extracted from the cell lines Ke15, *V. rupestris*, BY2 and Chardonnay when treated with 50 μM of AaE for 4 hours with respective controls. RNA was extracted using the Roboklon Universal RNA Kit (see Table 6) and loaded onto a 0.5 TAE-Buffer gel with 2 % agarose. RNA was stained using Midori Green Xtra (see Table 2). The electrophoresis was run for 20 minutes at 100 V and visualised using a Blue-Light Transilluminator (see Table 4). The two bands showed the rRNAs 25S and 18S.
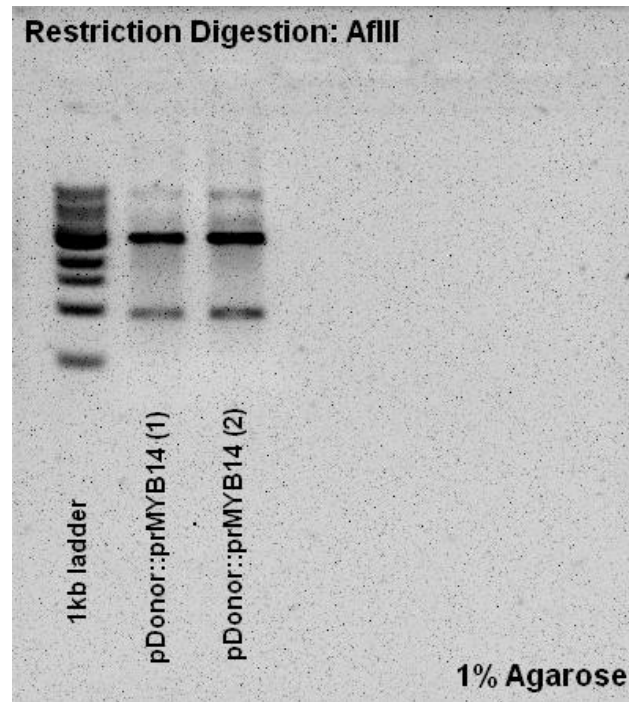
sFig. 4: AfIII restriction digestion of pDonor::prMYB14: 1 µg of the pDonor::MYB14 plasmid was digested with 10 U of the AfIII restriction enzyme. An *in silico* digestion of the plasmid resulted in two bands of both 2,559 bp and 868 bp which was confirmed by the fragments observed in the gel. Two separate stocks of the same plasmid were tested for their integrity.
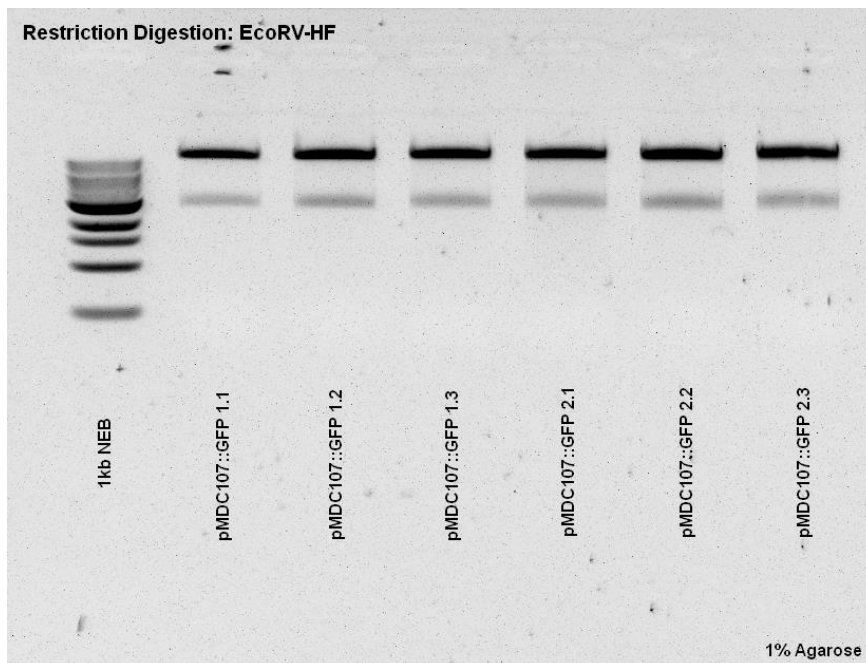
sFig. 5: EcoRV-HF restriction digestion of pMDC107: 1 µg of the isolated pMDC107 plasmid was digested by 10 U of the EcoRV-HF restriction enzyme. An in silico analysis of the digestion resulted in two bands of 9,120 bp and 2,624 bp in size. The transformed *E. coli* cells were plated on two separate plates and three colonies were tested on each plate. In all six samples, the resulting fragments confirmed the prediction done *in silico*.
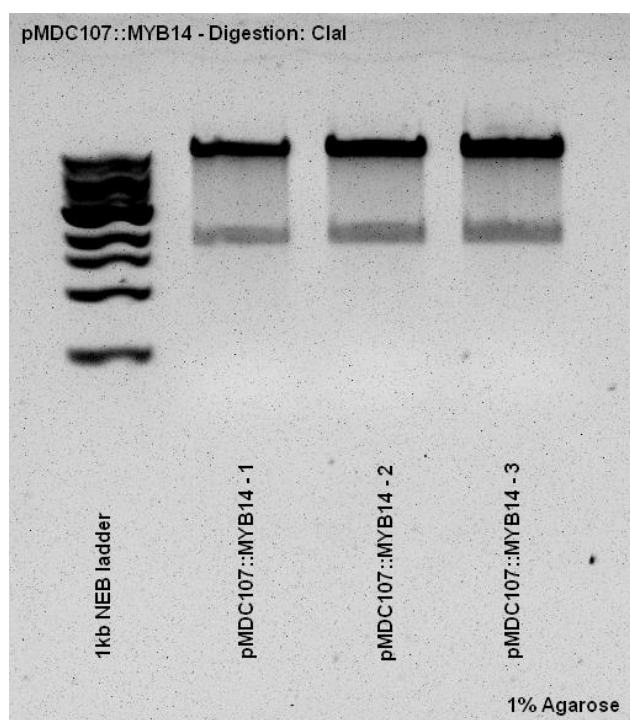
sFig. 6: ClaI restriction digestion of prMYB14::GFP: 10 U of the restriction enzyme ClaI is used to digest 1 µg of the isolated plasmid prMYB14::GFP (pMDC107::MYB14). The in silico analysis of the digestion results in two fragments in the sizes of 9,685 bp and 1,772 bp. E. coli transformed with the plasmid are plated on three separate plates and one colony was tested each. The fragments observed confirmed the prediction done *in silico*.
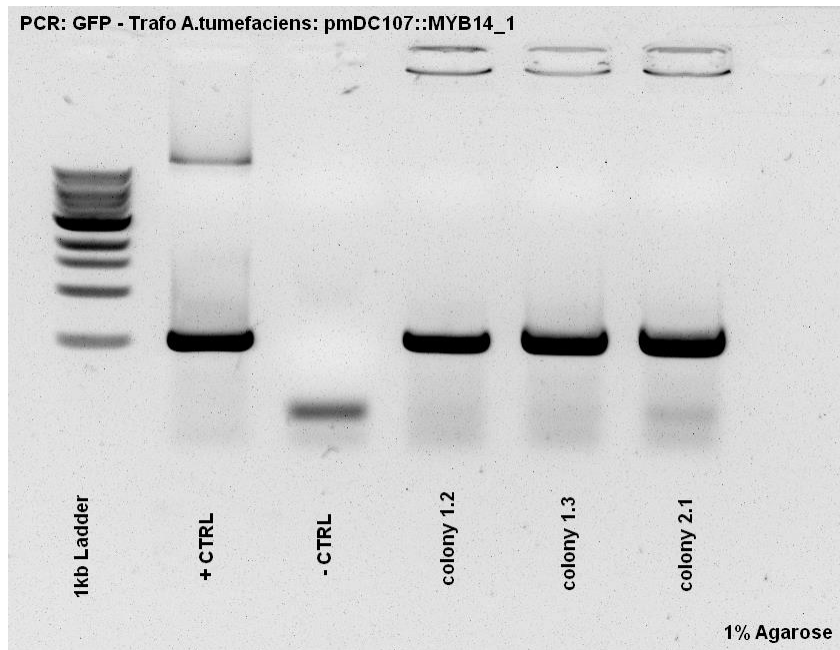
sFig. 7: PCR amplifying eGPF on prMYB14::GFP: A PCR was performed (see Chapter 3.2.2) using the primers eGFP_fw and eGFP_rv (see Table 8) to amplify the region of the plasmid prMYB14::GFP encoding the GFP. Three colonies of *A. fabrum* (formerly known as *A. tumefaciens*) hailing from two separate LB plates were selected due to their ideal and isolated growth and tested. Both a negative control (-CTRL) lacking the template and a positive control (+CTRL) using the prMYB14::GFP plasmid pre-transformation as the template were added to confirm the resulting fragment in the tested colonies to be the amplified region on the desired plasmid.

8.1   Establishing a reporter line

Cloning of pDonor::prMYB14

OVernight Cultures (OVC) of pDonor::prMYB14 were prepared in LB-medium containing 25 µg/mL zeocin (stock 50 mg/mL) and grown in the following condition: shaker with 180 rpm and 37°C in shaded conditions (indirect light) overnight (~18 h). Inoculation should occur in the afternoon and observation in the subsequent morning. The plasmid pDonor::prMYB14 was extracted from the OVCs using the "Roti-Prep Plasmid Mini" kit from Carl Roth according to protocol with the notable exception of using 40 µL of ddH$_2$O for the elution step. The elution step was performed by using the same 40 µL of ddH$_2$O twice to elute the maximum amount of DNA. The integrity of the plasmid was confirmed via restriction digestion (see sFig. 4) and sequencing.

Cloning of pMDC107 Gateway Vector

The isolated plasmid pMDC107 was transformed into the *E. coli* strain DB3.1 for plasmid multiplication via a heat shock protocol and subsequently plated onto selective

LB plates containing 50 µg/mL kanamycin. The plates were incubated in an incubator at 37°C overnight. Colonies that grew on the selective plates were used to inoculate OVernight Cultures (OVC) in liquid LB-medium containing 50 µg/mL kanamycin and cultivated on a shaker at 37°C in the dark, overnight (~18 h). The gateway vector pMDC107 was extracted from these overnight cultures the next day by using the "Roti-Prep Plasmid Mini" kit from Carl Roth according to the respective protocol. The plasmid was eluted in 40 µL of ddH$_2$O and the integrity of the plasmid was confirmed via restriction digestion (see sFig. 5) and sequencing.

LR reaction of pDonor::MYB14 into pMDC107

To create the desired construct; the promoter of MYB14 controlling the eGFP in the pMDC107 vector, the respective sequence was transferred from the donor plasmid into the gateway vector via an LR reaction. To start the reaction 150 ng of each plasmid was mixed with 1 µL of the LR clonase II mix (Gateway LR Clonase II Enzyme-Mix) and filled to 4 µL with TE buffer (pH=8.0). The mixture was incubated at 25°C for at least 3 hours, whereas overnight incubation periods (~18 h) yield better results. The LR reaction was terminated by adding 1 µL of proteinase K solution, briefly vortexing and incubating at 37°C for 10 min. 1 µL of the LR reaction product (prMYB14::GFP) was transformed into the *E. coli* strain DH5α via a heat shock protocol to multiply the plasmid. The transformed cells were plated on LB plates containing 50 µg/mL kanamycin. The integrity of the resulting plasmid was confirmed via restriction digestion (see sFig. 5) and sequencing.

Reaction of reporter line BY2 MYB14::GFP to elicitors

The transgenic line BY2 MYB14::GFP was intended to be used to screen substances for their ability to induce the plant's immune system. Controlling the expression of eGFP with the promoter of MYB14 should cause eGFP to be expressed when the synthesis of stilbenes should be induced (Höll et al. 2013), thus having the cells produce a green fluorescence when immune defence mechanisms are triggered. To test the feasibility of the cell line created, the cells were treated with different known elicitors and the fluorescence within the cells was measured. To quantify the fluorescence, the cells were transferred to objective slides and pictures were taken with an apotome microscope (see Table 4) using two sets of filters. A baseline of blue autofluorescence of the cells was measured using an excitation wavelength of 353 nm, an emission wavelength of 465 nm and an exposure time of 1,000 ms. The green

fluorescence, supposedly produced by the expression of the eGFP controlled by the MYB14 promoter, was measured using filters to produce an excitation wavelength of 488 nm, an emission wavelength of 509 nm and an exposure time of 3,000 ms. After taking the pictures, the fluorescence in the respective channels was quantified using the ImageJ software (see Table 5). The fluorescence was quantified in large overview pictures of a myriad of cells by measuring the mean grey value of the entire cell area. A time course observation was first performed with harpin. 4 days old BY2 MYB14::GFP cells were cultivated in 15 mL MS-medium with 27 µg/mL harpin, as a known inducer of the ETI response. A respective negative control with untreated MS medium was created as well. After adding the elicitor, the cell cultures were incubated at 26°C, in the dark, while shaking on an orbital shaker at 150 rpm. The fluorescence in the cells was observed and quantified at 4, 8 and 24 hours post-induction. Afterwards, a wider screening of stress elicitors was conducted. 4 days old BY2 MYB14::GFP cells were cultivated in 15 mL of MS medium, with one biological replicate per sample due to time and space restraints. A negative control with untreated MS-medium was performed. The other treatments included 1 µM flg22, 3 µM fusicoccin A, 200 µM AlCl$_3$, 100 µM MeJA, 150 nM NaCl and 5 µM of cis-hexenal (see Table 2). The treatments were incubated at 26°C, in the dark, while shaking at 150 rpm for 24 hours. Subsequent to the incubation, the cells were observed, and the fluorescence was measured and quantified.

Relative fluorescence
in BY2 MYB14::GFP under harpin exposure

Significance Level: 0,05
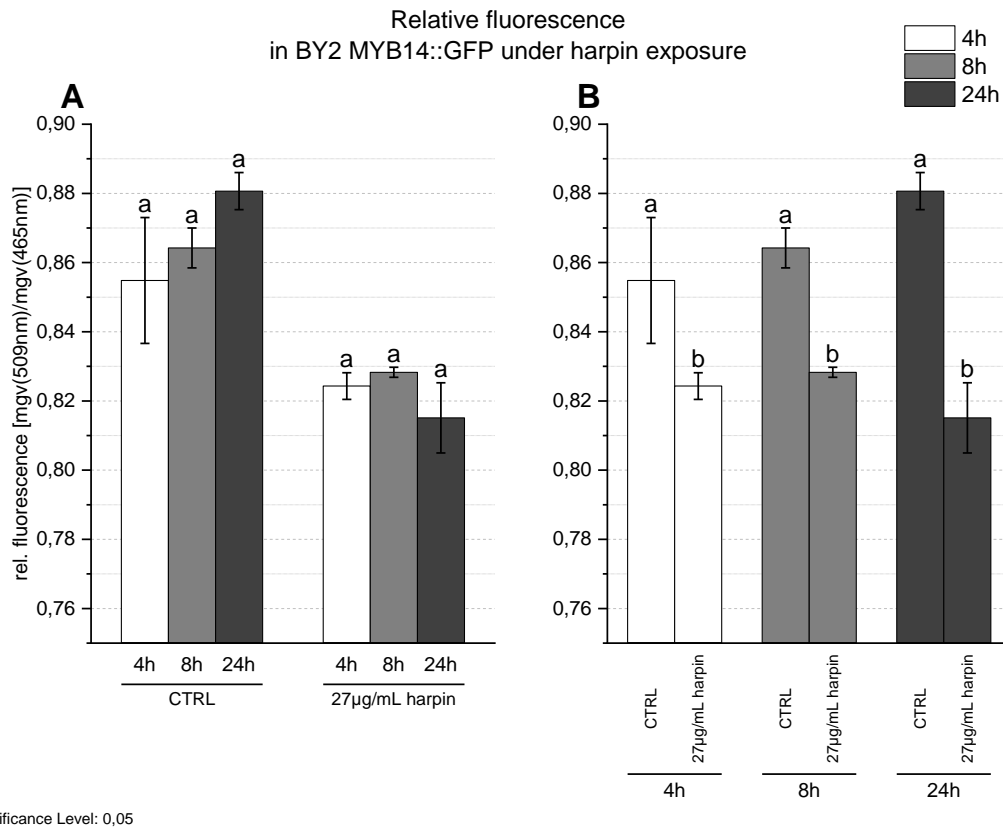
sFig. 8: Relative fluorescence in BY2 MYB14::GFP exposed to harpin: 4 days old BY2 MYB14::GFP cells were treated with 27 µg/mL harpin. Both the treated samples and the control (CTRL) were prepared in biological triplicates and the fluorescent signal was measured at 4 h, 8 h and 24 h post-elicitation. The green fluorescence (ex488 nm/em509 nm) was standardized to a baseline blue autofluorescence (ex353 nm/em465 nm). The significance of differences was calculated via a Fisher LSD ANOVA with a significance level of 0.05.

The untreated samples of BY2 MYB14::GFP showed a strong and evenly distributed green fluorescence. When treated with 27 µg/mL harpin the fluorescence intensity was significantly lower when compared to the respective CTRL in all time points observed (see sFig. 8 B). Comparing the samples within a treatment there was no significant difference observable between the different time points (see sFig. 8 A).

To check whether the reporter line BY2 MYB14::GFP produces a green fluorescent signal in reaction to different stressors, the cell line was treated with elicitors of different biotic and abiotic stresses. Time and spatial restrictions limited the number of replicates for each treatment to one for the preliminary screening. The cells were treated with 1 µM of flg22, 3 µM Fussicoccin A, 200 µM $AlCl_3$, 100 µM MeJA, 150 nM NaCl and 5 µM cis-hexenal (see Table 2).
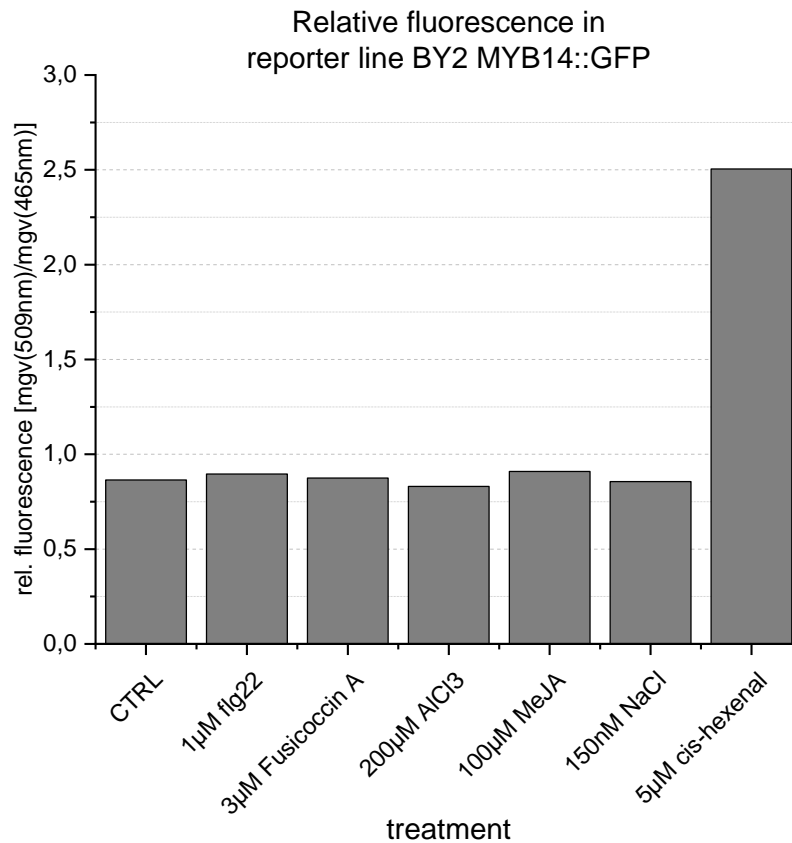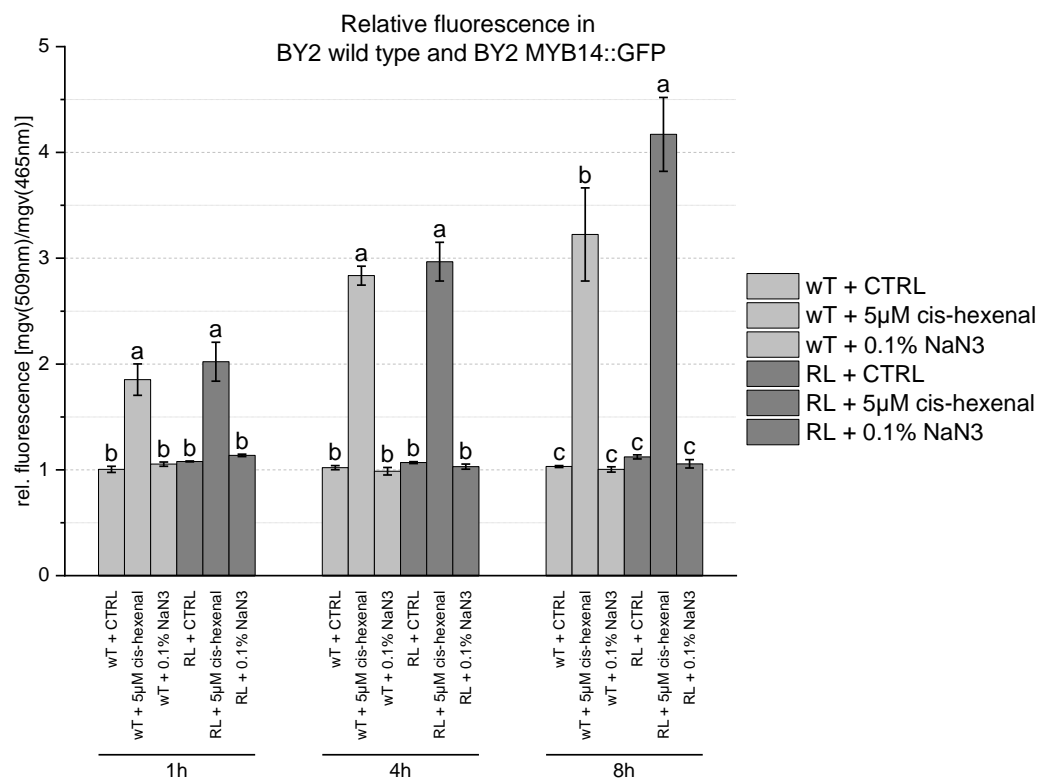
sFig. 9: Relative fluorescence in BY2 MYB14::GFP exposed to different stressors: 4 days old cells of BY2 MYB14::GFP were treated with either 1 µM flg22, 3 µM Fusicoccin A, 200 µM AlCl3, 100 µM MeJA, 150 nM NaCl and 5 µM cis-hexenal. Fluorescence was observed after 24 h of treatment. A green fluorescence (ex488 nm/em509 nm) was standardized to a baseline blue autofluorescence (ex353 nm/em465 nm). There was no statistical analysis due to the lack of replication.

In the reporter line treatments with flg22, fusiccocin A, AlCl$_3$, MeJA or NaCl there was little difference to the respective negative control (see sFig. 9). Treating BY2 MYB14::GFP with 5 µM of cis-hexenal produced a higher level of the relative fluorescence of 2.50424 compared to the relative fluorescence of 0.86443 in the negative control.

To further elucidate the reporter line's reaction to the treatment with cis-hexenal, biological triplicates of BY2 wildtype cells and the BY MYB14::GFP line were treated with cis-hexenal and NaN$_3$ to check whether the increase in fluorescence was caused by cell death. The cell lines were incubated in 15 mL of MS medium at 26°C, in the dark while shaking at 150 rpm and were treated with the respective substance at 4 days old. Both cell lines were treated with either 5 µM of cis-hexenal or 0.1 % (w/v) NaN$_3$ with a respective untreated negative control. After starting the treatment, the cells

were incubated as mentioned before. Observation of the induction of fluorescence was performed at 1 h, 4 h and 8 h post-induction. The cells were observed using an apotome microscope (see Table 4) with two sets of filters. A baseline blue fluorescence was measured using an excitation wavelength of 353 nm, an emission wavelength of 465 nm and an exposure time of 1,000 ms. The green fluorescence, intended to be produced by the expression of eGFP in the transgenic cell line, was measured using an excitation wavelength of 488 nm, an emission wavelength of 509 nm and an exposure time of 3,000 ms. The increase in green fluorescence was standardized to the blue baseline fluorescence that remained largely unchanged by the treatments applied.

Significance Level: 0,05

sFig. 10: Relative fluorescence: cis-hexenal exposure in BY2 wild-type and BY2 MYB14::GFP: 4 days old cells of BY2 wild-type (wT) and the reporter line BY2 MYB14::GFP (RL) were treated with 5 µM of cis-hexenal and 0.1 % NaN$_3$ respectively. These treatments and an untreated control were prepared in triplicates. Fluorescence was observed at 1 h, 4 h and 8 h post elicitation, whereas the green fluorescence (ex488 nm/em509 nm) observed was standardized to a baseline blue autofluorescence (ex353 nm/em465 nm). Whether the treatments differed significantly was calculated via a Fisher LSD ANOVA test using a significance level of 0.05.

In all time points observed, there was no significant difference between the control treatment (CTRL) and the NaN_3 treatment; both within a specific cell line nor when comparing the wild-type (wT) treatments to the respective reporter line (RL) treatments (see sFig. 10). In all treatments, both the wild-type and the reporter line treatment with 5 µM cis-hexenal resulted in a significantly higher fluorescence when compared to control and NaN_3 treatments. At time points 1 h and 4 h there was no significant difference between the cis-hexenal treatments of BY2 wild-type and BY2 MYB14::GFP (see sFig. 10). At the 8 h time point there was a slightly but significantly higher fluorescence in the cis-hexenal treatment of the reporter line when compared to the respective treatment of the wild-type line (see sFig. 10)

The transgenic reporter line BY2 MYB14::GFP was transformed with a genetic construct that controls the expression of eGFP with the promoter of MYB14 from *Vitis vinifera sylvestris* Hö29 (Höll et al. 2013; Duan et al. 2016). This was intended to create a cell line, that produces a green fluorescent signal once its immune system is engaged. The cloning of the construct and its transformation into the BY2 cell line was confirmed to have been successful (see sFig. 5, sFig. 6 and sFig. 7). The cell line produced a steady ground level of green fluorescence irrespective of the treatment (see sFig. 10). This might be due to a certain occurrence of reporter leakage. When testing the cell line for its intended purpose, BY2 MYB14::GFP showed no increase in fluorescence when treating the cells with 27 µg/mL harpin (see sFig. 8). Contrary to the assumption, the signal did not increase but significantly decreased when exposed to harpin. This was likely caused by the cell death induced in the effector-triggered immune response mounted by the cell line. The untreated control reproduced unhindered and expressed further fluorescent proteins, whereas the harpin-treated cells halted their lifecycle and engaged the programmed cell death, which ultimately caused the cells' structures to be dismantled. This might explain why the fluorescent signal in the harpin treatment significantly decreased when compared to the respective control group (see sFig. 8 B).

Since harpin treatment did not yield the intended result, a wider screening for transgenic activity was conducted to see whether the promoter would be engaged in other signalling pathways. BY2 MYB14::GFP was treated with 200 µM $AlCl_3$ and 150 nM NaCl to check whether the promoter would be triggered when signalling abiotic stresses. The line was also exposed to 100 µM MeJA to test for the involvement of

MYB14 in the jasmonate signalling pathway. Lastly, the reporter line was treated with 1 µM of flg22, 3 µM Fusicoccin A and 5 µM of cis-hexenal to elucidate the reaction to biotic stressors. Due to certain constraints, there was only one replicate of each. None of the treatments yielded any big change in relative fluorescence except for the treatment with 5 µM cis-hexenal (see sFig. 9). In the cis-hexenal treatment, a 2.9-fold increase in fluorescence could be observed but the habitus of the cell line hinted at the cells dying and the fluorescence potentially being the result of autofluorescent bodies present during cell death. To evaluate this possibility, BY2 MYB14::GFP cells, as well as a wild-type control of BY2 cells, were both treated with 5 µM cis-hexenal and 0.1 % NaN_3 as a positive control for cell death. NaN_3 is cytotoxic by inhibiting the cytochrome oxidase in mitochondria. The treatment with 5 µM cis-hexenal caused a significant increase in fluorescence in both the wild-type line and the reporter line BY2 MYB14::GFP (see sFig. 10). The difference was already observed in the earliest time point of 1 h post elicitation and increased at the 4 h and 8 h time points. After 8 h of incubation with cis-hexenal, there was a significant difference between the cis-hexenal treatment of the wild-type and the reporter line (see sFig. 10). NaN_3 did not cause an increase in fluorescence but did also not alter the general habitus of the cells, implying the treatment with 0.1 % NaN_3 did not cause the cells to die. Irrespective of the fact that there was a significant difference between the cis-hexenal treatment of the reporter line and the wild-type at the 8 hours time point, the fact remains that a significant increase in fluorescence was generated in the non-transgenic wild-type cell line. Therefore, the increase in fluorescence in the reporter line observable upon treatment with cis-hexenal cannot be attributed to the construct and an intended expression of eGFP when an immunity-related signalling pathway would be triggered.

The promoter of MYB14 used in this set of experiments was derived from the genotype *Vitis vinifera sylvestris* Hö29 (Duan et al. 2016). The transcription factor MYB14 is known to regulate and induce the synthesis of stilbenes in grapevine (Höll et al. 2013; Wong et al. 2016) during the mounting of a defence reaction to pathogen presence. The promoter of said transcription factor was transformed into cells of *Nicotiana tabacum* BY2. Currently, no stilbene synthases have been discovered in the genome of *N. tabacum*, therefore it is quite possible that BY2 does not have a similar sequence to prMYB14 in its transcriptional mechanism or the inherent defence reaction does not rely on the induction thereof. Defence reactions of BY2 and *Vitis sylvestris sylvestris* Hö29 might just be too different for prMYB14 to be activated by the defence reaction

of BY2. The BY2 cells were chosen as the preferred transformant due to their ease of handling and general vitality. To address this incompatibility it would be necessary to transform *Vitis* cells. To transform *Vitis* cells, an established transformation protocol for rice (Page et al. 2019) was slightly altered and tested on *Vitis vinifera sylvestris* Ke.
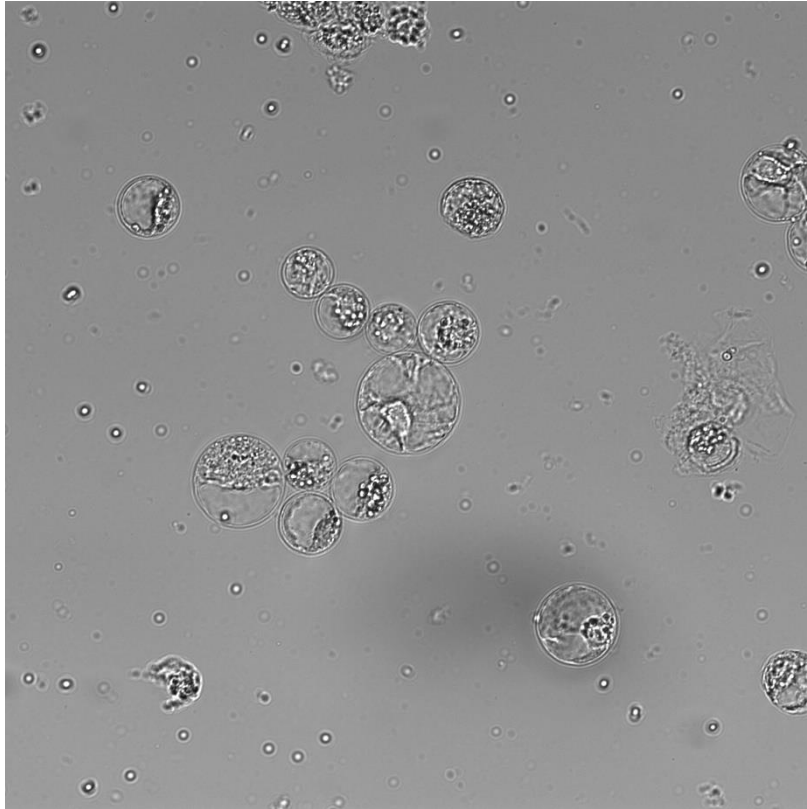
Transformation of *Vitis* protoplasts

In our lab, there are well-established routines to transform plant cells of *Nicotiana tabacum* BY2. The *Agrobacterium fabrum*-mediated transformation protocol is easy, quick and efficient and the resulting transgenic cells are quick to regenerate. Transferring the same protocol to the transformation of *Vitis* cells has proven difficult. To easily create transgenic cell lines of *Vitis* accessions to test constructs in these lines it is therefore important to establish improved protocols. A big barrier to the transformation of plant cells can be their cell wall. Page et al. (2019) established a method to rapidly generate protoplasts from rice seedlings to transform them by co-incubating the protoplasts with plasmids. The majority of the resulting transformations are transient. In this work, the protocol by Page et al. (2019) was slightly altered to test its feasibility to transform *Vitis* cells.

A slightly modified protocol by Page et al. (2019) was performed on *Vitis vinifera sylvestris* cells of the genotype Ke15. 4 days old cells of Ke15 were filtered using a Nalgene bottle top filter carefully replacing the MS medium the cells were cultivated in with 0.6 M mannitol (see Table 1). 40 mL of 0.6 M mannitol with the suspended Ke15 cells was transferred into a 50 mL reaction tube. The cells were incubated at room temperature (RT ~25°C) while gently shaking for 15 min to initiate plasmolysis. After incubation, the 0.6 M mannitol solution was drained off the cells by covering the reaction tube with a fine mesh and pouring out the solution. 30 mL of the enzyme solution (see Table 1) was added to the cells and incubated in the dark, at RT for 4 h while gently shaking the cells to aid the digestion of the cell wall. To stop the digestion 30 mL of W5 solution (see Table 1) was added to the solution and shaken gently. The cells were filtered through a mesh with a 40 µm pore size, thereby letting protoplasts pass and retaining cells with partially or entirely undigested cell walls. To improve yield, the cells can be rinsed with an additional 60 mL of W5 solution. The protoplast-containing solution was carefully centrifuged at 250 g for 3 min at room temperature (~25°C). The supernatant was gently decanted and the pellet was washed by resuspending the cells in 10 mL W5 buffer. The cells were centrifuged at 250 g for

3 min, the supernatant decanted and finally resuspended in 2 mL MMG solution. To increase the chances for a successful transformation 5 µg of the plasmid was to be diluted into 10 µL of ddH2O to mix with 60 µL of the protoplast suspension in MMG. Extraction of the plasmid p2FGW7-FABD$_2$-GFP yielded a maximum concentration of 76.2 ng/µL using the Roti-Prep plasmid mini kit (see Table 6). A full 10 µL of the plasmid sample with the highest concentration was used, yet the target concentration was not within reach. 70 µL of the PEG solution (see Table 1) was added to the plasmid-protoplast mixture, gently mixed by inverting the reaction tube and incubated in the dark at RT for 25 min. After these 25 minutes, the transformation process was stopped by adding 280 µL W5 solution and mixing by gently inverting the reaction tube. The protoplasts were centrifuged at 250 g for 3 min at RT and the supernatant was carefully aspirated. The pellet was resuspended in 500 µL WI solution (see Table 1) and separated into 125 µL aliquots. These aliquots were incubated for 16 h, preferably overnight at RT. During this time, transformed cells would accumulate the introduced transgenic proteins, if applicable. After the incubation period, *Vitis vinifera sylvestris* Ke15 protoplasts transformed with p2FGW7-FABD$_2$-GFP were observed using the apotome microscope (see Table 4) using a filter set to visualise the potentially induced actin-bound eGFP. The filters create an excitation wavelength of 488 nm and an emission wavelength of 509 nm. Pictures were taken of the green fluorescent channel mentioned before and the brightfield channel with an exposure time of 1,000 ms and 15 ms respectively. Additionally, pictures were taken before the transformation and subsequent 16 h incubation, only using the brightfield channel to evaluate the vitality of the protoplasts generated.

To check the general vitality and integrity of the protoplasts generated by the altered protocol of Page et al. (2019) a sample of protoplasts was taken right before the mixing of the protoplasts with the plasmid to be introduced into the cells. The Ke15 protoplasts were visualised using the brightfield channel of the apotome microscope (see Table 4).

sFig. 11: Protoplasts of *V. vinifera sylvestris* Ke15 cells, pre-transformation: *Vitis vinifera sylvestris* genotype Ke15 cells were treated according to a slightly altered protocol derived from the work of Page et al. (2019). The protoplasts were visualised in the pre-transformation step using the brightfield microscopy of the apotome microscope (see Table 4) and an exposure time of 15 ms.

Among cell debris, some protoplasts appeared to be healthy and contained intact proplastids, nuclei and vacuoles. There were different sizes of protoplasts in the sample observed (see sFig. 11).

To see whether the protoplasts were successfully transformed samples of cells that were treated to be transformed with the plasmid p2FGW7-FABD$_2$-GFP and a respective control group (CTRL) were observed using the apotome microscope using filters to visualise the eGFP present in the plasmid construct. The filters create an excitation wavelength of 488 nm and an emission wavelength of 509 nm.

CTRL **p2FGW7-FABD2-GFP**
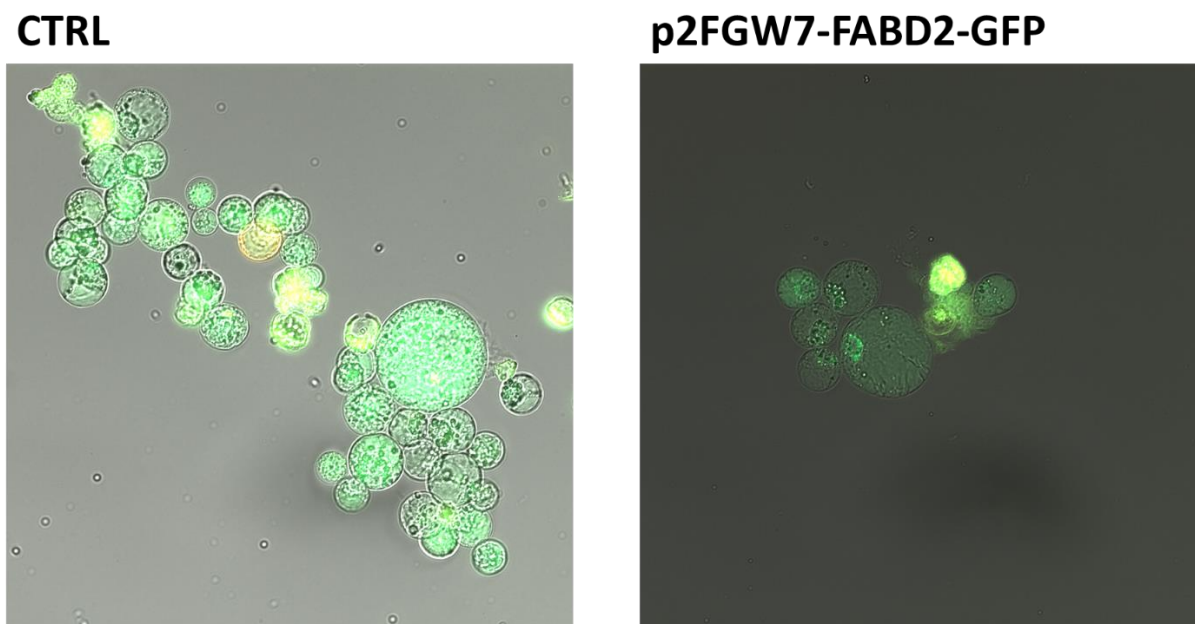
sFig. 12: Protoplasts of *V. vinifera sylvestris* Ke15 cells, post-transformation: *Vitis vinifera sylvestris* genotype Ke15 cells were treated according to a slightly altered protocol from Page et al. (2019). The protoplasts were visualised post-transformation using a brightfield channel with 15 ms exposure and a green fluorescent channel using a filter pair to create an excitation wavelength of 488 nm and an emission wavelength of 588 nm with an exposure time of 1,000 ms. The protoplasts were transformed with the plasmid p2FGW7-FABD2-GFP. A control group of cells (CTRL) was treated accordingly with no plasmid added during the transformation step.

Using a filter set (ex488 nm/em509 nm) to visualise the potential eGFP expressed in the transformed cell line, a green fluorescent signal was both visible within cells that were transformed with the p2FGW7-FABD$_2$ plasmid and within cells of the control group (CTRL) that had no plasmid added during the transformation process (see sFig. 12).

Transformation of *Nicotiana tabacum* BY2 cells is well-established and time-efficient but certain genes or promoters from different organisms might be inactive or behave differently. To research or exploit this genetic material it can help to transform them into cells closer related to the species of origin. The promoter of MYB14 from *Vitis vinifera sylvestris* Hö29 appeared to be inactive when transformed into BY2 cells (see sFig. 9). To create a transgenic cell line that produces eGFP controlled by prMYB14, BY2 cells were unsuitable. The same construct, prMYB14::GFP could be tested in *Vitis* cells. The closer relation of the cell line *V. vinifera sylvestris* Ke15 to *V. vinifera sylvestris* Hö29 increases the likelihood of the promoter being engaged. The transformation protocol used to transform BY2 cells proved less efficient when applied

to *Vitis* cells, therefore establishing a new protocol specifically for *Vitis* cells is desirable. In this work, a protocol to transiently transform rice protoplasts (Page et al. 2019) was altered to test the feasibility of transferring the protocol to transform *Vitis* cells of the genotype Ke15.

In the original publication, Page et al. (2019) used plant tissue of rice to generate protoplasts. To generate protoplasts of *Vitis* cells growing in liquid suspension culture, this step was replaced by substituting the MS medium the cells grow in a mannitol solution using a bottle-top filter. The rest of the protocol was transferred as is. Using the protocol on cells of *V. vinifera sylvestris* Ke15 yielded a sufficient amount of healthy protoplasts (see sFig. 11) to initiate transformation.

The transformation of the Ke15 cells with the control construct p2FGW7-FABD2-GFP according to the protocol yielded protoplasts that kept their integrity. The protoplasts were tested for green fluorescence via microscopy to check for successful transformation with the construct that constitutively produces GFP. Yet, green fluorescence was observed in both the transformed samples and the non-transformed control samples (see sFig. 12). It seems like the stress of generating protoplasts and the subsequent treatment for transformation caused the cell lines to generate substances with an auto-fluorescence in the same wavelength spectrum as GFP. Therefore, a successful transformation of the cell line could neither be confirmed nor ruled out.

The generation of protoplasts from *Vitis* cell lines using the protocol of Page et al. (2019) proved easy and efficient but the success of the subsequent transformation remains elusive. To confirm whether the transformation of the cell line is possible, the spectrum of the auto-fluorescence of the cells needs to be tested and the to-be-transformed construct to be chosen to avoid redundant spectra. Alternatively, the protoplasts could be selected via introduced antibiotic resistances and test their ability to regenerate.